Hypertrophic cartilage engineering for human bone and bone marrow regeneration

Inauguraldissertation

zur
Erlangung der Würde eines Doktors der Philosophie
vorgelegt der
Philosophisch-Naturwissenschaftlichen Fakultät
der Universität Basel

von

Sébastien Pigeot

Chaniers, France

Basel, 2020

Genehmigt von der Philosophisch-Naturwissenschaftlichen Fakultät

auf Antrag von

Prof. Ivan Martin, PhD
Prof. Peter Scheiffele, PhD
Prof. Prasad Shastri, PhD

Basel, den 27.02.2018

Prof. Dr. Martin Spies
The Dean of Faculty

"Facts do not cease to exist because they are ignored."

"Experience is not what happens to a man; it is what a man does with what happens to him."

Aldous Huxley

AKNOWLEDGMENT

En premier lieu, je souhaiterai remercier ma famille au sens large pour m'avoir offert un environnement propice au développement d'un esprit cultivé et critique sur de nombreux sujets. Bien sûr, mes parents, Marie-Christine et Serge Pigeot qui m'ont élevé et supporté tout au long de ma vie et de mes études et ceci même lorsqu'il s'agissait de choix « extravagant ». Ensuite, je tiens à remercier ma sœur Aurélie Soulice et son mari, Victorien Soulice avec qui j'ai toujours énormément de plaisir à discuter d'autres aspects de la vie en dehors de la science. Sonia et Iléana Soulice m'ont apporté des petits rayons de soleil au cours des moments difficiles de la thèse.

Following my family, I owe great thanks to Prof. Ivan Martin and Dr. Paul Bourgine to whom I owe to have been able to do my PhD in the University of Basel. They both helped me so much to grow as a person and as a scientist.

Also, this would never have been possible without the continuous support from my friends in Basel and elsewhere. They have been the pillars to support me during the good but most importantly the difficult times of the PhD.

Finally, I would like to take the opportunity to once again thank all the lab members, past and present, for their time, teaching, good spirit creating a very enjoyable atmosphere and enjoyable working environment.

Last but not least, I would like to thank all the members of my PhD committee Prof. Peter Scheiffele, Prof. Prasad Shastri, Prof. Ivan Martin, Dr. Paul Bourgine and Prof. Susan Treves for their help and advices during my PhD.

Abstract

Bone and bone marrow (BM) are major components of the human body, with a pivotal role in skeletal structure and hematopoietic cell function. Most bones in the human body form and heal through a process called endochondral ossification, whereby human mesenchymal stromal cells (hMSC) generate a hypertrophic cartilage (HyC) intermediate which progressively remodels into bone and BM. In my thesis, I propose to engineer HyC by recapitulating the key developmental features of endochondral ossification, and to exploit it for inducing bone repair and modelling human hematopoiesis.

Part I of my thesis aims at generating devitalized HyC to be used as a graft for bone repair by engineering hMSC with an inducible apoptotic cassette. Apoptosis devitalization showed that by preserving the factors embedded in the extracellular matrix, endochondral bone formation could be achieved by osteoinduction in an ectopic environment. In a second phase, the process to generate devitalized HyC was upscaled and streamlined using a perfusion-based bioreactor system. The resulting devitalized HyC was assessed against a clinically used human processed allograft in a rabbit calvarial model. Efficient and homogenous production of devitalized HyC could be accomplished in a single step process. Finally, orthotopic implantation demonstrated the superiority of devitalized HyC compared to a clinical standard-of-care.

Part II targets the exploitation of this developmental process to create a model for the study of interactions between human stroma and hematopoietic cells. Until now, most human hematopoiesis studies are carried out using humanized mice models, missing a human stromal compartment. By keeping alive the human stromal cellular fraction in the HyC, we generated an ectopic humanized bone organ (ossicle) in the mouse. The ossicles successfully engrafted long term functional human hematopoietic stem and progenitor cells (HSPC) and increased the fraction of quiescent human hematopoietic stem cells (HSC) as compared to the native mouse bone. Then, we asked whether the ossicles could be customized to visualize the human stroma and influence the hematopoietic environment. By engineering hMSC to overexpress a fluorescent reporter and the stromal cell-derived factor 1 alpha (SDF1α) cytokine, we visualized and quantified the human stromal cell fate in the ossicles and modified the hematopoietic cell homeostasis. Finally, this system allowed the visualization of putative human HSPC niches.

Overall, by using engineered hMSC and HyC tissue, this work tackles both a clinical application by developing a new material for bone repair, and the generation of fundamental knowledge by establishing a model of human hematopoietic cells interacting with their stromal niche.

Table of content

Chapter I:

Introduction

I. The bone organ

A. Skeletal structure

Bones are major components of some living organisms giving them their shape, dynamic and owing them to pertain to a specific phylogenetic class: the vertebrates. The human body is composed of over 200 bones which can be divided into two classes depending on their origins. Bones from the vertebral column, the rib cage as well as the appendicular skeleton come from the mesoderm whereas the craniofacial skeleton arises from the neural crest cells (ectoderm) [1,2]. Contrary to old beliefs giving bones the status of a relatively inert materials having a protective and scaffolding role shaping vertebrae, bones are highly complex and dynamic organs hosting the bone marrow (BM) where the hematopoietic system is homed and regulated [3,4]. Nevertheless, bones primary architectural role implies a stiff and robust structure [5]. Bones structures are comprised of cortical bone and trabecular bone (Fig. 1). The cortical bone is a very dense tubular ECM structure giving the shape and the stiffness to the organ and hosting the trabecular bone. Cortical bone is surrounded on the outside by the periosteum (except at the articulation where it is replaced by cartilage) and on the inside by the endosteum. Periosteum and endosteum are connective tissues tightly bound to the cortical bone and comprised of osteoblasts and additionally of osteoclast for the endosteum. Bone diameter growth is a slow process involving periosteal growth by osteoblasts matrix deposition and on the other side, endosteal bone resorption by osteoclasts [3].

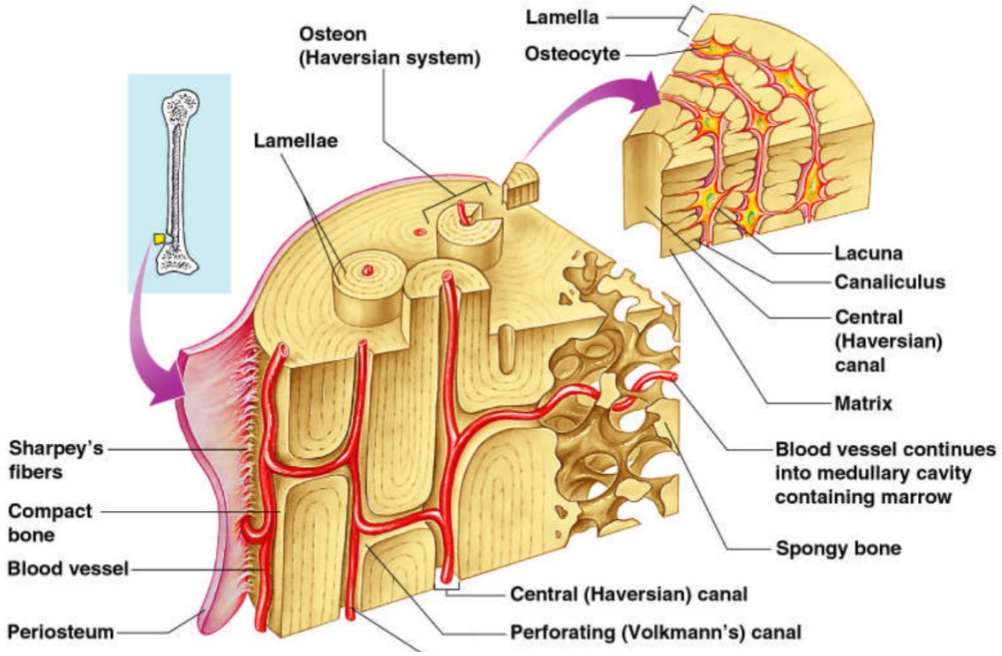

Figure 1: Overview of the general bone structure with the periosteum, cortical bone (compact bone) and the trabecular bone (spongy bone).

One of the main characteristic of the bone organs is their stiffness provided by a very dense and mineralized extracellular matrix (ECM) coupled to proteins such as collagen type I, osteocalcin, osteopontin, osteoconectin, sialoprotein, thrombospondin, and some serum proteins such as albumin [3,6,7].

During the embryonic development osteoblasts depositing the mineralized matrix are generated along two specific pathways namely the intramembranous ossification and the endochondral ossification [8,9]. Most bones are derived from endochondral ossification involving a primary differentiation of mesenchymal stromal cells into chondrocytes and the generation of a cartilaginous templates which upon subsequent remodeling will give rise to long bone organs with BM [10]. The details of this process will be described in a subsequent chapter. Intramembranous ossification on the other hand happens in the craniofacial bones, the mandibula as well as the clavicula. Also starting from mesenchymal cells condensation, they will undergo a direct differentiation into osteoblasts leading to the deposition of a mineralized matrix and bone formation [10,11].

B. Endochondral ossification

Most of the human bones in the body develop through an endochondral ossification process [10,12]. First, mesenchymal cells condense and differentiate into chondrocytes. Chondrocytes will then start producing an ECM composed of aggrecans and collagen type II. On the periphery of the mesenchymal condensation, some cells generate an outer layer called the perichondrium. Chondrocytes at the center undergo hypertrophy increasing by 5-10 folds in size and further depositing a dense matrix composed of collagen type X [13]. Other growth and remodeling factors such as VEGF attract blood vessels and macrophages while MMP13 triggers the action of osteoclast and ECM remodeling [14]. Chondrocytes will then develop along a gradient from the center of the future bone to the epiphysis. Chondrocytes closer to the center gradually become hypertrophic and organize into columnar patterns [15,16]. Further from the center, chondrocytes remain in a proliferating state generating new chondrocytes that can enter pre-hypertrophy and a columnar structure leading to the axial growth of long bones. Chondrocytes at the epiphysis remain in a resting state providing a pool for either proliferating chondrocytes or generating hyaline cartilage for the articulations. While the cartilaginous template undergoes longitudinal growth by chondrocytes columnar organization and hypertrophy. Part of the hypertrophic chondrocytes from the primary hypertrophic cartilage center undergo apoptosis while blood vessels as well as osteo-progenitors, osteoblasts and osteoclasts invade the hypertrophic cartilage and start a primary ossification center [12,16]. ECM is remodeled and generate a cavity for the establishment of the bone marrow space. It has long been believed that all hypertrophic chondrocytes underwent apoptosis. Recently some lineage tracing studies clearly shed the light on the fact that some of these hypertrophic chondrocytes also transdifferentiated into osteoblasts (Fig. 2A)

[9,16]. Osteoblasts from the perichondrium surrounding the hypertrophic ECM lay down mineralization and matrix deposition leading to the formation of the bone collar and the periosteum. The periosteum expands as the bone grows longitudinally. On the epiphysis, blood vessels also invade the cartilage and generate a second ossification center. Some osteoblasts on the bone collar get trapped in the ECM and further evolve towards osteocytes generating the cortical bone. The inner cavity remodels and become trabecular bone and BM (Fig. 2A) [17].

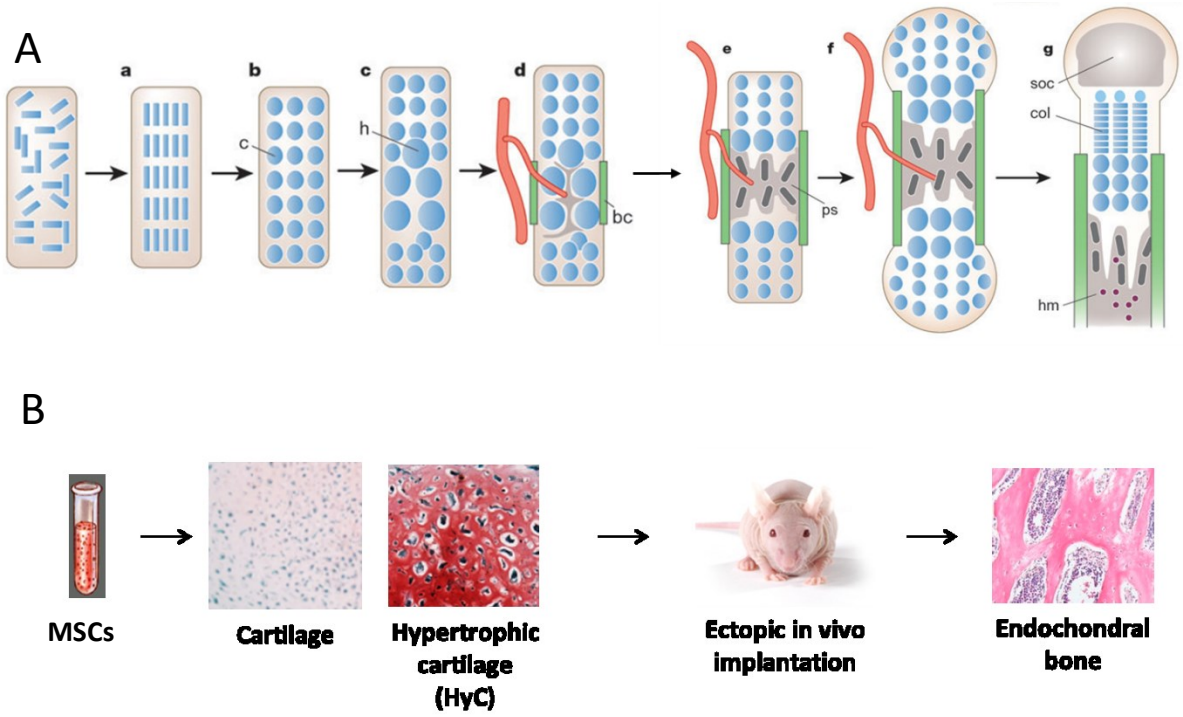

*Figure 2: Overview of the endochondral ossification pathway (**A**) and its recapitulation by different labs (**B**). Briefly, MSCs condensate (**a**) and differentiate into chondrocytes (c) (**b**) then hypertrophic (h) chondrocytes (**c**). Blood vessels and osteoprogenitors invade the hypertrophic cartilage and remodel it into bone and BM (hm) forming the primary spongiosa (ps) (**d, e**). Axial bone growth continues with columnar proliferating chondrocytes (col) while a secondary ossification center (soc) is generated at the epiphysis (**f, g**). Adapted from (Kronenberg 2003).*

Due to its implication in bone development, repair and bone marrow formation, scientists have tried to recapitulate the different steps of endochondral bone tissue formation [18,19]. Starting from different cells sources, cells were successively condensed and driven towards chondrogenic and hypertrophic chondrocytes differentiation (Fig. 2B). The final remodeling steps requiring invasion of the hypertrophic ECM by blood vessels, osteoclasts and osteoprogenitors was initially recapitulated by subcutaneous implantation of mineralized cartilaginous tissues subcutaneously in immunodeficient mice [20–22].

C. Home of the bone marrow

BM is present in most human bones' inner cavity. It is a complex, densely vascularized environment with a wide variety of cell types. It can be subdivided into three different sections with a cellular, extracellular and liquid compartment. The cellular compartment is composed cells involved in the bone and hematopoiesis homeostasis. Cells can be divided on one hand into stem and progenitor cells and on the other hand into mature, differentiated cells. Skeletal stem cells (SSC) and hematopoietic stem cells (HSC) represent the most undifferentiated cell types respectively responsible for the establishment of the bone and hematopoietic cells [23,24]. Stromal and bone cells in the BM are composed of MSC, osteoblasts, osteoclasts, chondroblasts and adipocytes. BM is the home of hematopoiesis and therefore, all blood cells types are present within the BM. HSCs are the only blood cells with true stem cells properties: long term self-renewal and multi-differentiation potential. The current model of hematopoiesis relies on a differentiation tree with HSCs being at the apex. Typically, HSC remain in a quiescent state [23]. To repopulate some hematopoietic populations, they differentiate to short-term HSC and multipotent progenitors (MPP) with multi lineages differentiation potential but limited self-renewal capacities. MPP can further differentiate into progenitors restricted to either the lymphoid lineage (multi lymphoid progenitor, MLP) or the myeloid lineage (common myeloid progenitors, CMP). Lymphoid lineage comprises T and B cells as well as natural killer cells (NK). Myeloid lineage contains erythrocytes and megakaryocytes. Both LMP and CMP can generate granulocyte and macrophages progenitors (GMP) leading to neutrophils, eosinophils, basophils, mast cells, macrophages and monocytes [25–27].

The extracellular compartment is mostly composed of bone ECM with dense mineralized matrix primarily composed of collagen type I [7,23]. Finally, the liquid compartment contains many growth factors involved in the autocrine and paracrine signaling as well as cytokines and other small molecules.

Cells present in the BM closely interact in bone growth and repair as well as hematopoiesis homeostasis, thereby instigating a specific microenvironment called HSC niche [28].

II. HSC niche modeling

A. General structure and function (Stem cell niche)

A stem cell niche is a microenvironment within a tissue where stem cells are maintained and regulated. This regulation is associated with other different cell types secreting growth factors and cytokines [29]. The HSC niche has different locations during the development and become mainly restricted under physiological condition to the bone marrow tissue within the bone organs in the human adults [30].

The maintenance of HSC is of primary importance as they are the one leading to the different blood lineages. They can replenish any blood cell type through tightly controlled regulation. Failure in their maintenance or regulation would lead to serious functional defect in physiological processes such as oxygen transport, coagulation and immune responses [31]. Therefore, deciphering and understanding the human HSC niche is of crucial importance towards the development of new therapies in a wide variety of pathologies.

The first postulate of a specific niche for HSC dates from 1978 by Schofield when he observed superior mature hematopoietic cells replacement following irradiation by bone marrow derived cells transplantation compared to cells derived from the spleen [32]. It was not until 2003 and due to major technical progresses in microscopy that the first evidences of osteoblast implication in the HSC niche could be suggested [33,34]. Since then, many studies complemented this finding and added to the description of the actual HSC niche [35–37]. The major fraction of HSCs is associated to the perivascular environment and more precisely next to sinusoidal vessels. Interestingly, the osteoblastic niche even though being the first to be described do not represent the main actor in HSC niche modeling [28,38]. Despite being extensively studied, the HSC niche composition and location remain controversial.

B. Main actors and role

The HSC niche is composed of hematopoietic and non-hematopoietic cells such as stromal cells, endothelial cells, endosteal cells and nerve cells. Despite being identified as a first cell type implicated in the establishment of HSC niches, osteoblasts do not seem to have a direct effect on the HSC niche [33,34,39]. They seem more involved in the direct maintenance of progenitors such as the lymphoid progenitors [28]. As described earlier, HSC are mainly associated to the perivascular environment and more specifically next to sinusoids [40]. Endothelial cells were shown to be of major importance in the HSC niche through the secretion of stem cell factor (Scf) and stromal derived factor 1 alpha (SDF1α, also known as CXC chemokine ligand 12 (CXCL12)) (Fig. 3). Other cells directly associated with the vasculature are stromal cells. Though being a very heterogenous cell population, specific subtypes have been identified has being of high importance in the HSC niche. CXCL12 abundant reticular (CAR) cells, Nestin-GFP positive cells and leptin receptor expressing cells (Lepr) showed high level of Scf and CXCL12 expression and functional depletion of HSC upon conditional knock out of these cells [28,38,41]. In humans, a specific CD146+ subtype of MSC showed similar characteristics to Nestin-GFP positive cells. Direct implication of these cells has been confirmed by mutant comparison expressing either soluble Scf or the membrane bound Scf. Depletion of HSC was only observed in the deletion of membrane bound Scf but not in the soluble Scf deletion [42]. This indicates the direct cell to cell contact requirement for the establishment of the HSC niche with Scf. Finally, other cell types like nerve cells, non-myelated Schwann cells, megakaryocytes and osteoclasts have been shown to influence and

regulate the HSC niche but rather in an indirect or less significant fashion by stimulating endothelial and stromal cells (i.e. CXCL12, Scf), modifying the micro-environment (calcium release by osteoclasts activity).

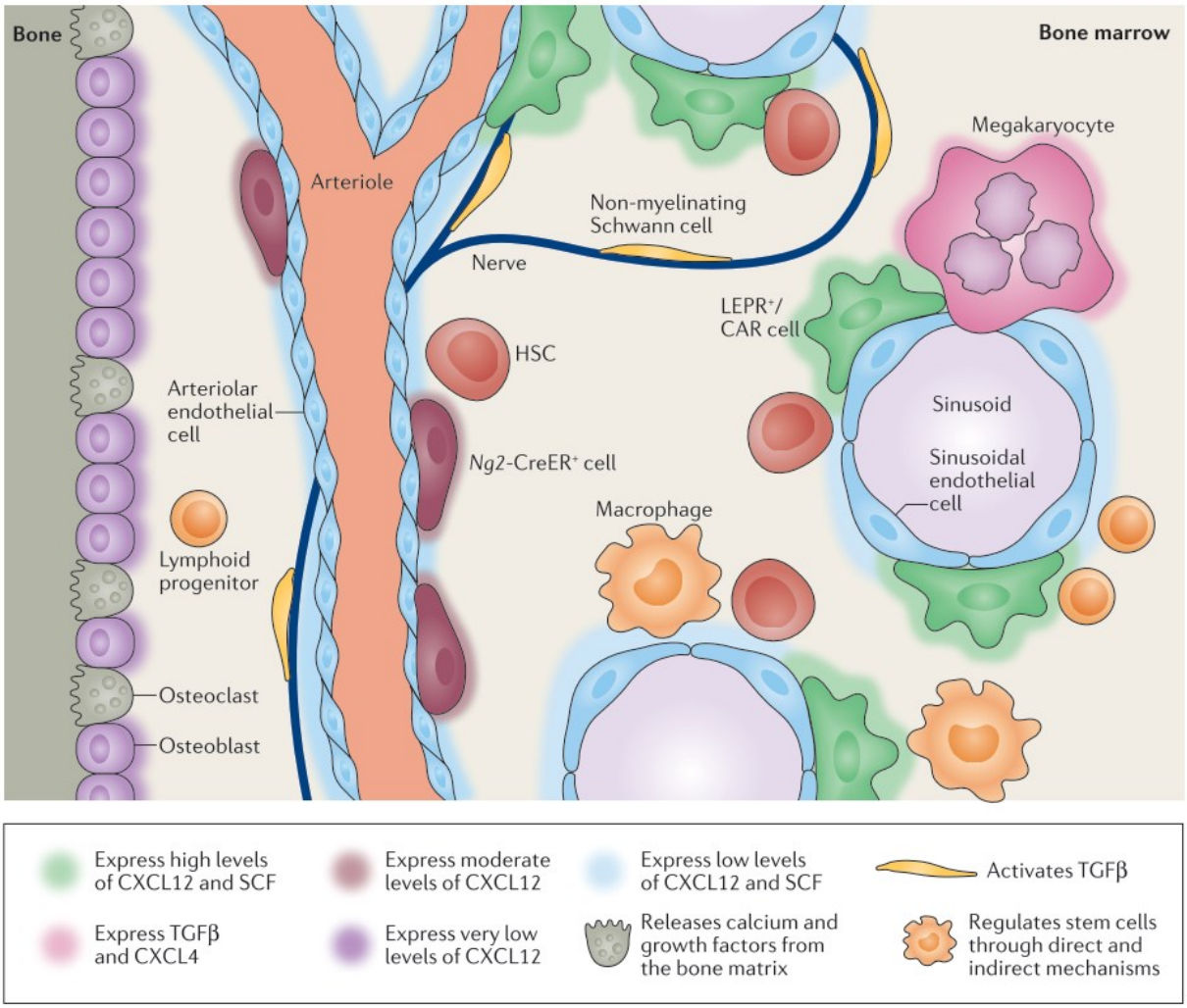

Figure 3: Overview of the current hematopoietic stem cell niche model with its different actors and Scf and CXCL12 secretion profiles. (Crane et al. 2017)

Despite the recent advances, much remains to be elucidated especially on specific roles of cells and growth factors on the HSC regulation, the role of stress on the HSC niche and other potential factors especially some possible long distance paracrine factors [38].

C. SDF1α (CXCL12)

CXCL12 is an important factor participating to the HSC niche. It was first characterized as a growth-stimulating factor for B cell precursor [43] and for the role of its receptor CXCR4 in HIV infection [44]. Since then the CXCL12 factor has been extensively described. It has an important role in B and lymphoid progenitors maintenance and proliferation [45,46]. More recent studies uncovered the major participation of CXCL12 in HSC quiescence, homing, maintenance and retention [47]. Many cells within

the bone marrow express CXCL12 at different levels and therefore have different levels of implication in the HSC niche. CXCL12 abundant reticular (CAR) cells, leptin receptor-expressing cells (LEPR+ cells) express the highest levels of CXCL12 and are mostly located in the perivascular and sinusoidal region. Other cells secreting CXCL12 are endothelial cells, Nestin-GFP cells and osteoblasts (Fig. 3).

D. Mouse vs Human

Since the discovery of HSCs by Till and McCulloch, most studies were conducted on the mouse hematopoietic system [48]. However, and despite being relatively close in the phylogenetic tree, mice and humans remain different species with some major differences (Fig. 4). Usually mice used for research studies are rather homogenous in population as compared to the diversity encountered in human population [25]. Therefore, studies carried out in the mice may not accurately reflect all the eventualities that may occur in humans. Mice are small animals exposed to different ecological cues and with a short lifespan and a precocious reproductive maturity. All these aspects influence their exposure to tumors, stress, telomerase activity and growth factors expression. Most of these parameters have a significant impact on hematopoiesis and therefore despite similarities, a direct correlation between the mouse and human biology cannot be established. It is also necessary to develop models closer to the actual human hematopoiesis.

First studies on human HSCs were conducted in vitro following the colony forming unit (CFU) paradigm previously validated with mice HSCs [49,50]. The evolution towards the in vivo engraftment in mice of human HSC was the logical next step. In 1988, several studies showed the first engraftment of human T and B blood cells in mice due to the generation of the severe combined immunodeficiency mice (Scid) [51–53]. Transplantation of differentiated cells however could not lead to long term engraftment. Further studies used the co-injection of human bone marrow cells and human growth factors in order to prolong the lifespan of human blood cells [54]. The persistence of the innate immune system did not allow a high and long-term engraftment of human HSC. Further mice models with more severe immunodeficiency were then generated in order to progressively shut-down the immune response establishing the non-obese diabetic (NOD), Scid, IL-2R common ɣ chain deletion ($gc^{-/-}$) (NSG). The final step towards better and longer engraftment was the generation of mice constitutively expressing human specific hematopoietic growth factors [25].

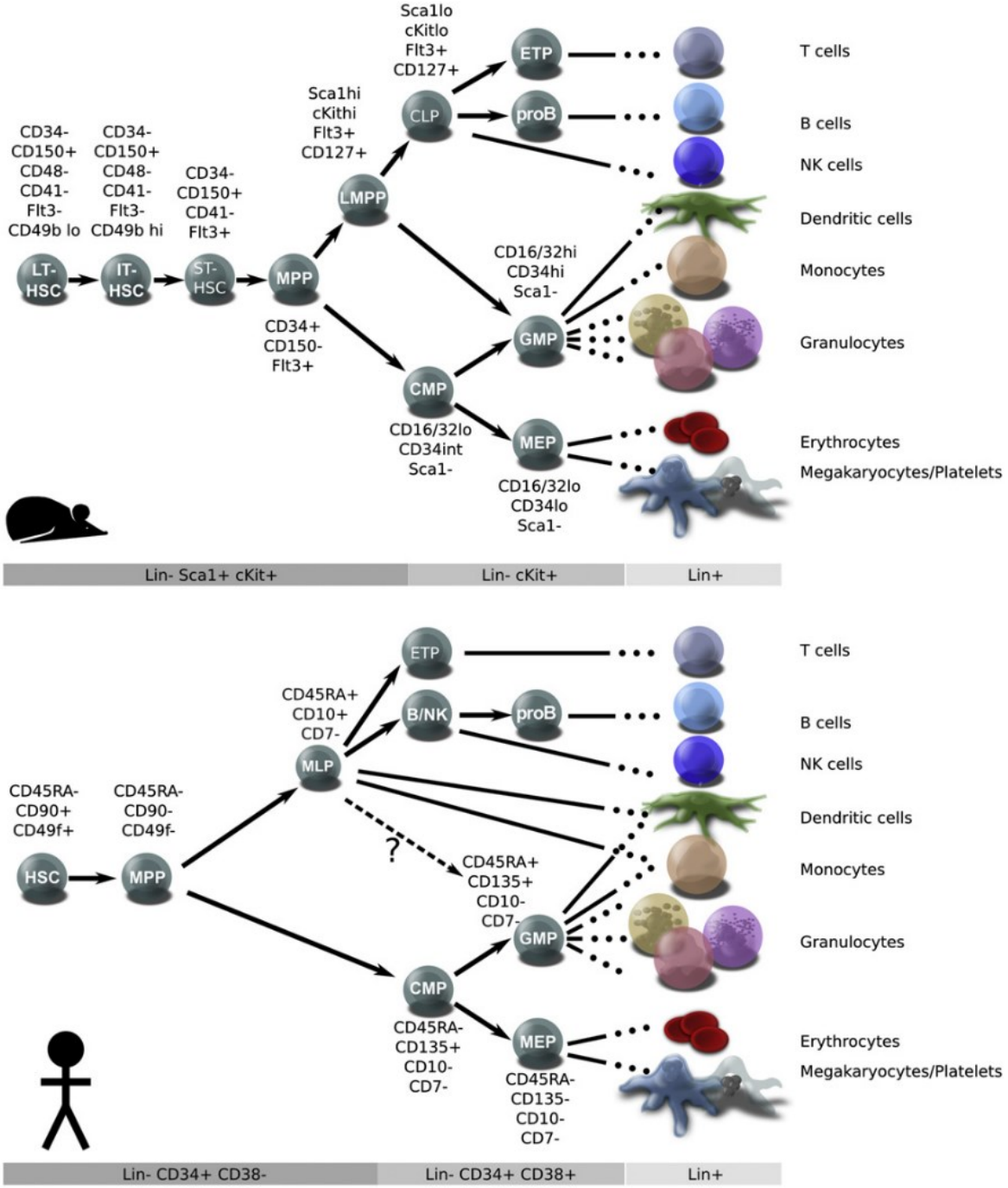

Figure 4: Current understanding of the mouse and human hematopoietic lineages. Despite some similarities, some major differences in the hematopoietic lineages and markers call for the development of humanized models. (Doulatov et al. 2012)

These mice models allowed to underline similarities and differences between the human and mouse hematopoiesis. Among the similarities are some signaling pathways like bmi1 and Notch as well as surprisingly the number of division per lifespan of HSCs [25]. Major differences could be found in the HobB4 pathway and in the DNA damage response with in the latter case a different response undertaken. While mouse HSCs tend to favor repair DNA repair and mutations accumulation, human HSCs favor an apoptotic approach. A possible explanation could be the difference in lifespan and

reproductive maturity between the two species [25]. These similarities and differences underline the need for a more thorough analysis of the human HSC niche, homing, engraftment and molecular pathways. In particular, the humanized mice models despite expressing some human cytokines do not reflect possible human HSC niche. There is a need for the establishment of a human stroma supporting human hematopoiesis model [55,56].

III. Bone fracture healing

A. Physiological fracture healing

Physiological fracture healing is a natural and efficient process regenerating broken bone without leaving any scar tissue. Most fracture heals through a developmental process resembling the endochondral bone formation (Fig. 5). It can be divided into four steps with an inflammation phase, soft callus formation phase, hard callus formation phase and remodeling phase [57].

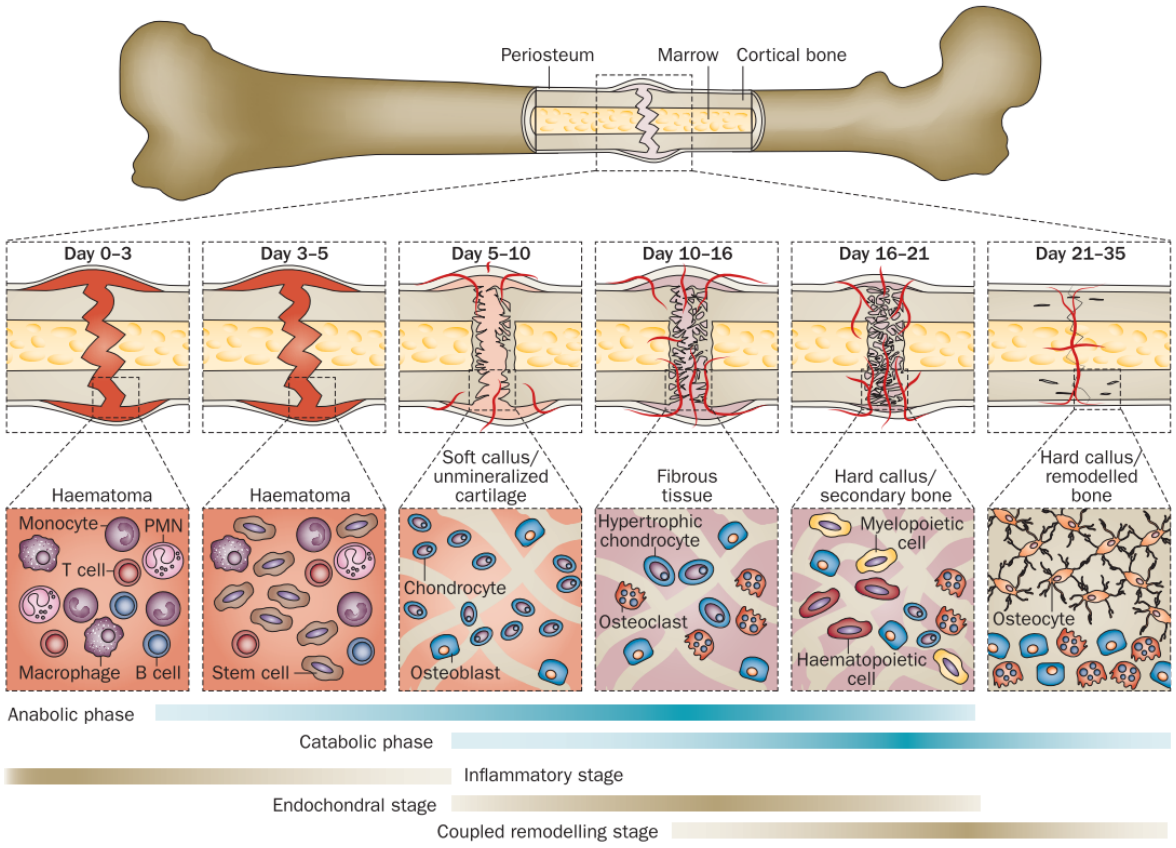

Figure 5: Physiological fracture healing in the mouse. (Einhorn, Gerstenfeld 2015)

Upon injury, the hematoma will lead to the aggregation of many inflammatory cells such as macrophages, monocytes and other phagocyting cells. They will secrete important quantities of cytokines and growth factors such as interleukins (IL-1 and IL-6, vascular endothelial growth factor

(VEGF), transforming growth factors-β (TGF-β), bone morphogenetic proteins (BMPs)… Secretion of these factors will lead to the recruitment of surrounding MSCs from the periosteum, and the bone marrow [58]. MSCs will differentiate into chondrocytes and recapitulate the endochondral pathway. Chondrocytes and fibroblasts will generate a soft tissue called soft callus. Gradually, the fibrous tissue will be replaced by expanding chondrocytes before undergoing hypertrophy and mineralization leading to the hard callus generation phase. Osteoblast from either exogenous location or transdifferentiated from hypertrophic chondrocytes lay down an intermediate extracellular matrix stably bridging the two broken pieces. This process happens simultaneously with an important vascularization process enhancing the remodeling of the hard callus [59]. Final remodeling involves the formation of lamellar and trabecular bone structures restoring the complete bone organ structure and function. This is carried out by osteoblast orchestrating the osteoclasts activity [57,60].

B. Current clinical treatments and limitations

Due to their actual structural role, bones are prone to damage and fractures but in most cases, can regenerate in a quick and efficient way without the need of any exogenous assistance other than immobilization. Moreover, newly regenerated bones do not show any sign of scar tissue and the border with the native bone can hardly if at all be noticed. However, for some clinical and pathological cases such as bone non-union, craniofacial reconstruction, bone tumor removal and hip implantation, there is a critical need for exogenous therapies to prime and enhance bone healing. Bone repair can be induced either by osteogenesis (e.g. autograft) where bone is generated by the transplanted tissue, by osteoconduction which is the passive process of bone formation from an already existing bone structure or by osteoinduction where cues induce a tissue to actively differentiate into bone [61]. The current clinical gold standard is autologous bone graft where bone from the patient is typically taken from the hip and re-allocated to the site of injury. While being quite efficient, it has several drawbacks such as creating a second site of injury, having a limited amount of material and cannot be used in some feeble patients and increasing the risks of infection. Therefore, there has been a critical need for exogenous therapies. Processed allo- and xenografts as well as synthetic bone substitutes such hydroxyapatite (one of the major bone component) or ceramics are typically used as a material for bone regeneration. However, these materials are inefficient in generating efficient osteoconduction and are often used in combination with osteoactive agents such as bone morphogenetic proteins (BMPs). The problem comes from the fact that important doses of BMPs are required. BMPs being an extremely potent growth factors, a careless and imprecise dosage as well as uncontrolled released in vivo can lead to dramatic effects like tumor formation or ectopic bone growth [61,62]. A most recent and promising approach consist in the use of stem and stromal cells either to generate tissue after

seeding on scaffolds [63]. This new area of research and development is called tissue engineering and will be developed in a subsequent chapter.

C. Cell source

Tissue engineering for bone regeneration requires a reliable cell source capable to efficiently differentiate into either chondrocytes (endochondral ossification) or osteoblasts (intramembranous ossification). To be used in clinical settings, some properties are recommended such as availability in term of access and quantities, robust and reproducible differentiation, low immunogenic response, safety post transplantation [64,65]. In this regard, several cell sources have been identified with different potential and attributes [66].

MSCs are the most studied and evident cells for bone regeneration as they have been among the first to be described for their potential to generate bone [67–69]. Cells designated as MSCs are present in many tissues and refer to heterogenous populations. They are defined as plastic adherent cells without hematopoietic marker and harboring CD44, CD73, CD90, CD105 and CD146. Additionally, these cells can differentiate into chondrocytes, osteocytes and adipocytes. MSCs can be harvested from many different tissues but predominantly from BM, adipose tissue, umbilical cord blood or periosteum for bone regeneration purposes. So far, there are no reliable and specific marker identifying MSCs. This impairs the research in the MSC field as MSC from various tissues or isolated using different methods (FACS sorting or plastic adhesion) harbor different potency regarding their proliferation and differentiation capacities. For bone regeneration, two sources of MSCs are mainly used, namely BM-MSCs and adipose derived mesenchymal stem cells (ASCs) [66,70–73]. BM-MSCs are the most potent for osteoblasts and chondrocytes differentiation leading to the two ossification pathways, namely intramembranous and endochondral ossification. ASCs are on the other hand much easier to harvest from patient in term of surgery procedure and available quantities. They also possess a potential for vascularization making them of great interest for bone grafts as a main factor for graft failure is the absence or delayed vascularization of the newly implanted graft.

D. 3D tissue engineering

Conventional cell culture relies on 2D systems to expand and differentiate cells towards a specific phenotype. It can result in the formation of ECM and tissues. However, their physiology and applications to clinical trials remains limited due to their size and lack of complexity. To better develop tissue engineering, the use of 3D scaffolds has become very attractive. The scaffolds must possess several characteristics to be used for clinical translation (Fig. 6). Ideally, scaffolds should allow or promote cell attachment, proliferation and viability, be resorbable to leave space to the newly formed and remodeled tissue, have a low or inexistent immunogenic response, be load bearing, and finally possess some osteoinductive properties [74,75]. There is a wide variety of scaffolds available for bone tissue engineering. They can be classified in four categories (i) ceramic scaffolds, (ii) synthetic polymers, (iii) natural polymers, (iv) acellular tissue.

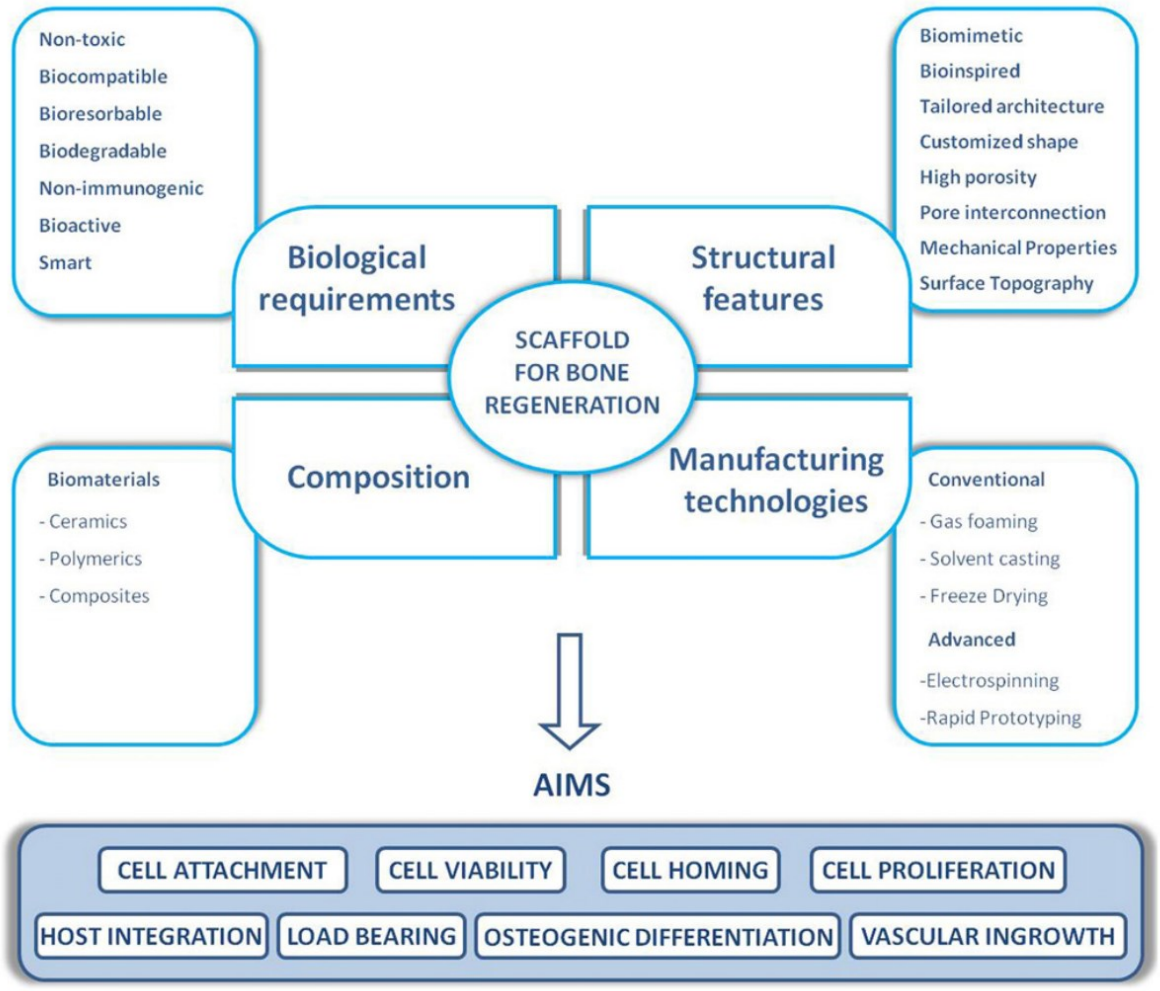

Figure 6: Criteria and features entering in the choice of a scaffold for bone regeneration using 3D tissue engineering. (Roseti et al. 2017)

Each scaffolding materials has a set of pros and cons making them suitable for different applications. Ceramic scaffolds are usually quite stiff and are the closest to the bone chemical composition. It naturally makes them a good candidate for bone tissue engineering. They however are difficult to shape to the defect size, resorb and remodel following in vivo implantation. Synthetic polymers have a great modularity but some concerns remain regarding their bioactivity and degradation products. Natural polymers are mainly composed of collagens and proteoglycans. They have the advantage of being bioactive and easily resorbable leading to the absence of residual scaffolding material following in vivo remodeling. The major drawback is their lack of load bearing properties. Finally, devitalized tissues either from cadavers or from tissue engineering can be used as a scaffolding material. They provide a very suitable ECM bioactive composition but are difficult to produce in large amounts and can be difficult to shape to the defect.

Scaffolds allow the generation of a 3D shape tissue with a larger size and complexity. However in vitro culture of large tissues does not provide a homogenous access to oxygen and nutrients throughout the tissue. In facts, 3D static culture generates tissues with non-homogenous cell seeding and therefore tissue formation coupled to a necrotic core at the center, with viable cells and tissues present only on the peripheral tissue located a few hundred microns from the culture medium. To circumvent this issue, perfusion bioreactors have been developed to allow a better repartition and diffusion of cells, oxygen and nutrients throughout the tissue leading to improved cell survival and tissue quality [76,77]. Also, 3D perfusion bioreactor provides a flow and a shear stress to the tissue thus better mimicking in vivo environment. Advanced 3D perfusion bioreactor can control culture parameters such as temperature, oxygen and pH allowing a tight regulation of the culture conditions. Finally, they allow to envision Good Manufacturing Practices (GMP) and streamlined processes towards the generation of clinically compatible grafts.

E. Devitalization Techniques

Bone repair requires the simultaneous action of a variety of factors initiated by inflammation in the standard healing process. The major problem of all the scaffolds mentioned above is that they do not possess any or very little osteoconductive or oestoinductive potential as they are lacking growth factors by themselves. They need to be combined to synthetic growth factors cross linked to the scaffold or not or used in combination with cells, generally MSCs, providing essentials factors for bone regeneration. These cells are commonly driven to either the osteo lineage or the chondrolineage to recapitulate either intramembranous or endochondral ossification. Growth factors by themselves or a combination of growth factors has a real potential for bone regeneration as they can be easily synthesized and added to any suitable scaffold. There is very limited risk of contamination, the process can be easily validated towards a GMP procedure and the efficiency remains high. Major concerns

however are related to the proper dosage. Indeed, BMP2 growth factor has been shown to induce ectopic bone formation and tumorigenesis when used in inadequate amounts. The number of growth factors bound to the scaffold as well as their kinetic release is also hard to control.

Cell seeded scaffold are coated with physiological doses and combination of growth factors making them ideal candidate for bone regeneration, yet it is inconceivable to implant allografts. The use of engineered tissues for bone regeneration therefore requires their devitalization. The different techniques used for tissue devitalization are (i) chemical agents (ii) biological agents (iii) physical agents [78–80]. Chemical agents are detergents, acid and basic solutions, hypo and hypertonic solutions, alcohols and other solvents. Biological agents comprise enzymatic (i.e. collagenase, trypsin, dispases…) and non-enzymatic agents such as ethylenediaminetetraacetic acid (EDTA). Physical agents are mostly temperature or pressure based by repetition of cycles of freezing and thawing. These techniques are either used alone or in combination to achieve efficient devitalization. All these techniques have an important effect on the ECM with major deterioration either to the ECM structure or proteins therefore reducing their potential following in vivo implantation.

IV. Aims of the thesis

In the past years, the possibility to recapitulate the developmental biology paradigm of endochondral ossification from human cells has been developed by several labs including ours. The recapitulation of endochondral ossification involves an in vitro phase with the generation of a hypertrophic cartilage tissue which upon in vivo implantation will be remodeled into a complete bone organ made of donor and host cells. This technological achievement paves the way for new perspectives both in translational and fundamental research. Generating human in vitro tissue graft for clinical bone regeneration applications is attractive but an efficient and protective decellularization method is required as well as an automated and upscaled production of the tissue graft. Moreover, the chimeric humanized bone organ generated ectopically contains human cells associated to the vasculature region corresponding to the localization of putative human HSC niches [38]. My thesis proposes to harness the endochondral ossification paradigm for either bone regeneration purposes by using in vitro generated devitalized hypertrophic cartilage ECM properties or the study of the human HSC niche compartment by the mean of in vivo subcutaneous humanized ossicles generation combined with human cord blood derived CD34+ cells.

The first chapter shows how preservation of the cartilaginous ECM is critical for bone formation. Primary human MSCs are engineered with an inducible apoptotic cassette using retroviral transduction. Following an in vitro differentiation towards hypertrophic cartilage, the cells within the

generated tissue are induced towards apoptosis. The resulting devitalized ECM has preserved growth factors content triggering bone remodeling by osteoinduction.

In the second chapter, devitalized hypertrophic cartilage is generated in a perfusion bioreactor and used to prime bone regeneration using an in vivo upscaled rabbit orthotopic model to move on closer to a potential clinical trial. To achieve this, the same techniques developed in the chapter one are used but within an upscaled perfusion bioreactor to achieve better tissue homogeneity and envisioning standardized streamlined process. Devitalized ECM shows superiority in de novo bone formation compared to current commercially available clinical gold standard for maxillofacial reconstruction.

The third chapter relates to the validation of the humanized ossicles [22] for human HSC long term engraftment. In this chapter, hypertrophic templates are implanted in humanized mice and following remodeling into bone, mice are sub-lethally irradiated and transplanted with human cord blood derived CD34+ cells. Engraftment, HSC functionality and cell cycle are tested in the ossicle in comparison to the native bone of the mice. Engraftment, colony forming unit assay, secondary transplant and cell cycle analysis show potential superiority of the ossicles in human HSC quiescence and functionality within the humanized ossicles.

To follow up on the validation of humanized ossicles for human HSC engraftment, the fourth chapter describes how the human MSC and therefore the ossicles can be genetically engineered to directly influence the human HSC niche interactions and composition. human MSC are engineered with a fluorescent reporter as well as the CXCL12 protein involved in HSC homing and homeostasis. Successful human HSC engineering led to the determination of the cell fate from the implanted tissue cells as well as functional engineering on the human HSC niche with modulation of the engraftment levels of human HSC within the engineered ossicles as opposed to the native ossicles.

Chapter II

Osteoinductivity of engineered cartilaginous templates devitalized by inducible apoptosis

Manuscript published in PNAS in 2014

Osteoinductivity of engineered cartilaginous templates devitalized by inducible apoptosis

Paul E. Bourgine[a,b], Celeste Scotti[a,b,c], Sebastien Pigeot[a,b], Laurent A. Tchang[a,b], Atanas Todorov[a,b], and Ivan Martin[a,b,1]

[a]Department of Surgery and [b]Department of Biomedicine, University Hospital Basel, University of Basel, 4031 Basel, Switzerland; and [c]IRCCS Istituto Ortopedico Galeazzi, via R. Galeazzi 4, 20161 Milano, Italy

Edited by Robert Langer, Massachusetts Institute of Technology, Cambridge, MA, and approved October 30, 2014 (received for review July 1, 2014)

The role of cell-free extracellular matrix (ECM) in triggering tissue and organ regeneration has gained increased recognition, yet current approaches are predominantly based on the use of ECM from fully developed native tissues at nonhomologous sites. We describe a strategy to generate customized ECM, designed to activate endogenous regenerative programs by recapitulating tissue-specific developmental processes. The paradigm was exemplified in the context of the skeletal system by testing the osteoinductive capacity of engineered and devitalized hypertrophic cartilage, which is the primordial template for the development of most bones. ECM was engineered by inducing chondrogenesis of human mesenchymal stromal cells and devitalized by the implementation of a death-inducible genetic device, leading to cell apoptosis on activation and matrix protein preservation. The resulting hypertrophic cartilage ECM, tested in a stringent ectopic implantation model, efficiently remodeled to form de novo bone tissue of host origin, including mature vasculature and a hematopoietic compartment. Importantly, cartilage ECM could not generate frank bone tissue if devitalized by standard "freeze & thaw" (F&T) cycles, associated with a significant loss of glycosaminoglycans, mineral content, and ECM-bound cytokines critically involved in inflammatory, vascularization, and remodeling processes. These results support the utility of engineered ECM-based devices as off-the-shelf regenerative niches capable of recruiting and instructing resident cells toward the formation of a specific tissue.

developmental engineering | endochondral | osteoinductive | extracellular matrix | hematopoisesis

The clinical gold standard solution to critical bone defects consists of autologous bone transplantation. However, it is associated with severe donor site morbidity, risks for infection, and limited availability of the material (1, 2). Off-the-shelf synthetic or naturally derived bone substitute materials (e.g., ceramics, collagen) allow bypassing of these issues (3) but have reduced regenerative potency, especially in challenging scenarios (e.g., atrophic nonunions, comminuted fractures, large substance loss, compromised environment). Cell-based approaches could introduce a superior biological functionality, but their clinical use remains rather limited (4), predominantly because of their nonpredictable effectiveness combined with their economic, logistic, and interpatient variability issues (5, 6).

Modern approaches to bone tissue engineering aim at triggering regenerative processes by matching the corresponding developmental program and thus recapitulating the embryonic stages of bone tissue development (7). During embryonic development, long bones typically develop by endochondral ossification, a process involving the formation and subsequent remodeling of a hypertrophic cartilage template (8). Following the principles of "developmental engineering," the process of endochondral ossification has been successfully reproduced using embryonic stem cells (9) and human mesenchymal stromal cells (hMSCs) (10–12). A further step was achieved with the upscaling of the graft size, leading not only to the successful formation of large bone tissue but also to the development of a mature organ that includes a fully mature hematopoietic compartment (13).

The increased recognition of the potency of the extracellular matrix (ECM)-derived materials in regenerative processes (14) led us to investigate whether a living cell compartment is strictly required or whether the endochondral route could be initiated by a cell-free ECM, represented by a devitalized hypertrophic template. Addressing this question may lead to a better understanding of the elements regulating the endochondral ossification process and to the generation of cell-based but cell-free off-the-shelf materials capable of instructing host osteoprogenitors toward bone formation. A devitalized approach to endochondral ossification has been envisioned from the beginning of the research in this field (9, 10), as it would bypass the complexity of delivering living cells of possibly autologous origin, but it has never been realized to date.

Existing studies converge on the importance of preserving ECM integrity to elicit the desired regenerative effect (15–17). This implies the use of a devitalization strategy reducing alterations in the composition and architecture of the generated template to mimic both the physiologic regenerative milieu and the 3D structure of the fracture callus. Toward this objective, a devitalization approach has been proposed via the induction of apoptosis (18). In particular, an inducible genetic system (19) can be incorporated into primary hMSCs to specifically induce their apoptosis on exposure to a clinical-grade chemical compound. This strategy offers the possibility to generate hypertrophic cartilage templates that can be subsequently devitalized with, theoretically, minimal changes in the ECM.

Significance

It has been previously reported that hypertrophic cartilage tissues engineered from human mesenchymal stromal cells can efficiently remodel in vivo into bone organs, recapitulating developmental steps of endochondral ossification. We have here demonstrated that the extracellular matrix (ECM) of such engineered cartilage, even in the absence of a living cell component, retains frankly osteoinductive properties. The use of an apoptosis-driven devitalization technique revealed the importance of preserving the ECM integrity and, in particular, the embedded factors to trigger the regenerative process. Although exemplified in a skeletal context, our work outlines the general paradigm of cell-based but cell-free off-the-shelf materials capable of activating endogenous cells toward the formation of specific tissues.

Author contributions: P.E.B., C.S., and I.M. designed research; P.E.B., C.S., S.P., L.A.T., and A.T. performed research; P.E.B. contributed new reagents/analytic tools; P.E.B., C.S., S.P., and A.T. analyzed data; and P.E.B. and I.M. wrote the paper.

The authors declare no conflict of interest.

This article is a PNAS Direct Submission.

[1]To whom correspondence should be addressed. Email: ivan.martin@usb.ch.

This article contains supporting information online at www.pnas.org/lookup/suppl/doi:10.1073/pnas.1411975111/-/DCSupplemental.

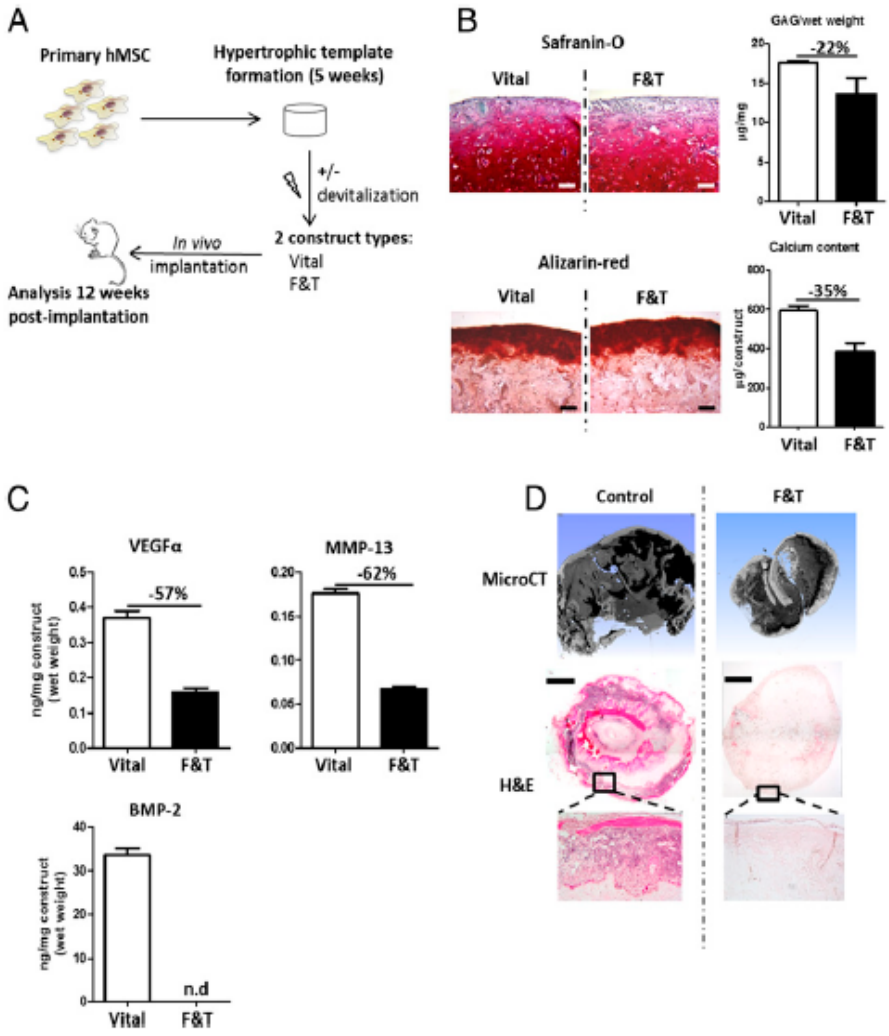

Fig. 1. Assessment of the osteoinductive properties of living (*Vital*) and F&T (*F&T*) devitalized engineered hypertrophic cartilage constructs. (*A*) Experimental scheme for the generation of hypertrophic tissues starting from hMSCs, devitalized and subsequently implanted in nude mice. (*B*) Representative sections of in vitro (5 wk) generated hypertrophic cartilage samples and the effect of the F&T treatment on the GAGs and calcium content ($n = 3$). (Scale bars, 100 µm.) (*C*) Effect of the F&T devitalization on the content of VEGF-α, BMP-2, and MMP-13 protein. (*D*) 3D reconstruction of microtomographic images (MicroCT) and hematoxylin and eosin (H&E) stained representative sections of samples retrieved 12 wk after ectopic implantation in nude mice ($n = 3$). (Scale bars, 1 mm.) Error bars represent SEMs of $n = 3$ measurements.

In this study, we aimed to induce de novo bone organ formation, using cell-free hypertrophic cartilage templates devitalized by apoptotic induction. We hypothesized that the preservation of the ECM integrity, serving as a reservoir of multiple growth factors at physiological levels, is a key prerequisite to recruiting and instructing endogenous progenitors to initiate bone regeneration.

Results

Assessment of the Osteoinductive Properties of Freeze & Thaw Devitalized Constructs. As a first attempt, we tested whether hypertrophic cartilage templates, engineered according to a previously established protocol (13) and devitalized by standard "freeze & thaw" (F&T) treatment, are capable of inducing bone formation (Fig. 1*A*). F&T is a well-established physical devitalization method efficiently leading to cell bursting and limited ECM alteration (20, 21). Primary hMSCs were then seeded at high density on cylindrical collagen meshes (8 mm diameter, 4 mm thickness) and cultured for 3 wk in chondrogenic medium, followed by 2 wk of hypertrophic medium. The resulting grafts successfully displayed the typical pattern of a hypertrophic cartilaginous tissue, consisting of a glycosaminoglycan (GAG)-rich core surrounded by a mineralized ring (*Vital*; Fig. 1*B*). Some constructs were subsequently devitalized, using a recognized method consisting of three F&T cycles followed by a bath in hypertonic solution (*F&T*) (22), leading to the absence of human living cells after implantation (Fig. S1*A*). The *F&T* constructs were still positively stained for GAG and mineral deposits, but quantitative assessments indicated a marked reduction in the wet weight percentage of GAG (−22%) and mineral content (−35%) (Fig. 1*B*). The F&T treatment also reduced the amount of growth factors that are known to play a critical role in hypertrophic cartilage remodeling into bone, including VEGFα (−57%), matrix metalloproteinase 13 (MMP-13; −62%), and bone morphogenetic protein 2 (BMP-2; below detection level; Fig. 1*C*).

On ectopic implantation in nude mice for 12 wk, *Vital* samples were macroscopically colonized by blood cells, in contrast to *F&T* tissues (Fig. S1*B*). *Vital* samples were extensively remodeled, resulting in interconnected mineralized bone trabeculae embedding bone marrow elements (Fig. 1*D*), with minimal cartilage residuals (Fig. S1*B*). In contrast, the retrieved *F&T* samples maintained an outer shell of calcified matrix and abundant remnants of devitalized cartilage, with no evidences of bone or bone marrow formation (Fig. 1*D* and Fig. S1*B*). The failure of *F&T* devitalized hypertrophic constructs to remodel and induce bone formation could be attributed to the absence of living cells within the implanted graft and/or the effect of the devitalization process, leading to a loss of osteoinductive (e.g., BMP-2), angiogenic (e.g., VEGFα), and remodeling (e.g., MMP-13) factors.

Generation of Hypertrophic Constructs Using Death-Inducible hMSCs. To assess whether a better-preserved devitalized hypertrophic ECM can induce endochondral bone formation, we introduced the strategy of devitalization by apoptosis induction (Fig. S2), which was previously proposed to target the living cell fraction with minimal changes in the ECM components (18). Primary hMSCs were thus retrovirally transduced with a death system based on the inducible dimerization of modified caspase 9 (iDS; Fig. S2*A*). To ensure the maximum cell death on induction, the

population was purified on the basis of the expression of the CD19 reporter surface marker (Fig. 2*A*). This allowed for the generation of hMSC-iDS capable of being efficiently induced toward apoptosis in 2D culture (>97%; Fig. 2*B*) by adding the soluble inducer in the culture media. hMSC-iDS could generate hypertrophic cartilage tissues similar to the untransduced cells, as assessed by histological stainings (Fig. 2*C*) and gene expression analysis showing successful induction of chondrogenic and hypertrophic genes (Fig. 2*D*). Hence, the gain of the inducible-apoptosis function did not impair the chondrogenic differentiation and subsequent hypertrophy of hMSC-iDS. Importantly, hMSC-iDS hypertrophic templates continued to express the iDS, as revealed by CD19 immunostaining (Fig. 2*C*), suggesting the possibility of devitalizing the engineered graft by activation of the system.

Devitalization by Apoptosis Induction of Hypertrophic Cartilaginous Templates. Treatment of hypertrophic constructs by *F&T* or apoptosis induction (*Apoptized*) allowed for an effective devitalization, leading to, respectively, 91% and 93% cell killing efficiency, as assessed by flow cytometry measurement of propidium iodide (PI) and annexin V staining (Fig. 3*A*). Conversely, most of the cells from the *Vital* group remained viable (16% of annexin V/PI positivity; Fig. 3*A*). Because the assay measures the apoptosis-driven extracellular translocation of annexin V, the measured cell death is not biased by the reported natural expression of annexin V by chondrocytes (23); in particular, during their mineralization phase (24). Histologic analyses indicated the successful activation of the apoptotic pathway, with clear morphologic evidence of cell and nuclear fragmentation (late stage of apoptosis) throughout *Apoptized* and *F&T* constructs, further confirmed by the presence of cleaved caspase 3 in nucleated cells (Fig. 3*B*). In the *Vital* group, apoptotic cells were mainly found within the hypertrophic outer ring. Luminex-based analysis showed, in *Apoptized* samples, the overall maintenance of factors involved in inflammation [monocyte chemoattractant protein-1 (MCP-1), macrophage colony-stimulating factor (M-CSF), IL-8], angiogenesis (VEGFα), and remodeling [MMP-13, osteoprotegerin (OPG)] processes, with levels similar to those of the *Vital* group. Instead, *F&T* treatment resulted in a severe impairment of ECM composition, with a significant loss in IL-8 (64.9%; $P < 0.0001$), MCP-1 (49.4%; $P = 0.0388$), OPG (37%; $P = 0.0015$), VEGFα (58.7%; $P < 0.0001$), and MMP-13 (32.1%; $P = 0.0307$) compared with the protein content in the *Vital* constructs. Thus, although the two devitalization methods led to a similar killing of the cells, the induction of apoptosis allowed for a better preservation of representative ECM components.

In Vivo Assessment of Hypertrophic Cartilaginous Templates. To assess whether a better-preserved acellular ECM is sufficient to induce vascularization and endochondral bone formation, *Apoptized*, *F&T*, and *Vital* templates were implanted ectopically in immunodeficient mice. On retrieval, samples displayed distinct morphologic patterns. Colonization by host blood cells was evident in *Vital* samples and, to a lower extent, in *Apoptized* ones, whereas *F&T* samples did not display macroscopic evidence of vascularization (Fig. 4*A*). Confocal microscopy confirmed these macroscopic observations, as *Vital* and *Apoptized* samples showed the presence of a mature vasculature characterized by CD31+ vessels stabilized by pericytic cells (NG2 staining; Fig. 4*B* and Fig. S3*A*). In contrast, *F&T* samples were marked by the absence of either cells or blood vessels within the constructs. Collectively, these data indicate the successful recruitment of the host vasculature by *Apoptized*, but not by *F&T* constructs, a prerequisite for the recapitulation of the endochondral ossification route.

Samples were further processed to investigate the presence of bone, cartilage, and bone marrow tissue. Remarkably, *Vital* and *Apoptized* samples, in strong contrast to *F&T* constructs, underwent

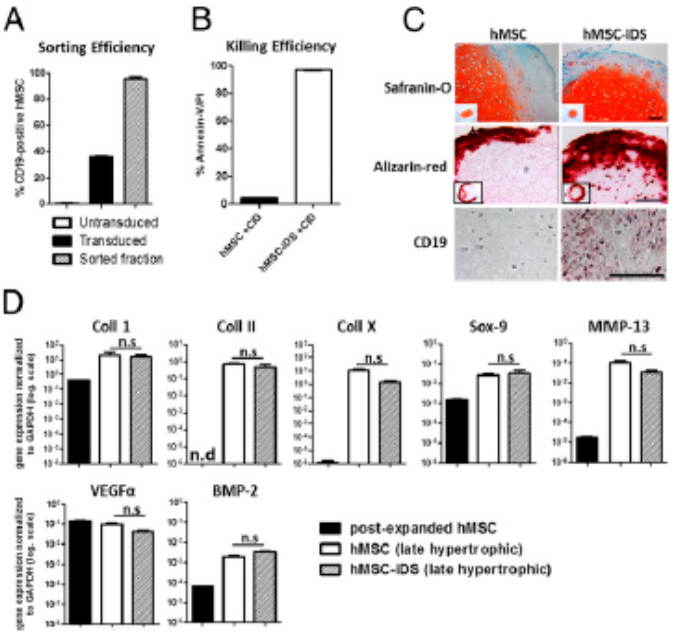

Fig. 2. Generation of hypertrophic constructs using death-inducible hMSCs. (*A*) Flow cytometry measurements of the CD19 (iDS reporter marker) expression by primary hMSC (Untransduced) after iDS retroviral transduction (Transduced) and subsequent enrichment using magnetic beads (Sorted fraction, hMSC-iDS) ($n = 5$). (*B*) Assessment of the efficiency of hMSC-iDS apoptosis induction in 2D culture on overnight exposure to the soluble inducer (+chemical inducer of dimerization) ($n = 4$). (*C*) Histologic sections of in vitro constructs (5 wk) generated by primary untransduced hMSCs and hMSC-iDS displayed a similar hypertrophic cartilage pattern (Safranin-O and Alizarin-red stainings). (Scale bars = 100 μm.) Only the hMSC-iDS expressed the iDS (CD19 immunostaining). (Scale bar = 50 μm.) (*D*) Gene expression analysis of hypertrophic templates generated by hMSCs and hMSC-iDS. Error bars represent SEMs of $n \geq 4$ measurements.

intense remodeling, giving rise after 12 wk to bone structures, including bone marrow spaces (Fig. 5*A*). Interestingly, although cortical external structures were observed in *Vital* and *Apoptized* groups, only *Vital* specimens displayed inner bone trabeculae (Fig. S3 *B* and *C*). The amount of mineralized tissue quantified after segmentation of micro-computerized tomography images was highest in the *Vital* specimens, followed by the *Apoptized* ones (Fig. S3*D*). However, as this technique does not allow discriminating between calcified cartilage and frank bone tissue, more specific quantification of the tissue types in the different groups was carried out, using histological sections. Histomorphometric analysis indicated in *Vital* samples the predominant formation of bone and bone marrow tissues (respectively, 24.9% and 32%), whereas cartilaginous regions were negligible (2%; Fig. 5*B*). *Apoptized* samples displayed a significantly higher bone (14.8%) and bone marrow formation (5.7%) than *F&T* samples (1.5% bone, 0.2% marrow). The latter, in turn, contained the highest percentage of cartilage remnants, confirming the limited efficiency of the remodeling process (Fig. 5*B*).

Ossicles of *Vital* and *Apoptized* constructs were characterized by the presence of osterix and tartrate-resistant-acid-phosphatase-expressing cells, respectively, representing osteoblastic and osteoclastic lineages (Fig. 5*C*). Those cells were predominantly lining the edges of the bone marrow regions, suggesting their involvement in tissue remodeling for marrow colonization. In *Vital* constructs, human cells participated in the bone formation, as assessed by the presence of cells positive for human Alu repeats among nucleated cells (Fig. 5*C*). In contrast, no human cells could be detected within *Apoptized* samples, so the formation of perichondral bone could only be attributed to host osteoprogenitors. *F&T* samples were also

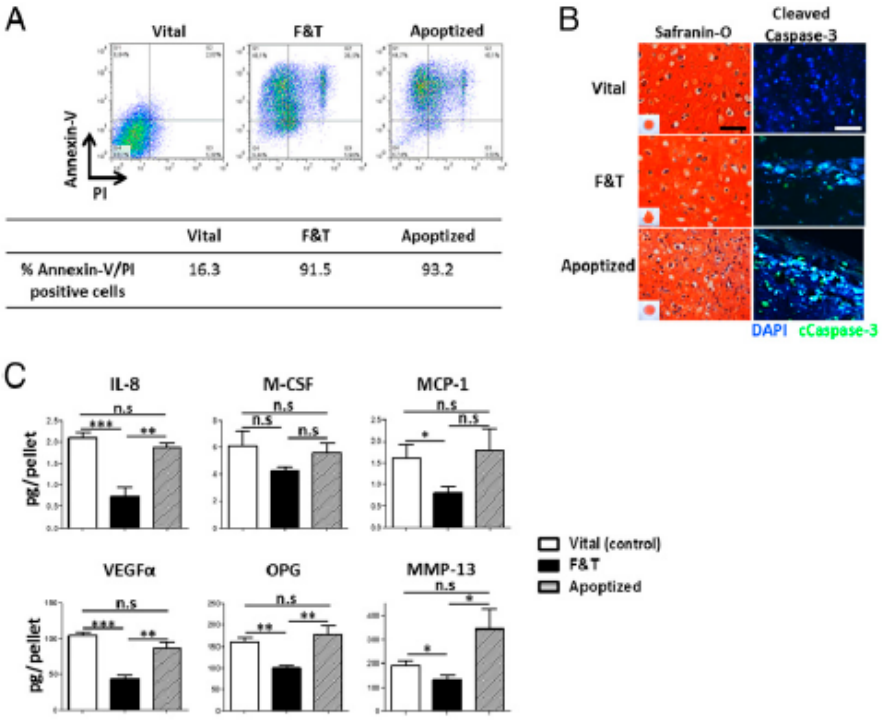

	Vital	F&T	Apoptized
% Annexin-V/PI positive cells	16.3	91.5	93.2

Fig. 3. Devitalization of hypertrophic cartilaginous templates. (*A*) Annexin V/PI flow cytometric analysis of cells retrieved from nondevitalized (*Vital*) or devitalized hypertrophic constructs, based on F&T cycles (F&T) or apoptosis induction (*Apoptized*). Both methods led to efficient tissue devitalization, with a killing efficiency superior to 90%. (*B*) Biochemical (Safranin-O) and immunofluorescence (Cleaved caspase-3) stainings of *Vital* and devitalized constructs. The devitalization processes efficiently induce cell death within the constructs. (Scale bars, 50 μm.) (*C*) Quantitative measurement of ECM proteins loss on devitalization of hypertrophic cartilage. Although the apoptotic method led to a minimal protein loss, the F&T treatment dramatically affected the ECM content. Error bars represent SEMs of $n = 6$ measurements. $^{*}P \leq 0.05$; $^{**}P \leq 0.005$; $^{***}P \leq 0.0005$.

marked by the absence of human cells, but with no evidence of frank bone structures or osteoblastic/osteoclastic cells (Fig. 5*C*).

Discussion

The present study demonstrates the hitherto unreported capacity of devitalized hypertrophic cartilage templates to induce de novo the formation of bone, including a mature vasculature and the presence of a bone marrow compartment, as well as the strict dependency of the regenerative process on the preservation of the ECM matrix and the growth factors and chemokines bound to it. In fact, the formation of heterotopic bone and bone marrow could be achieved only through the implementation of a devitalization strategy minimally affecting ECM integrity.

The deliberate activation of the apoptotic pathway allowed for the preservation of key embedded factors identified as being involved in inflammation (IL-8, MCP-1, M-CSF), vasculature recruitment (VEGFα), and bone remodeling processes (OPG, MMP-13). The initiation of the stage-specific cartilage template remodeling is known to require digestion of the engineered ECM through the identified factors, leading to the attraction of blood vessels via the release of entrapped VEGFα. The ingrowing blood vessels could subsequently deliver osteoblastic, osteoclastic, and hematopoietic precursors, completing cartilage resorption and directing formation of bone and associated stromal sinusoids, and in turn providing the microenvironment for hematopoiesis. Conversely, the use of the F&T as a "crude" devitalization technique led to the dramatic loss of those proteins, resulting in negligible vasculature, host cell recruitment, and tissue remodeling on implantation. These observations provide important information on the nature of the signals to be delivered to initiate endogenous formation of bone tissue and also warrant further investigation to identify the complete set of factors necessary and sufficient to instruct an efficient de novo formation of bone and bone marrow. In particular, our work highlights the paramount role played by the growth factors and chemokines embedded within the MSC-deposited ECM in triggering the tissue regeneration process. The potent biological role of the MSC secretome, appropriately bound to the ECM, is also in line with the recent view of MSCs as an "injury drugstore" and emphasizes the trophic effect of MSCs over their direct participation to the tissue formation (25).

In our study, the induced apoptosis of human hypertrophic chondrocytes is compliant with the physiological apoptosis of hypertrophic chondrocytes occurring during endochondral ossification. However, recent studies indicate that endochondral bone formation necessitates the presence of living hypertrophic chondrocytes, part of which directly contributes to the formation of trabecular structures (13) or the stromal niche for hematopoietic cells (26). As a consequence, despite the use of a cartilage intermediate, bone formation induced by devitalized ECM cannot be defined as being of canonical endochondral origin. Indeed, because the deposited bone tissue was predominantly

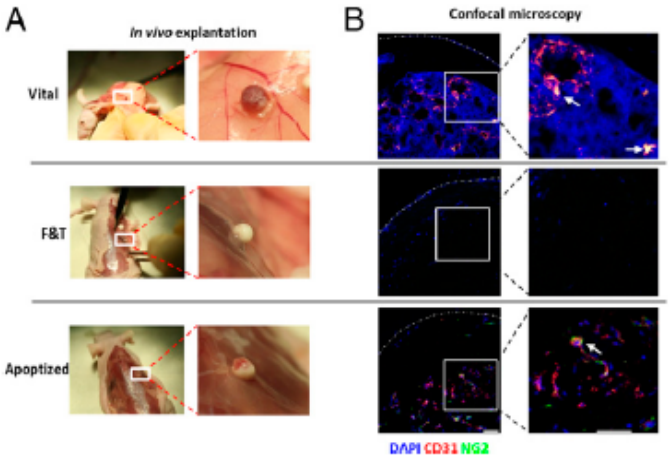

Fig. 4. Vascularization assessment of implanted hypertrophic cartilage tissues. (*A*) Macroscopic view of the samples at the time of explantation. *Vital* and *Apoptized* constructs displayed signs of blood cell colonization, in contrast to *F&T* samples. (*B*) Fluorescence microscopy of representative sections of explanted tissues. *Vital* and *Apoptized* constructs contained sinusoid-like vascular structures, positively stained for CD31 and stabilized by NG2+ pericytes. *F&T* devitalized constructs did not display evidences of vessel formation. (Scale bars, 50 μm.)

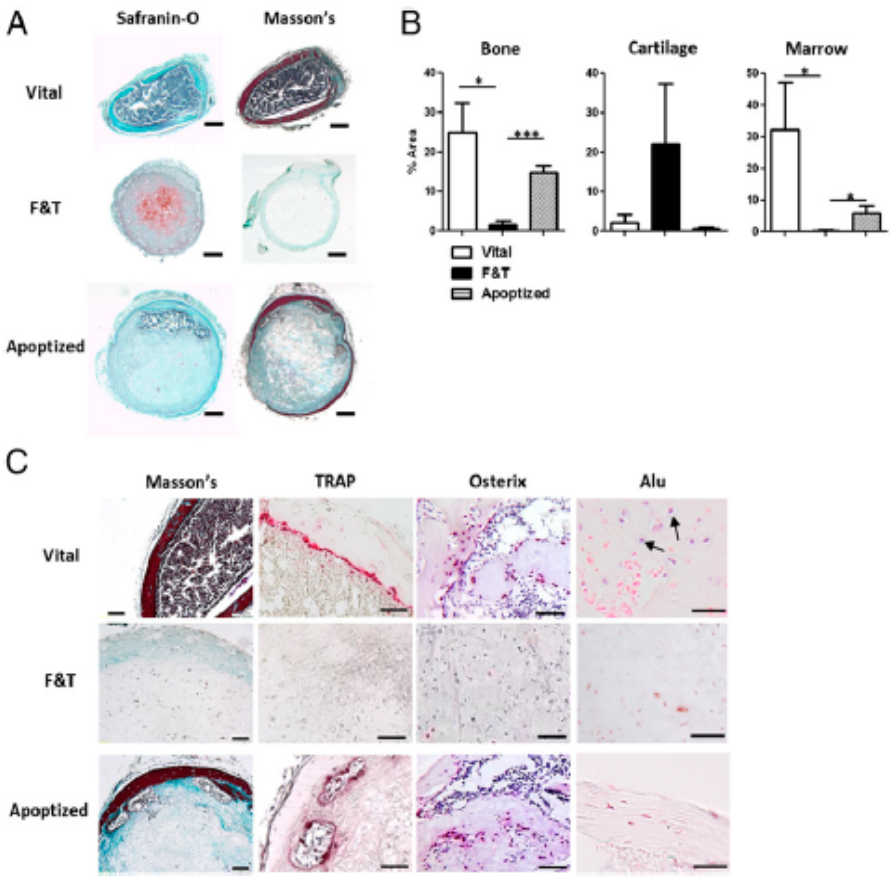

Fig. 5. Endochondral bone formation assessment of implanted hypertrophic cartilage tissues. (*A*) Safranin-O and Masson's Trichrome stainings of constructs retrieved 12 wk after implantation. *Vital* constructs underwent a full remodeling into bone, whereas *F&T* samples resembled an immature collagenous matrix with abundant cartilage remnants. *Apoptized* samples displayed evidence of perichondral bone formation, embedding a hematopoietic compartment. (Scale bars, 200 μm.) (*B*) Histologic quantification of bone, cartilage, and marrow tissue areas in sections of explanted living and devitalized constructs. (*C*) Masson's Trichrome, tartrate-resistant alkaline phosphatase, osterix, and Alu stainings were performed to, respectively, assess the presence of bone tissue, osteoclasts, osteoblasts, and human versus host cells. The presence of host-derived osteoclasts and osteoblasts was detected only in *Vital* and *Apoptized* samples. Human cells were present only in *Vital* constructs (black arrows). (Scale bars, 100 μm.)

perichondral, it could be attributed to the direct ossification of the mineralized cartilage template. A possible strategy to further improve the bone regeneration capacity of *Apoptized* constructs could thus be based on the increase of the surface:volume ratio by manufacturing channeled tissues, as recently described (27), to achieve a higher extent of perichondral bone formation.

Current acellular osteoinductive materials are typically enhanced by the delivery of single growth factors (BMPs). Because of the absence of critical accessory cues and ECM ligands that potentiate their effect, these strategies require supraphysiological doses of the morphogen, raising economic and safety issues (28, 29). Conversely, the osteoinductivity of the devitalized hypertrophic template relies on a mixture of factors accumulated at doses within physiological ranges and presented through a backbone of ECM molecules. Thus, *Apoptized* devitalized hypertrophic cartilage could offer an attractive alternative to currently available off-the-shelf osteoinductive materials, with the potency of cell-based grafts but bypassing both the logistically complex and regulatory costly use of autologous cells and the still-controversial introduction of allogeneic MSCs. As opposed to ECMs derived from native tissues, which are receiving an increased therapeutic interest (30), the present approach offers the opportunity not only to mimic a developmental process to efficiently form bone tissue but also to enrich the engineered templates in targeted proteins. This could be achieved through the overexpression of key identified factors (e.g., BMP-2, VEGFα) during in vitro culture by modified cells, leading to their embedding in the ECM and their preservation by apoptotic induction. The production of "customized" grafts, with an enhanced angiogenic or osteoinductive potency, would be required to target specific classes of patients or compromised environmental conditions at the repair site (e.g., atrophic nonunions requiring extensive vascularization, or simple bone losses requiring only osteoinduction) (31, 32). The ECM-based embedding of different growth factors in a controllable and customizable fashion for specific clinical needs clearly distinguishes the proposed approach from the "smart" ceramic materials, which have been proven to be osteoinductive in large animal models (33).

Obviously, the clinical translation of the proposed system necessitates further development and extensive preclinical studies. In the present work, the apoptosis induction relies on the use of a retroviral vector, leading to the integration of the system in the target cells. Although the approach has been validated for clinical practice (34), the development of alternative nonviral methods capable of efficiently devitalizing hypertrophic cartilaginous templates (e.g., proapoptotic adjuvants) may be preferred. One important issue with clinical implementation of the developed approach is also related to the efficacy in bone formation of *Apoptized* versus *Vital* grafts. At the assessed time, *Apoptized* constructs remained inferior to *Vital* ones, probably because of the lack of donor cells initially contributing to bone formation. Our study thus needs to be extended to a longer time of observation to assess whether this initial difference will be overcome.

The ectopic model used in the present work allows using human cells and investigating the de novo formation of bone tissue independent from osteoconductive events. Therefore, it

represents the most stringent proof of effective osteoinductivity of the devitalized grafts. However, a relevant assessment of the long-term bone-forming capacity of the implanted constructs will require an orthotopic model in immunocompetent animals. This will also allow the study of the regulatory role of osteoprogenitor and inflammatory cells from a bone environment, as well as of mechanical loading parameters.

In conclusion, we demonstrated that engineered hypertrophic cartilaginous matrix, provided a suitable devitalization technique, can deliver the set of factors to induce its remodeling and develop into bone tissue and bone marrow tissue. The findings outline a broader paradigm in regenerative medicine, relying on the engineering of cell-based but cell-free niches capable of recruiting and instructing endogenous cells on the formation of predetermined tissues. The approach can thus be extended to other biological systems to support both innovative translational strategies and fundamental investigations on the role of engineered ECM, decoupled from that of living cells.

Materials and Methods

All human samples were collected with informed consent of the involved individuals, and all mouse experiments were performed in accordance with Swiss law. All studies were approved by the responsible ethics authorities and by the Swiss Federal Veterinary Office.

HMSC-iDS were generated with the use of a retrovirus carrying the inducible death system (iCasp9-ΔCD19) and were purified by magnetic bead sorting based on CD19 expression (35). Cells were expanded for up to four passages (accounting for an average of 15–20 population doubling) to minimize the loss of chondrogenic potential, and were characterized by flow cytometry for putative MSC markers, with results consistent with our previous report (13).

Hypertrophic templates were generated by either the seeding of cells onto type I collagen meshes at a density of 70×10^6 cells/cm^3 (upscaled construct) (13) or using transwell culture seeded at 5×10^5 cells per insert (10). Constructs were cultured in chondrogenic conditions for 3 wk in a serum-free chondrogenic medium, followed by 2 wk in a serum-free hypertrophic medium (13). Samples were devitalized following two different protocols: F&T treatment or apoptosis induction. Samples were implanted in s.c. pouches of nude mice (four samples per mouse) and retrieved after 12 wk. The resulting in vitro and in vivo tissues were analyzed histologically, immunohistochemically, biochemically (glycosaminoglycans, DNA, protein content), by real-time RT-PCR, and by microtomography. Tissue development in vivo was evaluated histologically, immunohistochemically, and by microtomography. The survival and contribution to bone formation by HMSCs was evaluated with in-situ hybridization for human Alu sequences. A more complete and detailed description of the methods is included in *SI Materials and Methods*.

ACKNOWLEDGMENTS. We are grateful to Prof. Stefan Schären for the kind provision of bone marrow aspirates. This work was partially funded by the Swiss National Science Foundation (Grant 310030_133110, to I.M.) and by the Eurostars program (Grant FO132513, to I.M.).

1. Arrington ED, Smith WJ, Chambers HG, Bucknell AL, Davino NA (1996) Complications of iliac crest bone graft harvesting. *Clin Orthop Relat Res* 329:300–309.
2. Boden SD (2000) Biology of lumbar spine fusion and use of bone graft substitutes: Present, future, and next generation. *Tissue Eng* 6(4):383–399.
3. Kolk A, et al. (2012) Current trends and future perspectives of bone substitute materials - from space holders to innovative biomaterials. *J Craniomaxillofac Surg* 40(8):706–718.
4. Martin I (2014) Engineered tissues as customized organ germs. *Tissue Eng Part A* 20(7-8):1132–1133.
5. Rosset P, Deschaseaux F, Layrolle P (2014) Cell therapy for bone repair. *Orthop Traumatol Surg Res* 100(1, Suppl):S107–S112.
6. Meijer GJ, de Bruijn JD, Koole R, van Blitterswijk CA (2007) Cell-based bone tissue engineering. *PLoS Med* 4(2):e9.
7. Leucht P, Minear S, Ten Berge D, Nusse R, Helms JA (2008) Translating insights from development into regenerative medicine: The function of Wnts in bone biology. *Semin Cell Dev Biol* 19(5):434–443.
8. Kronenberg HM (2003) Developmental regulation of the growth plate. *Nature* 423(6937):332–336.
9. Jukes JM, et al. (2008) Endochondral bone tissue engineering using embryonic stem cells. *Proc Natl Acad Sci USA* 105(19):6840–6845.
10. Scotti C, et al. (2010) Recapitulation of endochondral bone formation using human adult mesenchymal stem cells as a paradigm for developmental engineering. *Proc Natl Acad Sci USA* 107(16):7251–7256.
11. Janicki P, Kasten P, Kleinschmidt K, Luginbuehl R, Richter W (2010) Chondrogenic pre-induction of human mesenchymal stem cells on beta-TCP: Enhanced bone quality by endochondral heterotopic bone formation. *Acta Biomater* 6(8):3292–3301.
12. Farrell E, et al. (2011) In-vivo generation of bone via endochondral ossification by in-vitro chondrogenic priming of adult human and rat mesenchymal stem cells. *BMC Musculoskelet Disord* 12:31.
13. Scotti C, et al. (2013) Engineering of a functional bone organ through endochondral ossification. *Proc Natl Acad Sci USA* 110(10):3997–4002.
14. Benders KE, et al. (2013) Extracellular matrix scaffolds for cartilage and bone regeneration. *Trends Biotechnol* 31(3):169–176.
15. Badylak SF (2007) The extracellular matrix as a biologic scaffold material. *Biomaterials* 28(25):3587–3593.
16. Song JJ, Ott HC (2011) Organ engineering based on decellularized matrix scaffolds. *Trends Mol Med* 17(8):424–432.
17. Crapo PM, Gilbert TW, Badylak SF (2011) An overview of tissue and whole organ decellularization processes. *Biomaterials* 32(12):3233–3243.
18. Bourgine PE, Pippenger BE, Todorov A, Jr, Tchang L, Martin I (2013) Tissue decellularization by activation of programmed cell death. *Biomaterials* 34(26):6099–6108.
19. Tey SK, Dotti G, Rooney CM, Heslop HE, Brenner MK (2007) Inducible caspase 9 suicide gene to improve the safety of allodepleted T cells after haploidentical stem cell transplantation. *Biol Blood Marrow Transplant* 13(8):913–924.
20. Burk J, et al. (2014) Freeze-thaw cycles enhance decellularization of large tendons. *Tissue Eng Part C Methods* 20(4):276–284.
21. Lu H, Hoshiba T, Kawazoe N, Chen G (2012) Comparison of decellularization techniques for preparation of extracellular matrix scaffolds derived from three-dimensional cell culture. *J Biomed Mater Res A* 100(9):2507–2516.
22. Sadr N, et al. (2012) Enhancing the biological performance of synthetic polymeric materials by decoration with engineered, decellularized extracellular matrix. *Biomaterials* 33(20):5085–5093.
23. Ludc D, Mollenhauer J, Kilpatrick KE, Cole AA (2003) N-telopeptide of type II collagen interacts with annexin V on human chondrocytes. *Connect Tissue Res* 44(5):225–239.
24. Kirsch T, et al. (1997) Annexin V-mediated calcium flux across membranes is dependent on the lipid composition: Implications for cartilage mineralization. *Biochemistry* 36(11):3359–3367.
25. Caplan AI, Correa D (2011) The MSC: An injury drugstore. *Cell Stem Cell* 9(1):11–15.
26. Serafini M, et al. (2014) Establishment of bone marrow and hematopoietic niches in vivo by reversion of chondrocyte differentiation of human bone marrow stromal cells. *Stem Cell Res (Amst)* 12(3):659–672.
27. Sheehy EJ, Vinardell T, Toner ME, Buckley CT, Kelly DJ (2014) Altering the architecture of tissue engineered hypertrophic cartilaginous grafts facilitates vascularisation and accelerates mineralisation. *PLoS ONE* 9(3):e90716.
28. Garrison KR, et al. (2010) Bone morphogenetic protein (BMP) for fracture healing in adults. *Cochrane Database Syst Rev* 6:CD006950.
29. Woo EJ (2013) Adverse events after recombinant human BMP2 in nonspinal orthopaedic procedures. *Clin Orthop Relat Res* 471(5):1707–1711.
30. Sicari BM, et al. (2014) An acellular biologic scaffold promotes skeletal muscle formation in mice and humans with volumetric muscle loss. *Sci Transl Med* 6(234):234ra58.
31. Garcia P, et al. (2012) Temporal and spatial vascularization patterns of unions and nonunions: Role of vascular endothelial growth factor and bone morphogenetic proteins. *J Bone Joint Surg Am* 94(1):49–58.
32. Grayson WL, et al. (2010) Engineering anatomically shaped human bone grafts. *Proc Natl Acad Sci USA* 107(8):3299–3304.
33. Yuan H, et al. (2010) Osteoinductive ceramics as a synthetic alternative to autologous bone grafting. *Proc Natl Acad Sci USA* 107(31):13614–13619.
34. Zhou X, et al. (2014) Long-term outcome after haploidentical stem cell transplant and infusion of T cells expressing the inducible caspase 9 safety transgene. *Blood* 123(25):3895–3905.
35. Bourgine P, et al. (2014) Combination of immortalization and inducible death strategies to generate a human mesenchymal stromal cell line with controlled survival. *Stem Cell Res (Amst)* 12(2):584–598.

Supporting Information

Bourgine et al. 10.1073/pnas.1411975111

SI Materials and Methods

hMSC Isolation, Transduction, in Vitro Culture, and in Vivo Implantation. hMSCs were isolated from bone marrow aspirates and processed as previously described (1). Briefly, marrow aspirates (20 mL volume) were harvested from healthy donors (seven males and one female, 23–49 y old) during routine orthopedic procedures involving exposure of the iliac crest. A bone marrow biopsy needle was inserted through the cortical bone, and the aspirate was immediately transferred into plastic tubes containing 15,000 IU heparin. For hMSC-iDS generation, cells were plated at 6,000 cells/cm^2 in 60-mm dishes the day preceding the transduction. hMSCs were transduced by incubation with retroviral vector (iCasp9-ΔCD19) supernatants supplemented with 8 μg/μL polybrene (Sigma Aldrich) for 5 min at 37 °C and centrifuged at 1,100 × *g* for 30 min at room temperature in the dishes, followed by fresh medium replacement (1). Cells were expanded for up to four passages and seeded onto type I collagen meshes (disks 8 mm in diameter, 2 mm thick; Ultrafoam, Davol) at a density of 70 × 106 cells/cm^3 to generate upscale constructs. Alternatively, smaller hypertrophic templates were generated by seeding in transwell culture at 5 × 10^5 cells per insert cells. Constructs were cultured in chondrogenic conditions for 3 wk in a serum-free chondrogenic medium (2), followed by 2 wk in a serum-free hypertrophic medium, supplemented with 50 nM thyroxine, 7 mM β-glycerophosphate, 10 nM dexamethasone, and 0.25 mM ascorbic acid and IL-1β (50 pg/mL). Samples were implanted in s.c. pouches of nude mice (four samples per mouse) and retrieved after 12 wk.

Real-Time RT-PCR Quantitation of Transcript Levels. Total RNA extraction, cDNA synthesis, and real-time RT-PCR (7300 AB; Applied Biosystems) were performed to quantitate expression levels of the following genes of interest: type I (Coll I; Applied Biosystems, ref. no. Hs00164004_m1), type II (Coll II; Applied Biosystems, ref. no. Hs01060345_m1), or type X collagen (2); Sox-9 (Applied Biosystems, ref. no. Hs00165814_m1); MMP-13 (Applied Biosystems, ref. no. Hs00233992_m1); VEGFα (Applied Biosystems, ref. no. Hs00900055_m1); and BMP2 (Applied Biosystems, ref. no. Hs00154192_m1). GAPDH was used as reference gene to normalize gene expression values (Applied Biosystems, ref. no. Hs02758991_g1).

Histological Stainings, Immunohistochemistry, and in Situ Hybridization for Alu Repeats. After in vitro and in vivo cultures, constructs were fixed in 4% (vol/vol) paraformaldehyde; if necessary, decalcified with 7% (vol/vol) EDTA solution (Sigma); and embedded in paraffin. Sections (5 μm thick) were stained with H&E (Baker), Masson's trichrome, or Alizarin red or for tartrate-resistant acid phosphatase activity by means of the leukocyte acid phosphatase kit (Sigma, ref. no. 387A-1KT). Immunohistochemical analyses were performed to characterize the ECM using the following antibodies: CD19 (AbCam, ref. no. 31947). On rehydratation in ethanol series, sections were treated according to the manufacturer's instructions. The immunobinding was detected with biotinylated secondary antibodies and using the appropriate Vectastain ABC kits. The red signal was developed with the Fast Red kit (Dako Cytomation), and sections were counterstained by hematoxylin. Negative controls were performed during each analysis by omitting the primary antibodies. Chromogenic in situ hybridization (Zytovision kit) to detect human Alu repeat sequences was performed following the manufacturer's instructions, using nuclear fast red (Sigma) as nuclear counterstaining. Histological and immunohistochemical sections were analyzed using an Olympus BX-61 microscope.

Immunofluorescence Images. After in vivo explantation, samples were fixed in 4% (vol/vol) paraformaldehyde (Sigma), decalcified with EDTA (Sigma) solution, embedded in optimal cutting temperature compound, and snap frozen in liquid nitrogen. Sections (20 μm thick) were incubated with the primary antibodies against CD31 (platelet endothelial cell adhesion molecule 1; BD Pharmingen), NG2 (Chemicon International), and α-smooth muscle actin. As appropriate, secondary antibodies labeled with Alexa Fluor 647, Alexa Fluor 488, or Alexa Fluor 546 (Invitrogen) were used, and DAPI was used to stain nuclei. Fluorescence images were acquired using a confocal Zeiss LSM 710 microscope.

Microtomography. Microtomography was performed with in vivo implants. After fixation in formalin and storage in PBS, microcomputerized tomography data were acquired using a Phoenix nanotom m scanner (General Electric) with 0.5 mm aluminum filtered X-rays (applied voltage, 70 kV; current, 260 μA). Transmission images were acquired during a 360° scan rotation with an incremental rotation step size of 0.25°. Reconstruction was made using a modified Feldkamp algorithm at an isotropic voxel size of 2.5 μm. Threshold-based segmentation and 3D measurement analyses (bone mineral density and volume) were performed using the ImageJ software (ImageJ; National Institutes of Health) with the BoneJ (4) and 3D Shape (5) extensions. 3D rendering of the structures was performed using VGStudio MAX 2.2 software (Volume Graphics).

Statistical Analysis. The results of real-time RT-PCR, protein, and tissue quantification are presented as mean ± SEM. Statistical analysis was performed using the unpaired *t* test. *P* values of 0.05 or less were considered statistically significant.

Proteins Quantification. Protein levels were determined in devitalized (F&T and apoptized) and nondevitalized (living) tissue lysates collected from constructs cultured for 5 wk in vitro. Samples were analyzed for their content of a panel of growth factors, chemokines, and metalloproteinases, according to the manufacturer's instructions (Procarta Immunoassay Kit; Panomics).

1. Bourgine P, et al. (2014) Combination of immortalization and inducible death strategies to generate a human mesenchymal stromal cell line with controlled survival. *Stem Cell Res (Amst)* 12(2):584–598.
2. Scotti C, et al. (2010) Recapitulation of endochondral bone formation using human adult mesenchymal stem cells as a paradigm for developmental engineering. *Proc Natl Acad Sci USA* 107(16):7251–7256.
3. Barbero A, Ploegert S, Heberer M, Martin I (2003) Plasticity of clonal populations of dedifferentiated adult human articular chondrocytes. *Arthritis Rheum* 48(5):1315–1325.
4. Doube M, et al. (2010) BoneJ: Free and extensible bone image analysis in ImageJ. *Bone* 47(6):1076–1079.
5. Sheets KG, et al. (2013) Microglial ramification and redistribution concomitant with the attenuation of choroidal neovascularization by neuroprotectin D1. *Mol Vis* 19:1747–1759.

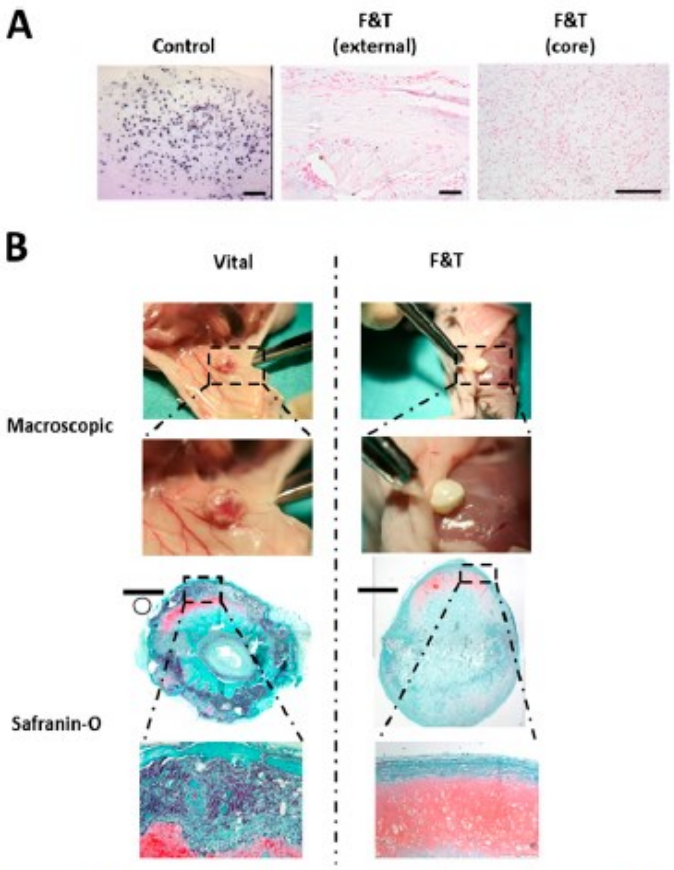

Fig. S1. (*A*) In situ hybridization for Alu repeats. No human cells could be detected in F&T devitalized ossicles 5 wk after in vivo implantation, as demonstrated by the absence of blue positively stained cells in both the external and core part of the ossicle. Purple stained cells (hematoxylin) corresponded to host cell invasion. The control sample consists of an in vitro-generated hypertrophic cartilage template, nondevitalized. (Scale bar, 100 μm.) (*B*) Explantation of non-devitalized (Vital) and F&T devitalized (F&T) ossicles 12 wk after ectopic implantation in nude mice. The Vital ossicles underwent an intense remodeling, giving rise to a mature bone organ with evidence of perichondral and trabecular bone and of a hematopoietic compartment (Safranin-O staining). Conversely, the F&T devitalized ossicles did not showed macroscopic evidences of remodeling and blood cell colonization, as confirmed by histological analysis revealing the absence of bone and bone marrow throughout the samples (Safranin-O). (Scale bar, 1 mm.)

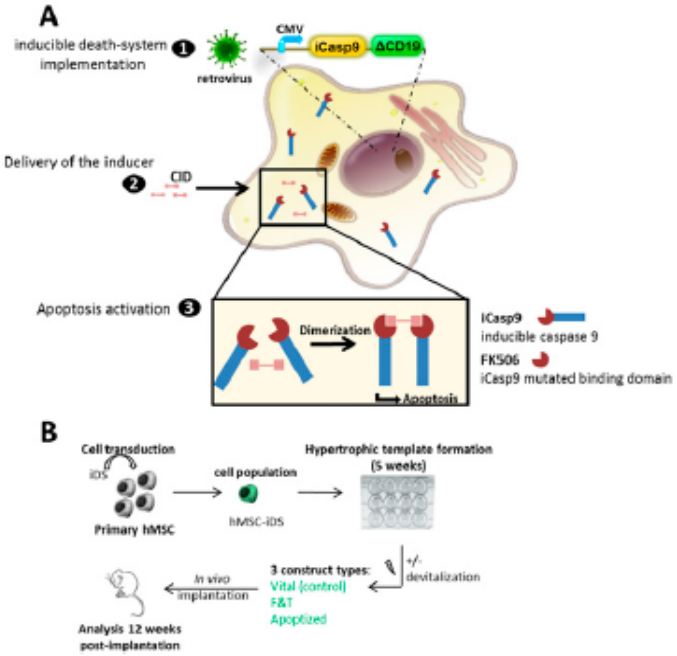

Fig. S2. (*A*) Mode of action of the iDS. The iDS is implemented in the genome of the target cells by the use of a retrovirus (1). Successfully transuded cells constitutively expressed a modified caspase 9 (iCasp9) displaying a mutated binding domain (FK506). The truncated CD19 is used as reporter marker. The delivery of the chemical inducer of dimerization (2) results in the dimerization of the iCasp9 by specific binding. The iCasp9 dimerization leads to the activation of the intrinsic apoptosis pathway (3). (*B*) Experimental set-up to assess the osteoinductive potential of devitalized hypertrophic templates. hMSC-iDS were generated by retroviral transduction. Hypertrophic templates were generated by 5 wk of culture (3 wk chondrogenesis + 2 wk hypertrophy) in the transwell system. Obtained constructs were either nondevitalized (Vital) or devitalized by F&T or apoptosis induction and were subsequently implanted ectopically in nude mice. After 12 wk, samples were retrieved for analysis.

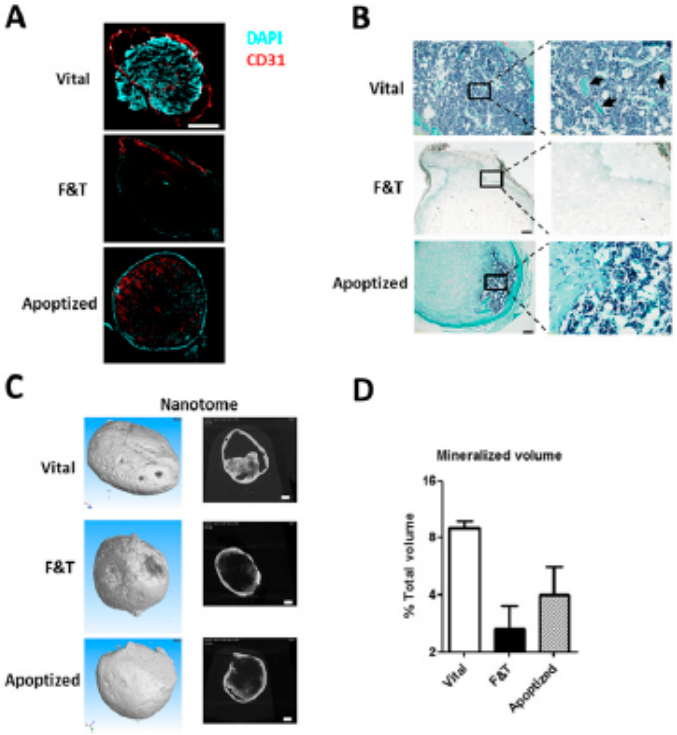

Fig. S3. (*A*) Fluorescence microscopy (DAPI, CD31) of hypertrophic templates retrieved 12 wk after ectopic implantation. F&T samples were characterized by the absence of vessel perfusion and host cell colonization. Apoptized samples were shown to be perfused by vessels although to a lower extent than the Vital constructs. (Scale bar, 0.5 mm.) (*B*) Masson's Trichrome staining revealing the presence of trabecular structure (arrow) only in Vital samples. Despite the presence of perichondral bone and bone marrow, no trabecular bone was found in Apoptized samples. F&T constructs did not show any evidence of frank bone structures. (Scale bar, 0.5 mm.) (*C*) 3D reconstructed microtomographic images of samples cultured for 5 wk in vitro and implanted ectopically in nude mice for 12 wk. (Scale bar, 0.35 mm.) (*D*) Microcomputed tomographic quantification of the mineralized volume in Vital, F&T, and Apoptized samples retrieved 12 wk after in vivo implantation. The measured volume includes both bone and calcified cartilage tissues.

Chapter III

Engineered and devitalized human extracellular matrix for orthotopic bone repair

Manuscript in preparation

Engineered and devitalized human extracellular matrix for orthotopic bone repair

Pigeot S, Bourgine P, Jacquiery C, Scotti C, Papadimitropoulos A, Todorov A, Epple C, Peretti G, Martin I

Departments of Surgery and of Biomedicine, University Hospital Basel, University of Basel, Hebelstrasse 20, CH-4031 Basel, Switzerland

ABSTRACT

Most bones of the human body form and heal through endochondral ossification, whereby hypertrophic cartilage (HyC) is formed and subsequently remodeled into bone. We previously demonstrated that HyC can be engineered from human mesenchymal stromal cells (hMSC), and subsequently devitalized by apoptosis induction. The resulting tissue retained osteoinductive properties leading to ectopic bone formation. In this study, we aim at engineering and devitalizing HyC in an upscaled, streamlined process within a perfusion bioreactor and subsequently test it in an orthotopic bone repair model. We hypothesized that such HyC would outperform a clinical product currently used for bone reconstructive surgery.

Human MSC were seeded, differentiated and devitalized on a collagen type I scaffold within a perfusion bioreactor. The resulting apoptosis-devitalized HyC was implanted in a 10-mm rabbit calvarial defect model, with human bone processed allograft as control (Botiss, Maxgraft®).

Human MSC culture in the perfusion bioreactor enabled the generation of homogenous HyC, upscaled in volume by 100-fold from classic static pellet culture. Following 6 weeks of in vivo implantation, microcomputed tomography analysis of the defects indicated that devitalized HyC induced a 15-fold higher mineralized volume than the Botiss material. Histological assessment confirmed an increased bone formation in the defects filled with HyC as compared to Botiss, with a 2.5-fold higher total amount of bone formed in the central 5-mm core and an 8-fold higher amount of bone formed in direct contact with the implanted material.

This work demonstrates the suitability of engineered devitalized HyC to be used as a bone substitute material, with a performance superior to a state-of-the-art commercial graft. Importantly, the tissue transplant was generated in an upscaled streamlined fashion envisioning standardization, automation toward design of a product for clinical applications.

ABSTRACT

Most bones of the human body form and heal through endochondral ossification, whereby hypertrophic cartilage (HyC) is formed and subsequently remodeled into bone. We previously demonstrated that HyC can be engineered from human mesenchymal stromal cells (hMSC), and subsequently devitalized by apoptosis induction. The resulting tissue retained osteoinductive properties leading to ectopic bone formation. In this study, we aim at engineering and devitalizing HyC in an upscaled, streamlined process within a perfusion bioreactor and subsequently test it in an orthotopic bone repair model. We hypothesized that such HyC would outperform a clinical product currently used for bone reconstructive surgery.

Human MSC were seeded, differentiated and devitalized on a collagen type I scaffold within a perfusion bioreactor. The resulting apoptosis-devitalized HyC was implanted in a 10-mm rabbit calvarial defect model, with human bone processed allograft as control (Botiss, Maxgraft®).

Human MSC culture in the perfusion bioreactor enabled the generation of homogenous HyC, upscaled in volume by 100-fold from classic static pellet culture. Following 6 weeks of in vivo implantation, microcomputed tomography analysis of the defects indicated that devitalized HyC induced a 15-fold higher mineralized volume than the Botiss material. Histological assessment confirmed an increased bone formation in the defects filled with HyC as compared to Botiss, with a 2.5-fold higher total amount of bone formed in the central 5-mm core and an 8-fold higher amount of bone formed in direct contact with the implanted material.

This work demonstrates the suitability of engineered devitalized HyC to be used as a bone substitute material, with a performance superior to a state-of-the-art commercial graft. Importantly, the tissue transplant was generated in an upscaled streamlined fashion envisioning standardization, automation toward design of a product for clinical applications.

technique by engineering primary hMSC with a caspase inducible apoptotic system [13]. Following their in vitro chondrogenic differentiation and HyC tissue formation, addition of a clinical grade adjuvant in the culture medium leads to efficient devitalization of the tissue and preservation of the ECM. Upon in vivo implantation, the devitalized HyC formed ectopic bone by osteoinduction, underlying the importance of ECM preservation as well as its potential for bone regeneration [13].

To generate a cell-free osteoinductive material recapitulating physiological bone healing for clinical applications, additional validations are required. The generation of a large quantity of homogenously devitalized tissues in a single step process would contribute to the translation of the production towards an upscaled and streamlined process. Moreover, apoptosis devitalized HyC must be assessed in a relevant animal model against current clinical standard-of-care materials to confirm the therapeutic potential.

In this work, we engineered an upscaled devitalized HyC within a bioreactor system and assessed its potential as a graft for bone repair in an orthotopic environment. To this aim, hMSC were engineered with an apoptosis inducible cassette, seeded and differentiated on a collagen type I scaffold towards HyC formation within a perfusion bioreactor chamber. Apoptosis was then induced in the same chamber, resulting in the streamlined generation of a homogenous devitalized HyC. We hypothesized that devitalized HyC would enable superior bone regeneration in an orthotopic environment as compared to a clinical standard-of-care ECM-based material, namely a human processed allograft (Botiss, Maxgraft®).

MATERIAL AND METHODS

Cell culture

Human bone marrow aspirates were obtained during routine orthopedic surgical procedures involving exposure of the iliac crest, after ethical approval (EKBB, Ref.78/07) and informed donor consent. Marrow aspirates (20 ml volumes) were harvested from healthy donors (20 to 60 years old) using a bone marrow biopsy needle inserted through the cortical bone and immediately transferred into plastic tubes

containing 15,000 IU heparin. After diluting the marrow aspirates with phosphate buffered saline (PBS) at a ratio of 1:4, nucleated cells were counted and seeded at a density of 3.10^6 cells/cm² in complete medium supplemented with 5 ng/ml of fibroblast growth factor-2 (FGF-2, R&D Systems) and cultured in a humidified 37 °C/5% CO_2 incubator. Complete medium consisted of α-minimum essential Medium (αMEM) with 10% fetal bovine serum, 1% HEPES (1 M), 1% Sodium pyruvate (100 mM) and 1% of Penicillin–Streptomycin–Glutamine (100×) solution (all from Gibco). hMSCs were expanded to passage 1 (P1) before lentiviral transduction. for maximum four passages and seeded onto

Lentivirus production

The lentiviral vector was kindly provided by the San Raffaele Institute in Milan. It consists of a bidirectional promoter driving the transcription on one hand of the inducible truncated caspase 9 (iCas9) and on the other hand of the ΔNGFR reporter. 3rd generation packaging plasmids pCMV-VSVG, pRSV-REV, pRRE were ordered from Addgene (Respectively, Plasmid #8454, Plasmid #12253, Plasmid #12251). Lenti-X™ 293T Cell Line from Clontech (Cat# 632180) was plated on 10cm diameter plastic dishes the day before to reach a confluency of 60% on the day of tranfection. Lentiviral packaging was performed by co-transfecting overnight and per plate, 4ug piCas9, 2ug pCMV-VSVG, 2ug pRSV-REV, 2ug pRRE using FugeneHD (Promega, Ref E2311) according to manufacturer's recommendation. The day after, medium was changed and supernatant collected 72 hours later, filtered using 0.45µm filters and centrifugated on a 20% sucrose bedding at 13000rpm for 3h00 and deceleration without break. Lentivirus was then resuspended in PBS, aliquoted and stored at -80°C until use. Transduction of primary hMSCs was carried out at P1 using a MOI of 1 to limit the number of integration per hMSC. Upon reaching confluency, hMSCs were labeled and sorted using a FACS BD SORPAria III sorter and NGFR antibody.

Cell seeding

Sorted hMSCs to a purity ≥95% were further expanded until P3. Cells were seeded either statically or in perfusion on type I collagen meshes (round disks with 6-mm-diameter and 2-mm-thickness; Ultrafoam, Davol) at a density of 35×10^6cells/cm³ and cultured in a serum-free chondrogenic medium (DMEM supplemented with penicillin-streptomycin glutamine (Invitrogen), HEPES (Invitrogen), sodium pyruvate

(Invitrogen), ITS (Insulin, Transferrin, Selenium) (Invitrogen), Human Serum Albumin 0.12% (CSL Behring), 0.1mM ascorbic acid (Sigma), 10^{-7}M dexamethasone (Sigma) and 10ng/ml TGF-β3 (Novartis)) for 3 weeks, followed by another 2 weeks culture in a serum-free hypertrophic medium, (DMEM supplemented with 50 nM thyroxine, 10mM β-glycerophosphate (Sigma), 10^{-6}M dexamethasone, and 0.1mM ascorbic acid and 50 pg/mL IL-1β (Sigma)).

Cells seeded statically were allowed to attach for 1h00 in the incubator before addition of the medium. Cells seeded in perfusion bioreactor (U-CUP, Cellec Biotek AG) were perfused at a speed of 3ml/min overnight and then differentiated at a speed of 0,3ml/min, corresponding to a superficial velocity of 100µm/sec [14]. Apoptosis induction was carried on overnight by addition of the AP20187 dimerizer at a concentration of 100nM (ApexBio).

Orthotopic in vivo implantation

All studies were approved by the responsible ethics authorities and by the Swiss Federal Veterinary Office (permit 2783).

Before implantation, the retrieved devitalized grafts were washed in PBS. A volume of 157mm3 was considered to fill up the rabbit calvaria (10-mm diameter and 2-mm height). Therefore, 3 bioreactors were pulled together and chopped into heterogenous granules (≤2-mm) resembling the Botiss composition. Before implantation, granules were embedded in a fibrin gel (TISSEEL, Baxter). Analgesia was provided with Buprenorphin 0.05mg/kg body weight subcutaneously prior to anesthesia and every 6h during the first 48h and by the drinking water during the night. Meloxicam 0.3mg/kg was administered orally at the end of the procedure and every 24h thereafter for the first week. Anesthetic induction was performed with Ketamin 25mg/kg body weight and Xylazin 2.5mg/kg body weight subcutaneously. Anesthesia with isofluran was maintained on demand and regulated by pulsoximetry. Oxygen was used as a carrier gas at a ratio of 1:2 (O2:N2O). Prior to surgery the skin of the head is shaved and disinfected. A midline longitudinal incision is made from the nasofrontal area to the external occipital protuberance along the midsagittal suture. Skin and underlying tissues are reflected bilaterally

RESULTS

A perfusion bioreactor allows the generation of upscaled, homogenous hypertrophic cartilage

Primary hMSCs were efficiently transduced with the inducible apoptotic cassette and sorted to obtain a homogenous population (≥ 95%, data not shown) (Fig 1). To validate the ability of the perfusion bioreactor to generate devitalized HyC of 56,5mm^3 compared to the 0,53mm^3 as previously reported [13]. Tissues of 6-mm diameter by 2-mm height were produced either statically or in the perfusion system. Assessment of in vitro cartilage formation was first carried out by measurement of glycosaminoglycans (GAG), a major cartilaginous tissue component detectable both in the supernatant and in the generated tissue. Cartilage in perfusion bioreactors released 6- to 20- fold higher GAG in the supernatant over the culture time (Fig. 2A). The GAG present within the tissue was on the other hand comparable in static and perfusion culture (Fig. 2B). This difference revealed that HyC in the bioreactor produced a higher amount of GAG. Tissues were retrieved after 5 weeks of in vitro differentiation and analyzed histologically to assess quality and homogeneity. Cartilage and hypertrophic cartilage formation were respectively validated by Saf-O and collagen type X staining (Fig. 2C). While perfused HyC displayed a homogenous Saf-O and collagen type X distribution, statically cultured tissue showed the presence of a necrotic core, negatively stained for Saf-O and collagen type X, as previously reported [10]. HyC had identical mineralization (Alizarin red) patterns surrounding the tissue, independently of the culture process (Fig. 2C). Gene expression analysis confirmed the chondrogenic (SOX9, ColII) and hypertrophic (IHH, VEGF, ColX, BSP) state of the tissues (Fig. 2D). HyC quality was analogous in static and perfused conditions. Overall, perfused HyC displayed similar differentiation stage and quality as statically cultured HyC but with a homogenous cartilage tissue distribution. This feature was essential to reliably generate minced HyC with reduced variability in quality.

Engineered HyC is efficiently devitalized in the perfusion bioreactor

Following validation of the perfusion bioreactor-based culture, the built-in devitalization strategy based on apoptosis induction was assessed by addition of the adjuvant to the medium in perfusion and compared to non-induced (living) tissue. Devitalization efficiency was measured and quantified by live-dead assay directly upon tissue retrieval from the bioreactor. Both living and devitalized HyC displayed a homogenous cell distribution (Fig. 2E). Living tissues showed very few dead cells, whereas apoptosis induced HyC had negligible living cells in the whole tissue, with over 95% efficiency in the devitalization (Fig. 2E). The perfusion bioreactor system thus supported an efficient built-in devitalization of upscaled HyC.

Microcomputed tomography (µCT) reveals increased mineralization from devitalized HyC

Orthotopic in vivo implantation in a NZW rabbit calvarial model was used to assess the performance of the devitalized HyC graft generated in the bioreactor versus the clinically available standard-of-care Botiss (Fig. 1). Prior to implantation, the devitalized HyC discs were minced to obtain heterogenous granules of similar shape and size (≤ 2-mm) than the Botiss material. In each rabbit, two 10-mm calvarial defects were generated and filled with a volume of 169,5-mm³ (corresponding to 3 bioreactors) of either minced HyC ECM or Botiss granules.

After 6 weeks of in vivo implantation, calvaria were retrieved and mineralization assessed by µCT. To exclusively quantify the newly formed mineralization volume within the Botiss defect, a corresponding amount of Botiss was measured by µCT and subtracted to the total mineralization volume. The mineralization volumes of the defect were quantified in each defect using two cylindrical regions of interest of different sizes (Fig. 3A). In the first case, a 10-mm diameter cylinder was analyzed, corresponding to the full defect and thus to the total newly formed mineralization. HyC filled defects showed a 15-fold increase in mineralization volume compared to the Botiss ones (Fig. 3B). To determine whether this difference was mainly due to osteoconduction from the cortical bone or to newly formed mineralization at the inner of the defect, a 5-mm diameter central cylinder was analyzed. A 3.7-fold

DISCUSSION

We previously demonstrated the capacity of apoptosis devitalized HyC to induce bone formation in an ectopic environment by osteoinduction [13]. Here, we demonstrated the possibility to engineer and subsequently devitalize HyC within a perfusion bioreactor system. The method allowed the formation of upscaled HyC tissue in a streamlined fashion. The homogenous generated HyC was then efficiently devitalized within the bioreactor. Finally, we validated the superiority of the devitalized tissue as a graft for bone repair against a clinical standard-of-care, the human processed bone ECM Botiss.

The upscaled generation of HyC was previously achieved using static seeding and differentiation on a collagen type I scaffold (Ultrafoam) [15]. Nevertheless, statically upscaled HyC developed a necrotic core in the center due to the lack of nutrients and oxygen. Here we established the advantage of perfusion bioreactor-based to form homogenous qualitative HyC tissues confitmed by a higher GAG production. Perfusion mimics a more physiological environment with shear-stress and accessibility of nutrients/oxygen throughout the tissue [14,16]. Therefore, they represent an interesting opportunity for in vitro tissue formation in a single step process [17]. In this study we describe for the first time the homogenous formation of mature HyC tissue as well as their subsequent devitalization in a single closed-in system. The bioreactor used in this study could be developed to include a fully automated system with real time control over oxygen levels, pH, metabolites and nutrients enabling a fine tuning of the culture [18]. Automation reduces human manipulation and mechanically, the risks of errors and contaminations envisioning a standardized streamlined process for devitalized HyC tissue production to be used as a bone substitute material.

Within the defects, bone was constituted in different ways either (i) in contact with the calvarial bone, (ii) in contact with the implanted material, (iii) isolated from the calvarial bone and the implanted material. Bone in contact with the calvaria represented most of the newly formed bone with an increase in the HyC emphasizing the osteoconductive effect of the HyC. Bone formed on the implanted material

was found in higher amounts on the devitalized HyC underlining a biological functionalization in preserved ECM. Finally, bone constituted independently of calvaria and implanted material showed similar, heterogeneously distributed bone formation. This newly formed bone is likely due to osteoprogenitors migration from the periosteum [19] and therefore not material dependent. Despite being a clinical standard-of-care, defect filled with the Botiss material showed significantly less bone formation in all the analyzed areas consistent with the limited potency of current processed bone allograft [2].

Regardless of superior bone formation in the calvarial defect, the remodeling of the implanted HyC ECM was only partial. We can speculate that by increasing the speed and extent of the remodeling, higher bone creation in the defect would prompt a more efficient healing process. A recently developed strategy consists in customizing the ECM by overexpression and embedding of key factors by genetic engineering or using different in vitro cues [20–22]. Cells forming the HyC ECM could be engineered with crucial growth factor recapitulating key bone repair stages such as angiogenesis (e.g. vascular endothelial growth factor (VEGF) [23]) or bone formation (e.g. bone morphogenetic protein 2 (BMP2) [24]) [4,25].

In our work, the generation of devitalized HyC requires the use of primary hMSC leading to high heterogeneity in the HyC quality depending on the donor. Additionally, there is currently no marker allowing the prediction of primary hMSC potential to form HyC [26]. This remains a major limitation from the perspective of tissue upscaling and proceeding towards potential clinical trials. Further research should aim at engineering a cell line capable to reproducibly and efficiently form HyC before apoptosis induction. Ideally, genetic engineering of hMSC would be combined with the cell line generation allowing for fine tuning of the ECM properties.

The immunogenicity of the devitalized HyC was not extensively assessed but no serious rejection could be observed. The use of apoptosis, generating apoptotic bodies instead of cell bursting through necrosis may lead to attenuated immune response [27]. Additionally, perfusion of the tissue during the apoptotic process likely removed most of the potential immunogenic material from the tissue. Noticeably, in some

cases, graft decellularization was not sufficient to avoid graft rejection [28]. Therefore, additional studies should characterize the immunogenicity of apoptosis devitalized HyC.

A final step in the standardized streamlined generation of HyC as a bone graft material is the definition of a suitable storage strategy. Major allograft storage strategy include cryopreservation, deep freezing (fresh-freezing) and lyophilization (freeze-drying) [29]. Cryopreservation and deep freezing are the most common storage procedure. Despite some recent report suggesting storage at -20°C [30], frozen tissues are usually kept at -70°C making it technically challenging for the clinic [31]. Future research should aim at characterizing the quality and preservation of the engineered HyC as potential graft for bone repair.

To conclude, we showed that apoptosis-devitalized HyC can be fully engineered using bioreactor systems and has the potential to outperform the clinical standard-of-care Botiss in an immunocompetent orthotopic environment. This approach will lead to the generation of biological material as a graft with preserved biological function. Ultimately, we envision that the combination of a cell line with defined pattern of cytokine expression in an automated streamlined bioreactor could lead to the standardized manufacturing of specifically enriched HyC material for enhanced bone repair.

ACKNOWLEDGEMENT

The work was funded by the Eurostars program (grant n. E!7865 to A.P., G.P. and I.M.)

CONFLICTS OF INTERESTS

The authors declare no potential conflicts of interest.

REFERENCES

[1] M.A. Fernandez-Yague, S.A. Abbah, L. McNamara, D.I. Zeugolis, A. Pandit, M.J. Biggs, Biomimetic approaches in bone tissue engineering: Integrating biological and physicomechanical strategies, Advanced drug delivery reviews 84 (2015) 1–29.

[2] Y. Fillingham, J. Jacobs, Bone grafts and their substitutes, The bone & joint journal 98-B (1 Suppl A) (2016) 6–9.

[3] E.M. Thompson, A. Matsiko, E. Farrell, D.J. Kelly, F.J. O'Brien, Recapitulating endochondral ossification: A promising route to in vivo bone regeneration, Journal of tissue engineering and regenerative medicine 9 (8) (2015) 889–902.

[4] T.A. Einhorn, L.C. Gerstenfeld, Fracture healing: Mechanisms and interventions, Nature reviews. Rheumatology 11 (1) (2015) 45–54.

[5] H.M. Kronenberg, Developmental regulation of the growth plate, Nature 423 (6937) (2003) 332–336.

[6] S.M. Oliveira, I.F. Amaral, M.A. Barbosa, C.C. Teixeira, Engineering endochondral bone: In vitro studies, Tissue engineering. Part A 15 (3) (2009) 625–634.

[7] S.M. Oliveira, D.Q. Mijares, G. Turner, I.F. Amaral, M.A. Barbosa, C.C. Teixeira, Engineering endochondral bone: In vivo studies, Tissue engineering. Part A 15 (3) (2009) 635–643.

[8] C. Scotti, B. Tonnarelli, A. Papadimitropoulos, A. Scherberich, S. Schaeren, A. Schauerte, J. Lopez-Rios, R. Zeller, A. Barbero, I. Martin, Recapitulation of endochondral bone formation using human adult mesenchymal stem cells as a paradigm for developmental engineering, Proceedings of the National Academy of Sciences of the United States of America 107 (16) (2010) 7251–7256.

[9] E. Farrell, S.K. Both, K.I. Odörfer, W. Koevoet, N. Kops, F.J. O'Brien, R.J. Baatenburg de Jong, J.A. Verhaar, V. Cuijpers, J. Jansen, R.G. Erben, G.J.V.M. van Osch, In-vivo generation of bone via endochondral ossification by in-vitro chondrogenic priming of adult human and rat mesenchymal stem cells, BMC musculoskeletal disorders 12 (2011) 31.

[10] C. Scotti, E. Piccinini, H. Takizawa, A. Todorov, P. Bourgine, A. Papadimitropoulos, A. Barbero, M.G. Manz, I. Martin, Engineering of a functional bone organ through endochondral ossification, Proceedings of the National Academy of Sciences of the United States of America 110 (10) (2013) 3997–4002.

[11] J.J. Song, H.C. Ott, Organ engineering based on decellularized matrix scaffolds, Trends in molecular medicine 17 (8) (2011) 424–432.

[12] P.M. Crapo, T.W. Gilbert, S.F. Badylak, An overview of tissue and whole organ decellularization processes, Biomaterials 32 (12) (2011) 3233–3243.

[13] P.E. Bourgine, C. Scotti, S. Pigeot, L.A. Tchang, A. Todorov, I. Martin, Osteoinductivity of engineered cartilaginous templates devitalized by inducible apoptosis, Proceedings of the National Academy of Sciences of the United States of America 111 (49) (2014) 17426–17431.

[14] M. Cioffi, J. Küffer, S. Ströbel, G. Dubini, I. Martin, D. Wendt, Computational evaluation of oxygen and shear stress distributions in 3D perfusion culture systems: Macro-scale and micro-structured models, Journal of biomechanics 41 (14) (2008) 2918–2925.

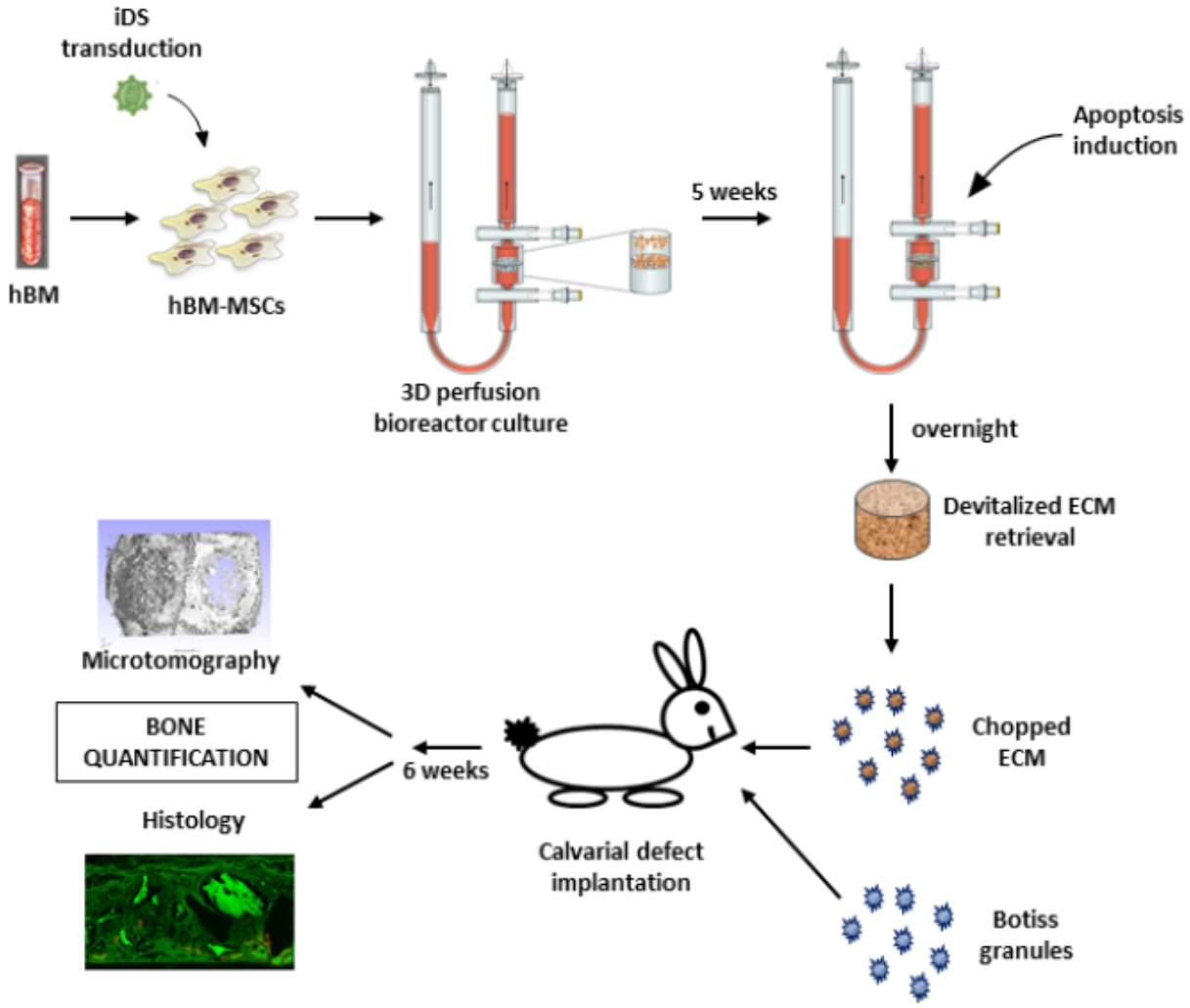

Figure 1: Overview of the experimental plan. Briefly, human MSCs are isolated from total human iliac crest bone marrow (hBM) samples by plastic adhesion. hBM-MSCs are then transduced with lentivirus carrying the inducible caspase 9 (iDS). FACS sorted hBM-MSCs carrying the iDS are then expanded and seeded on collagen sponge within the 3D perfusion bioreactor system. Following the 3 weeks chondrogenic and 2 weeks hypertrophic differentiation protocol, apoptosis is induced overnight in the perfusion bioreactor. Hypertrophic tissues are then retrieved, chopped and implanted into 10mm orthotopic bilateral calvarial defects. Analysis of the calvarial defects is done 6 weeks post-implantation.

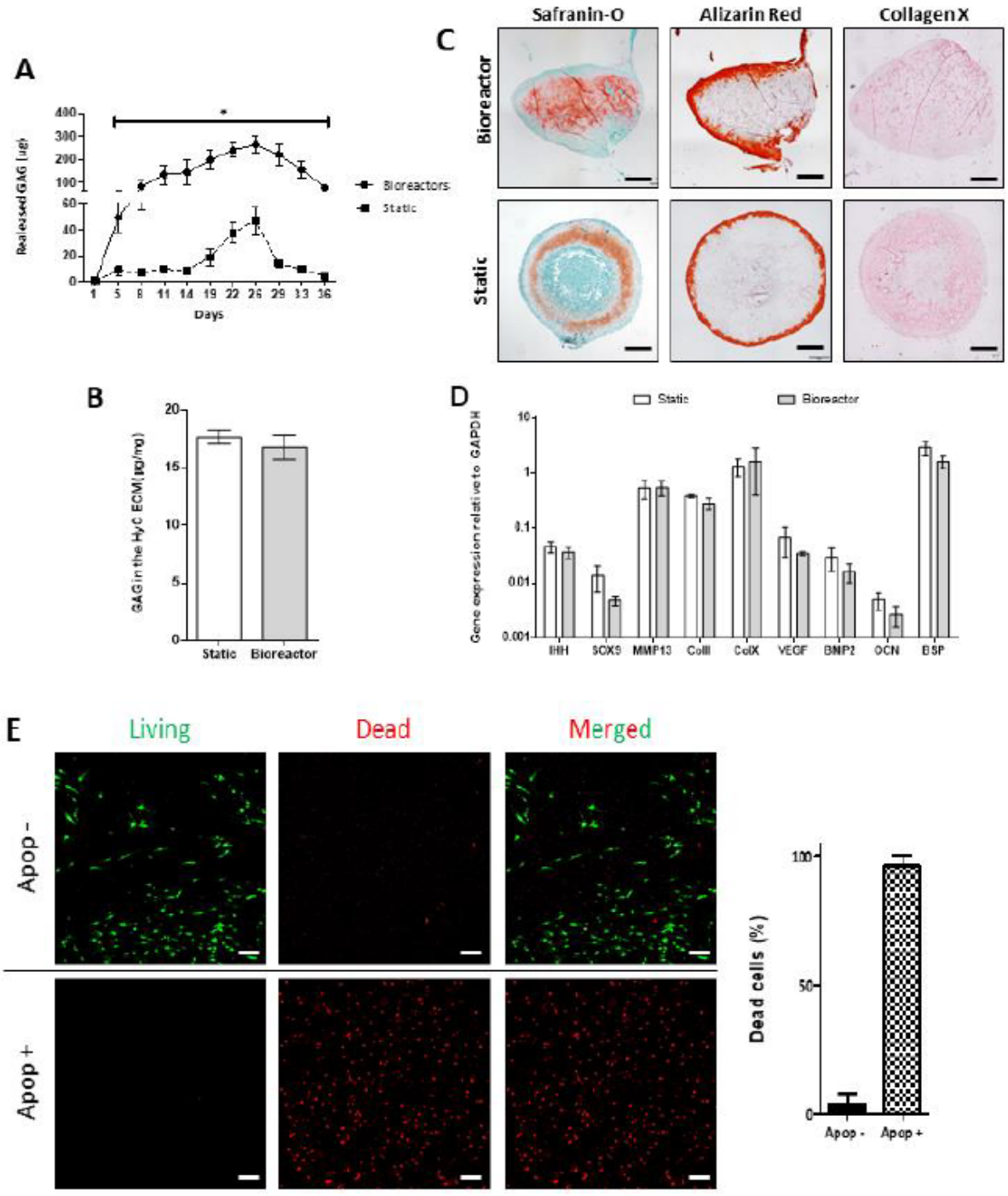

Figure 2: In vitro hypertrophic cartilage (HyC) characterization. (A) GAG released quantities in the cell culture media during the 5 weeks in vitro differentiation towards hypertropgic cartilage. (B) GAG measured in the HyC ECM after the 5 weeks in vitro differentiation. The GAG is measured per mg of ECM (n = 6). (C) Histology of the hypertrophic cartilage following 5 weeks in vitro differentiation and before being chopped for orthotopic implantation (scale bar = 1mm). GAG is stained in red on the Safranin-O staining (Saf-O). Mineralization stains in red on the Alizarin Red. Collagen type X stains in pink on the immunohistochemistry staining. (D) Gene expression analysis by qRT-PCR following the 5 weeks in vitro differentiation protocol (n ≥ 3). (E) Pictures of the live/dead assay staining in living (apop-) and devitalized (apop+) hypertrophic cartilage and the related cell quantification (scale bar = 200µm) (n = 15). Graphs show the average and SEM. Statistics are two tailed unpaired t-test, P=0.05.

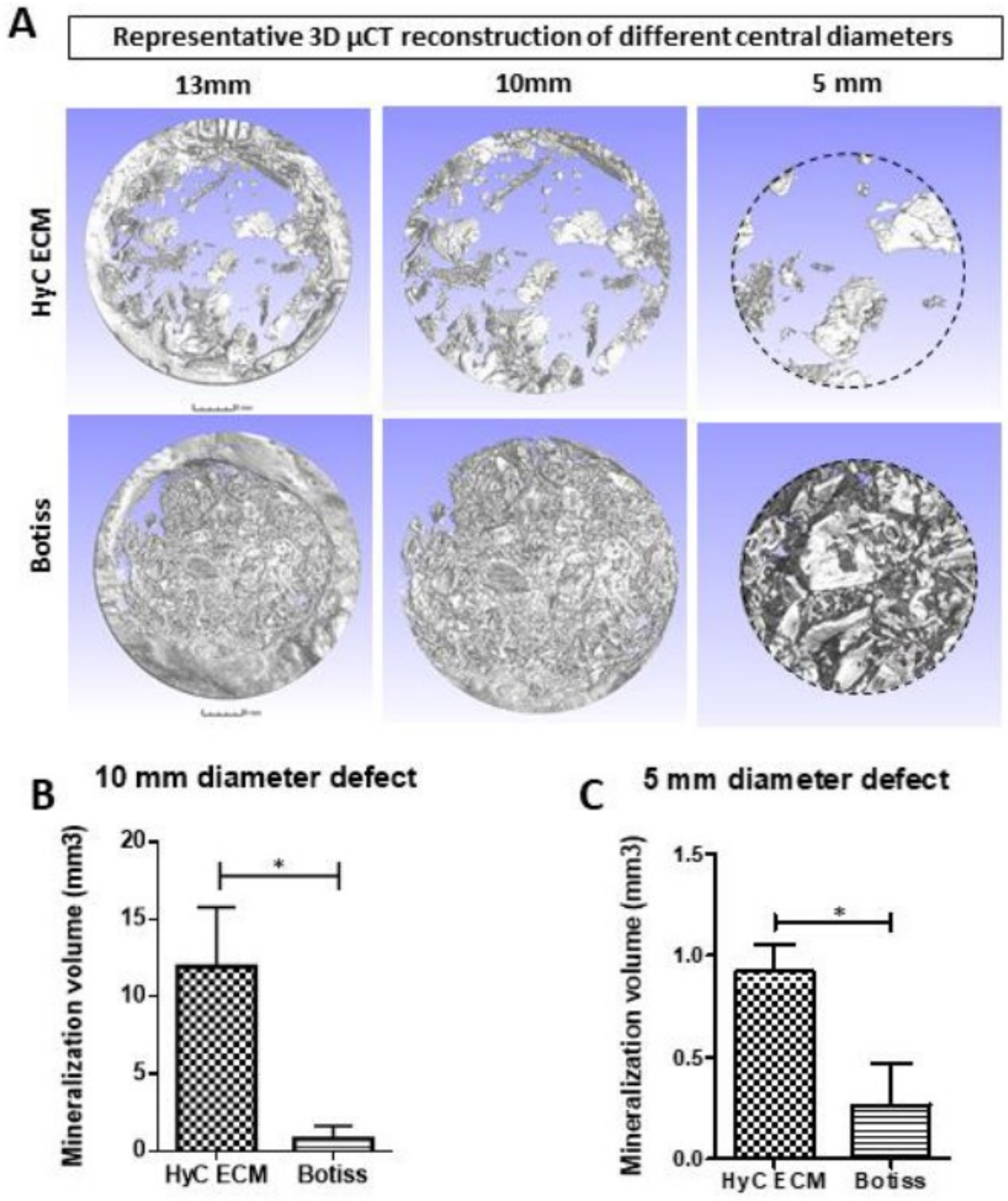

Figure 3: µCT analysis of the calvarial defect. (A) Representative picture of different 3D µCT reconstruction of the analyzed volumes. (B) Bone and mineralization volume quantification in the 10mm diameter area and (C) in the 5mm diameter area. Graphs show the average and SEM. Statistics are two tailed unpaired t-test, P=0.05.

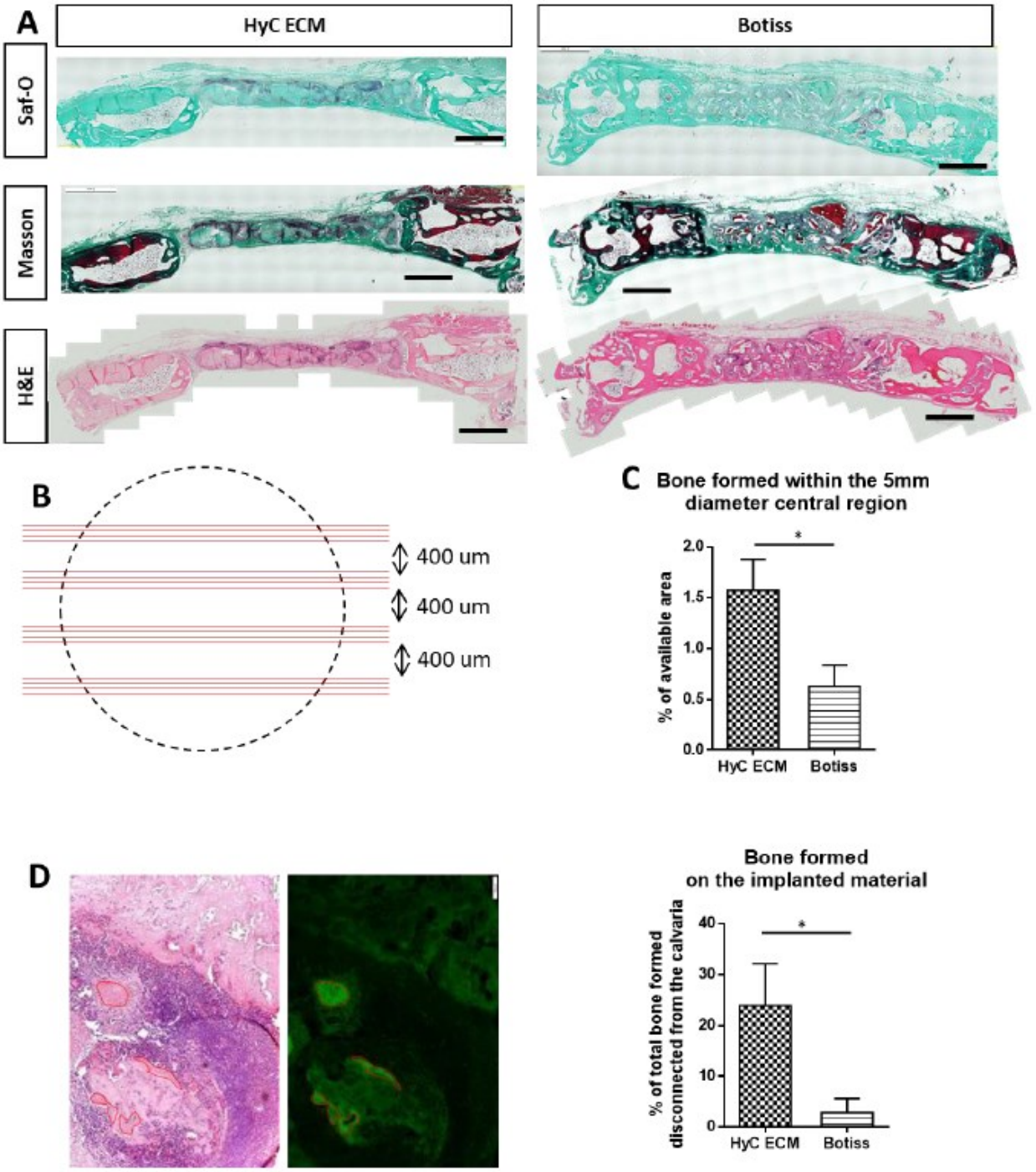

Figure 4: Histological analysis of the retrieved calvarial samples. (A) Representative sections of the calvaria 6 weeks after in vivo implantation. Saf-O stains bone in deep green and cartilage in red. Masson stains mature bone in brown and newly formed bone in deep green. H&E stains bone in deep pink. (B) Scheme of measured area on slides stained by H&E staining. Quantifications were made on H&E stained sections by comparison of bright field and auto-fluorescence. (C) Histomorpho-quantification of bone formation in the 5mm central region of the defect. (D) Examples of direct bone formation on the implanted material on sections stained by H&E. The green picture shows the tissue auto-fluorescence after H&E staining. Bone has an intense green auto-fluorescence. Quantification was made by comparison of bright field and auto-fluorescence with H&E staining. Graph represents the quantified bone in direct contact with the implanted granules (HyC or Botiss). The percentage of bone is normalized to the implanted material area. Graphs show the average and SEM. Statistics are two tailed unpaired t-test, P=0.05.

Chapter IV:

Engineered human bone organs maintain human hematopoiesis in vivo

Manuscript accepted in Experimental Hematology

Engineered humanized bone organs maintain human hematopoiesis *in vivo*

Kristin Fritsch[1,5], Sébastien Pigeot[2,5], Xiaomin Feng[4], Paul E. Bourgine[2,3], Timm Schroeder[3], Ivan Martin[2], Markus G. Manz[1,*], Hitoshi Takizawa[1,4,*]

[1] Hematology, University Hospital Zurich and University of Zurich, CH-8006 Zurich, Switzerland, [2]Department of Biomedicine, University Hospital Basel, University of Basel, Basel, CH-4031 Switzerland, [3]Department of Biosystems Science and Engineering, ETH Zurich, Basel, CH-4058 Switzerland, [4]International Research Center for Medical Sciences, Kumamoto University, Kumamoto 860-0811, Japan, [5]These authors contributed equally

[*]Correspondence: markus.manz@usz.ch or htakizawa@kumamoto-u.ac.jp

Short title: Human hematopoiesis maintained in human ossicles
Category: hematopoietic stem cells, hematopoietic niche
Word count: abstract 174 words; text: 1469 words
Figure: 3 Figures; 3 Supplementary figures
Reference: 17 References

Correspondence :
Prof. Hitoshi Takizawa, Ph.D.
International Research Center for Medical Sciences, Kumamoto University
2-2-1 Honjo, Chuo-ku, Kumamoto 860-0811, Japan
Phone: +81 96 373 6879
htakizawa@kumamoto-u.ac.jp

Highlights

- Human MSCs-derived ossicles can support multi-lineage human hematopoiesis
- Functional human HSPCs are maintained in the human ossicle
- Human HSCs cycle less in human ossicles than in mouse bone marrow

Introduction

Lifelong self-renewing and multilineage repopulating capacity of HSCs is maintained in a specialized microenvironment in the BM, the so-called "niche". Development of genetically modified animals advanced our understanding on the mouse BM niche which consists of a variety of non-hematopoietic cells that provide HSCs with vital factors for their maintenance and quiescence[1]. However, relatively little is known about the cellular and molecular components of the human BM niche, in part due to lack of *in vivo* models recapitulating the human BM microenvironment.

Several studies have suggested that subcutaneous implantation of mouse or human mesenchymal stromal cells (MSCs) into immunodeficient mice results in formation of a bone marrow cavity which is seeded by hematopoietic cells and bony tissues, and which can attract and support murine hematopoiesis[2-6]. A recent study has shown that human BM-derived MSCs are able to form a marrow cavity supporting engraftment of functional human HSCs as well as acute myeloid leukemia (AML)-initiating cells[7,8]. However, to our knowledge, these systems have not been used to study of human HSC quiescence.

We recently reported on a tissue developmental approach in which human BM-derived MSCs *ex vivo* differentiate into hypertrophic cartilage, and, upon implantation *in vivo*, remodel to a fully mature bone organ via endochondral ossification[5]. Here, we show that human ossicles can support multi-lineage hematopoietic repopulation and maintain self-renewal and quiescence of human HSC.

Material and Methods

In vitro MSC culture, and *in vivo* implantation.

Two millions in vitro expanded MSCs from human bone marrow aspirates were seeded onto type I collagen sponges (round disks with 6-mm-diameter and 2-mm-thickness; Ultrafoam, Davol) and cultured in a chondrogenic medium for 3 weeks, followed by another 2 weeks culture in a hypertrophic medium as previously reported[5]. The resulting human cartilage templates were subcutaneously implanted on the back of immunodeficient mice (STRG or MSTRG). Four ossicles were implanted per mice for a total of 121 ossicles, and 4 weeks later, mice were intravenously transplanted with 6-8x10^5 cord blood derived CD34+ cells following sublethal irradiation (400cGy) as previously reported[5,9-11].

Flow cytometry

Cells were isolated from implanted pooled ossicles (4 per mice) and mouse bones and incubated with anti-mouse CD45.2 antibody and human antibodies against mature and immature human hematopoietic cells. For cell cycle analysis, the isolated cells were stained with cell surface markers and intracellularly with anti Ki67 and Hoechst or DAPI.

CFU and Serial transplantation

One thousand human CD45+Lin-CD34+ cells were sorted from ossicles and femurs, respectively, and plated onto cytokine-containing methylcellulose medium (Stem Cell Technologies). Cells were classified by their morphologies and scored after a 12-14 day-incubation. For serial transplantation, 4 $x10^5$ human CD45+CD34+ cells were FAC-sorted from pooled ossicles and femurs, and intravenously transplanted into sublethally irradiated (400cGy) STRG mice without ossicles.

Further materials and methods are provided in the supplemental materials and methods.

Results and Discussion

Human hematopoiesis is repopulated and maintained in human ossicles

To determine ossicle structure and compare human hematopoietic engraftment in human ossicles versus mouse bone marrow, two immunodeficient mice strain (STRG or MSTRG) were implanted with human cartilage templates generated from human MSCs as previously described[5]. One month later, mice were intravenously transplanted with human cord-blood (CB)-derived CD34+ HSPCs and engraftment analysis was performed 8 weeks after hematopoietic cell transplantation (Figure 1A and Supplemental figure 3). Histological and micro-CT analysis revealed that upon *in vivo* implantation, the hypertrophic cartilage underwent extensive remodeling with formation of trabecular bone-like structures, efficient vascularization and increased cellularity, confirming and extending our previous findings[5] (Supplemental Figure 1).

In situ hybridization for human specific sequences (Alu) reveals human cells in close vicinity with bone structures, demonstrating long-term human cell survival (12 weeks post-implantation) and suggesting a functional role of these cells in bone structure formation and maintenance (Supplemental Figure 1C). Flow cytometric analysis identified multi-lineage repopulated hematopoiesis including mature T cells (CD45+CD3+), myeloid cells (CD45+CD3-CD33+), B cells (CD45+CD3-CD33-CD5+CD19+) immature B (CD45+CD3-CD33-CD5-CD19+), pro-B (CD45+CD3-

CD33-CD5-CD19+CD10+CD34+) and pre-B (CD45+CD3-CD33-CD5-CD19+CD10+CD34-) cells in the human ossicles (Figure 1B-C, and supplemental figure 2) at levels as high as in the mouse BM. Furthermore, we also detected immune-phenotypically defined human HSCs (CD34+CD38-CD90+CD45RA-), multipotent progenitor cells (MPP, CD34+CD38-CD90-CD45RA-) multi-lymphoid progenitors (MLP, CD34+CD38-CD90-CD45RA+), common myeloid progenitors/ megakaryocyte-erythrocyte progenitors (CMP/MEP, CD34+CD38+CD45RA-), and granulocyte/macrophage progenitors (GMP, CD34+CD38+CD45RA+) within the myeloid progenitor compartment (MyelP, CD34+CD38+) in the human ossicles (Figure 1D-E). Despite similar human cell engraftment (CD45+), host mouse strain led to significant differences with similar repopulation of hematopoietic stem and progenitor cells (HSPCs) in the human ossicle versus the mouse bone with a significant decrease in MyelP and GMP in the ossicles in STRG mice. On the contrary, MSTRG mice showed significantly higher repopulation and maintenance of HSPC, GMP, MPP and HSC in the ossicles as compared to mouse BM. This might be because additional M-CSF expression enhances HSPC myeloid differentiation in the mouse environment, while human ossicles better maintain HSPC without differentiation. We confirmed the results by calculating the fold change in the frequency of human HSPCs in the ossicles compared to that in BM of the same mouse (Figure 1F-G).

Figure 1.

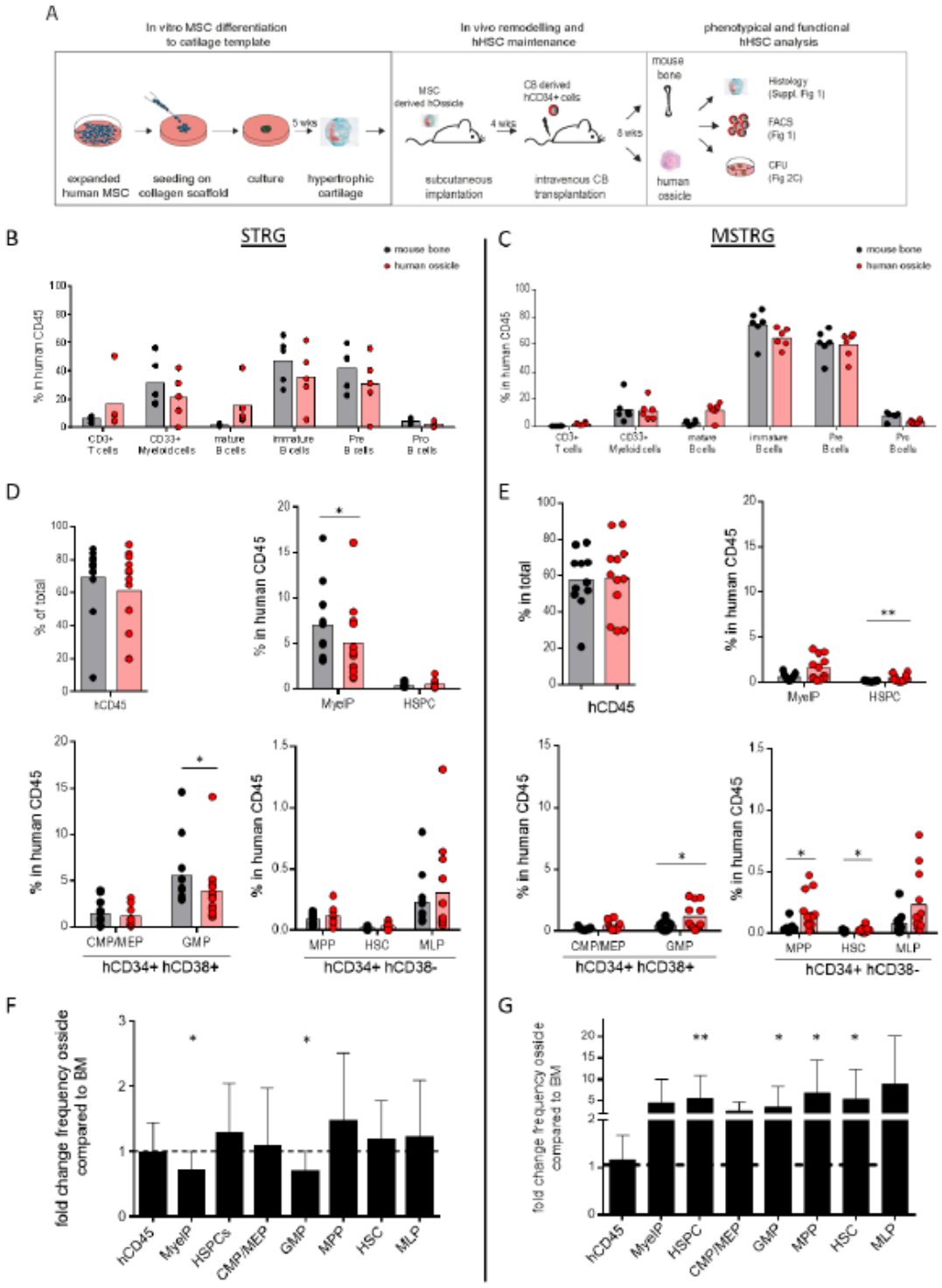

Figure 1. Human bone organs maintain phenotypic human hematopoiesis and hematopoietic stem and progenitor cells. (A) Experimental scheme: human bone marrow mesenchymal stromal cells (BM-MSCs) were cultured on a collagen scaffold for 5 weeks under chondrogenic and hypertrophic conditions, and subcutaneously implanted into STRG or MSTRG mice. At 4 weeks post implantation, the mice were

sub-lethally irradiated and transplanted with human cord blood (CB)-derived CD34+ cells. Eight weeks later, cells were harvested from mouse bones (1 femur and 1 tibia per mouse) and human ossicles (4 pooled ossicles), and analyzed. (B-C) Summary of percentage of mature hematopoiesis in the mouse bones and the *in vivo*-remodeled human ossicles at 8 weeks after CB transplantation. CD3+ T cells, CD45+CD3+; CD33+ myeloid cells, CD45+CD3-CD33+; mature B cells, CD45+CD3-CD33-CD5+CD19+; immature B cells, CD45+CD3-CD33-CD5-CD19+; pre-B cells, CD45+CD3-CD33-CD5-CD19+CD10+CD34-; pro-B cells, CD45+CD3-CD33-CD5-CD19+CD10+CD34+. Bar graphs represent mean of the percentage of indicated population within hCD45+ cells (B, n=5 from one experiment; C, n≥6 from 2 experiments) (D-E) Summary of immature cell analysis. Bar graphs represent mean (D, n=14 from 3 experiments; E, n≥11 from 3 experiments). Engraftment cut-off was >10% hCD45+ cells. (F-G) Fold change of HSCs and progenitors in human ossicles compared to those in mouse bone. Bar graphs represent mean+s.e.m. (n≥11 from 3 experiments).

Multi-lineage repopulating and self-renewing human HSCs are maintained in human ossicles

To test if human ossicles can maintain functional HSPCs, we first performed in vitro myeloid-colony forming unit (CFU) assays with human cells derived from the human ossicles or the corresponding mouse BM from STRG mice. Cells from human ossicles formed significantly higher numbers of myeloid colonies including CFU-G and -GM, as compared to respective cells from the mouse bone (Figure 2A). This demonstrates a higher maintenance of functional HSPCs within CD45+Lin-CD34+ fraction in human ossicles compared to respective populations in mouse BM.

We next assessed the presence of *in vivo* functional, self-renewing human HSCs in the human ossicle by performing serial transplantation in STRG mice. Human CD34+ cells were separately isolated from human ossicles and mouse BM from STRG mice, and intravenously transplanted into sublethally irradiated secondary recipients without ossicle implantation (Figure 2B). Eight weeks later, analysis of secondary recipient mouse BM showed a trend to higher frequencies of mature and immature cellular compartments (HSPCs, HSC, MPP and MLP) in mice transplanted with cells from the human ossicles compared to those transplanted with cells from the mouse BM, suggesting higher self-renewal potential of human ossicle-maintained cells (Figure 2C). Interestingly, the human ossicle-derived CD34+ cells repopulated significantly more mature myeloid cells, an observation that is in line with the increased number of myeloid colonies formed in the CFU assay (Figure 2A).

Despite some lower frequencies in some cases, these data suggest that the human ossicle model provides an optimized environment for maintenance of human self-renewing and repopulating HSCs.

Figure 2.

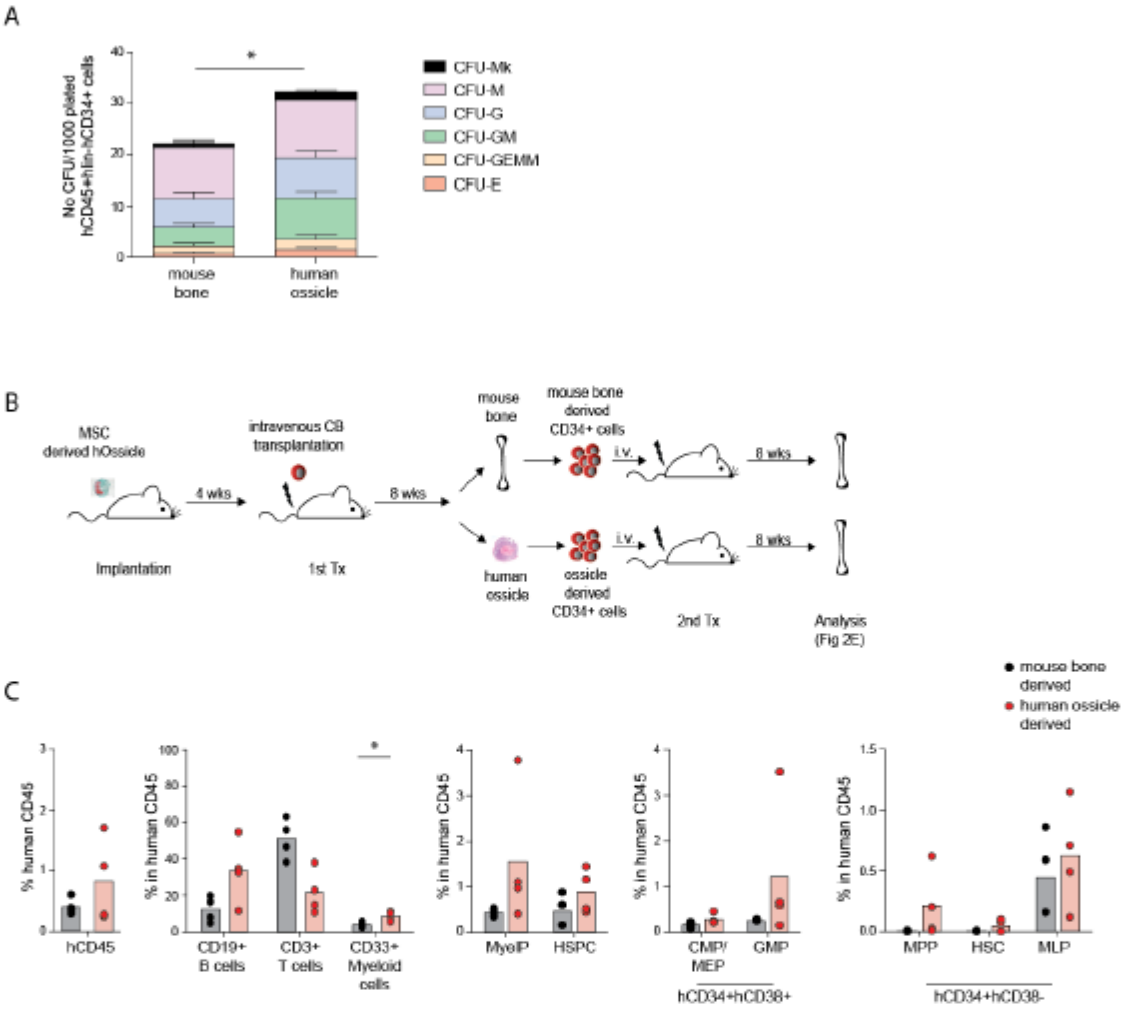

Figure 2. Functional human HSCs are maintained in the implanted human bone organ. (A) Number of hematopoietic colony-forming cells (CFUs) in 1,000 CD45+Lin-CD34+ cells isolated from the mouse bone and from human ossicles (4 pooled ossicles) at 8 weeks after CB transplantation. Graphs represent number of myeloid colony subtypes that are classified at day 14 of culture; CFU-Mk, megakaryocyte; CFU-G or -M, granulocyte or macrophage; CFU-GEMM, mixture of granulocyte, erythrocyte, macrophage and megakaryocyte; CFU-E, erythrocyte; CFU-GM, granulocyte and macrophage. Data are pooled from two independent experiments (n=9). (B) Experimental scheme of serial transplantation: human CD34+ cells from mouse bones and human ossicles were harvested, and enriched for human CD45+CD34+ cells at 8 weeks after primary transplantation (1st Tx). Subsequently, $4x10^5$ sorted CD45+CD34+ cells were transplanted into sub-lethally irradiated STRG

mice (2nd Tx). Eight weeks later, the hematopoietic composition in the mouse bone and human ossicles were analyzed. (C) Summary of percentages of human CD34+ HSPC in mouse BM. Bar graphs represent mean (n=4).

Human HSC are more quiescent in human ossicles compared to mouse bone marrow in MSTRG mice

At any given time, a major fraction of mouse HSCs are in a quiescent phase of cell cycle. This quiescence is mediated through the interaction with the surrounding environment, and HSC quiescence is associated with self-renewal potential[12]. In contrast, human HSCs are highly proliferative in conventional xenograft mouse models[13]. This suggests that the mouse BM does not support human HSC quiescence, which might lead to attenuation of human HSC self-renewal capacity in mouse BM. To test whether human ossicles can maintain human HSCs quiescence, we determined the cell cycle status of human HSPCs in human ossicles and compared it to those in BM of either STRG or MSTRG mouse. Cell cycle analysis revealed that whereas 40% of HSCs in fresh CB were found quiescent as reported previously[14], only a minor fraction of HSPCs (<5%) were quiescent in both human ossicles and BM of STRG mice (Figure 3). On the contrary, MSTRG mice maintained higher HSCs quiescence in the human ossicles (63%) compared to that found in mouse bone (34%) or the fresh cord blood (42%), while the other HSPCs showed similar levels of quiescence (Figure 3B and 3D). It has been shown that M-CSF addition accelerate myeloid differentiation of HSCs as well as myeloid progenitor cells, thereby leading to early recovery of homeostasis[15]. Taking together, our data indicate that additional M-CSF expression in MSTRG BM environment might enhance myeloid differentiation of HSPCs with decreased quiescence, while the human ossicles protect HSCs from proliferation and enhance their quiescence relative to mouse BM, resulting in higher quiescence in the human ossicles. Other factors, such as vascularization might differ within the human ossicles of MSTRG and STRG mice, which might in addition affect oxygen status within the human ossicles, and thus regulate their quiescence through cell metabolism, especially glycolytic pathways.

In summary, using a standardized and reproducible tissue engineering approach we report that human MSC-remodeled ossicles display features of a bone organ with engraftment and maintenance of multi-lineage human hematopoiesis. The human ossicles potentially increase the quiescence and self-renewal of human HSCs. This experimental approach could offer a platform to re-engineer a human niche to

study normal and malignant human hematopoiesis, as well as a preclinical model for the development of new therapies.

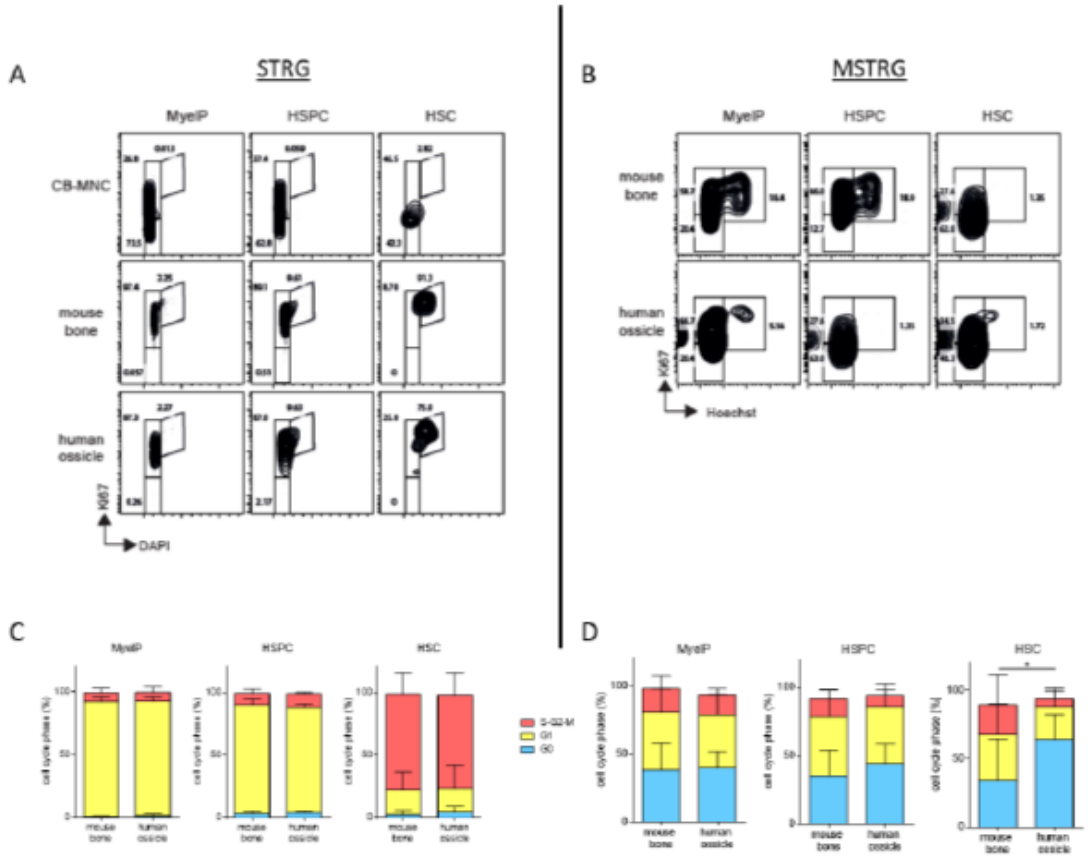

Figure 3. Cell cycle status of human HSCs maintained in the implanted human bone organ. (A and B) Representative cell cycle profiles of immature hematopoiesis in the mouse bones and *in vivo*-remodeled human ossicles at 8 weeks after CB transplantation in STRG (A) and MSTRG (B) mice. (C and D) Summary of percentage of each cell cycle phase of MyeIP, HSPC and HSC in the mouse bone and human ossicles in STRG (C, n=5, single experiment) and MSTRG (D, n≥11, 3 independent experiment) mice. Bars represent mean±SD.

Acknowledgment

This work was supported by the Swiss National Science Foundation (Systems-X program, 2014/266) to T.S., I.M., and by the Swiss National Science Foundation (310030_146528/1), the Promedica Foundation (Chur, Switzerland), and the Clinical Research Priority Program of the University of Zurich to M.G.M, and by Japanese Society of the Promotion of Science (15H05669), The Cell Science Research Foundation, Friends of Leukemia Research Fund, and The Tokyo Biochemical Research Foundation to H.T.

Authorship contribution

K.F., S.P., P.B., and X.F. designed research, performed experiments, analyzed results and wrote the paper. K.F. and S.P. made the figures. T.S., I.M. M.G.M. and H.T., designed research and wrote the paper.

Disclosure of Conflicts of Interest

The authors declare no competing financial interests.

References

1 Morrison, S. J. & Scadden, D. T. The bone marrow niche for haematopoietic stem cells. *Nature* **505**, 327-334, doi:10.1038/nature12984 (2014).
2 Chan, C. K. *et al.* Endochondral ossification is required for haematopoietic stem-cell niche formation. *Nature* **457**, 490-494, doi:10.1038/nature07547 (2009).
3 Sacchetti, B. *et al.* Self-renewing osteoprogenitors in bone marrow sinusoids can organize a hematopoietic microenvironment. *Cell* **131**, 324-336, doi:10.1016/j.cell.2007.08.025 (2007).
4 Kuznetsov, S. A. *et al.* Single-colony derived strains of human marrow stromal fibroblasts form bone after transplantation in vivo. *J Bone Miner Res* **12**, 1335-1347, doi:10.1359/jbmr.1997.12.9.1335 (1997).
5 Scotti, C. *et al.* Engineering of a functional bone organ through endochondral ossification. *Proc Natl Acad Sci U S A* **110**, 3997-4002, doi:10.1073/pnas.1220108110 (2013).
6 Antonelli, A. *et al.* Establishing human leukemia xenograft mouse models by implanting human bone marrow-like scaffold-based niches. *Blood* **128**, 2949-2959, doi:10.1182/blood-2016-05-719021 (2016).
7 Reinisch, A. *et al.* Epigenetic and in vivo comparison of diverse MSC sources reveals an endochondral signature for human hematopoietic niche formation. *Blood* **125**, 249-260, doi:10.1182/blood-2014-04-572255 (2015).
8 Reinisch, A. *et al.* A humanized bone marrow ossicle xenotransplantation model enables improved engraftment of healthy and leukemic human hematopoietic cells. *Nat Med* **22**, 812-821, doi:10.1038/nm.4103 (2016).
9 Rongvaux, A. *et al.* Human thrombopoietin knockin mice efficiently support human hematopoiesis in vivo. *Proc Natl Acad Sci U S A* **108**, 2378-2383, doi:10.1073/pnas.1019524108 (2011).
10 Saito, Y. *et al.* Peripheral blood CD34+ cells efficiently engraft human cytokine knock-in mice. *Blood*, doi:10.1182/blood-2015-10-676452 (2016).
11 Rongvaux, A. *et al.* Development and function of human innate immune cells in a humanized mouse model. *Nat Biotechnol* **32**, 364-372, doi:10.1038/nbt.2858 (2014).
12 Mercier, F. E., Ragu, C. & Scadden, D. T. The bone marrow at the crossroads of blood and immunity. *Nat Rev Immunol* **12**, 49-60, doi:10.1038/nri3132 (2011).
13 Shima, H. *et al.* Acquisition of G(0) state by CD34-positive cord blood cells after bone marrow transplantation. *Exp Hematol* **38**, 1231-1240, doi:10.1016/j.exphem.2010.08.004 (2010).
14 Wilpshaar, J. *et al.* Similar repopulating capacity of mitotically active and resting umbilical cord blood CD34(+) cells in NOD/SCID mice. *Blood* **96**, 2100-2107 (2000).
15 Mossadegh-Keller, Noushine; Sarrazin, Sandrine; Kandalla, Prashanth K.; Espinosa, Leon; Stanley, E. Richard; Nutt, Stephen L. et al. M-CSF instructs myeloid lineage fate in single haematopoietic stem cells. In Nature 497, 239 EP -. DOI: 10.1038/nature12026 (2013).
16 Rathinam, C. *et al.* Efficient differentiation and function of human macrophages in humanized CSF-1 mice. *Blood* **118**, 3119-3128, doi:10.1182/blood-2010-12-326926 (2011).
17 Strowig, T. *et al.* Transgenic expression of human signal regulatory protein alpha in Rag2-/-gamma(c)-/- mice improves engraftment of human hematopoietic cells in humanized mice. *Proc Natl Acad Sci U S A* **108**, 13218-13223, doi:10.1073/pnas.1109769108 (2011).

Supplemental Figures

Supplemental Figure 1.

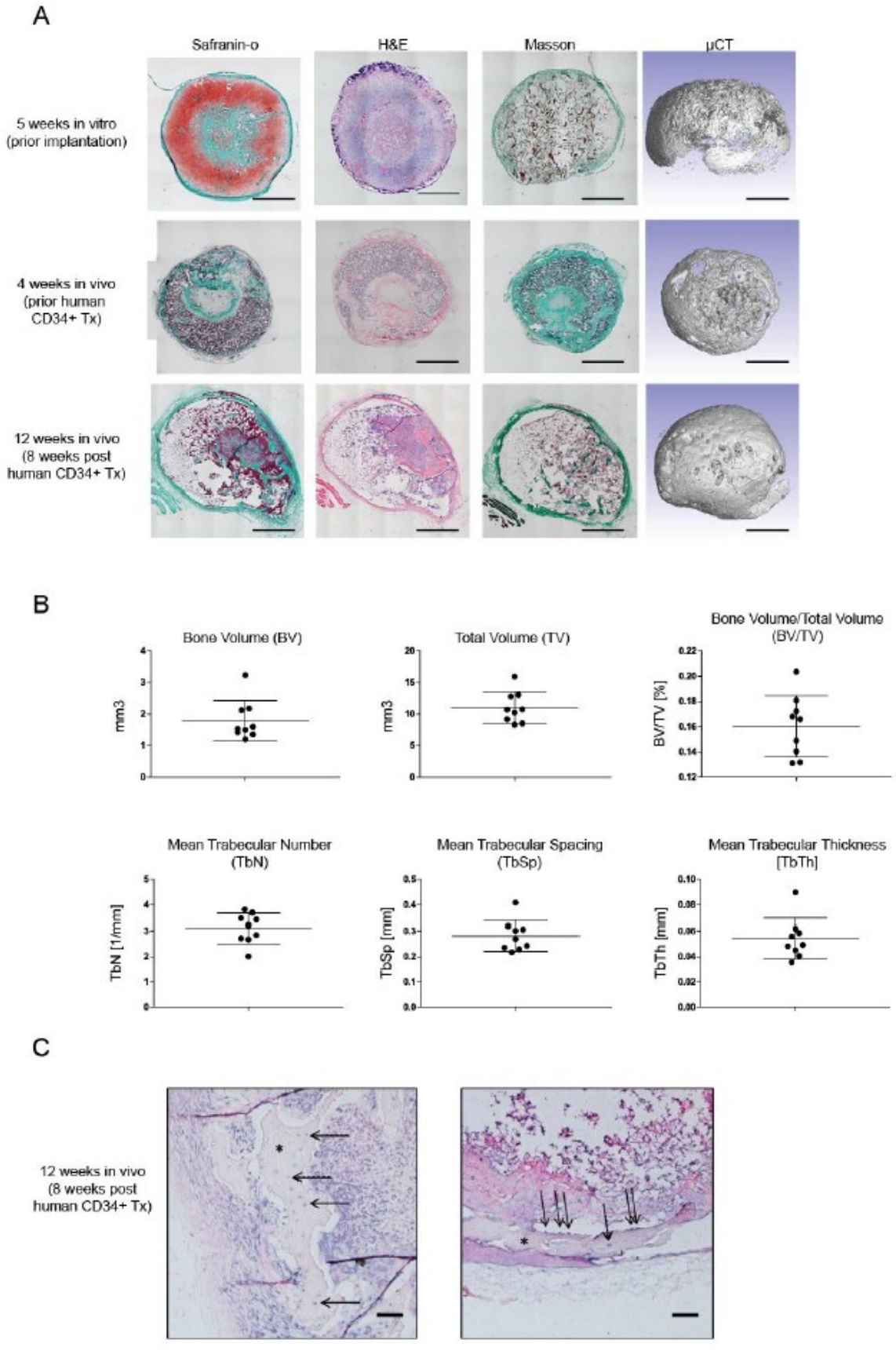

Supplemental Figure 1. Histological characterization of *in vitro* and *in vivo* remodeled human bone tissues.

(A) Representative histological sections (Safranin O, H&E and Masson's Trichrome) and 3D reconstructed micro tomographic (µCT) images of samples after 5 week *in vitro* culture, 4 weeks after implantation *in vivo*, and 12 weeks after implantation and 8 weeks after CB transplantation *in vivo*. Scale bar indicates 1mm. (B) Quantitative histomorphometric data of the total volume of the ossicle (TV) as well as the bone volume within an ossicle (BV) and its ratio (BV/TV). The trabecular bone number (TbN) represents the average number of trabeculae per unit length, their average thickness (TbTh) as well as the mean distance between the trabeculae (TbSp) is represented on the lower graphs (n=9). (C) Alu staining specific for human sequences. Human cells are stained in violet and mouse cells in pink. The staining shows the presence of human cells either embedded in the bone matrix (osteoblast/osteocytes) and on the inner cortical bone as bone lining cells (e.g. osteoblasts).

Supplemental Figure 2

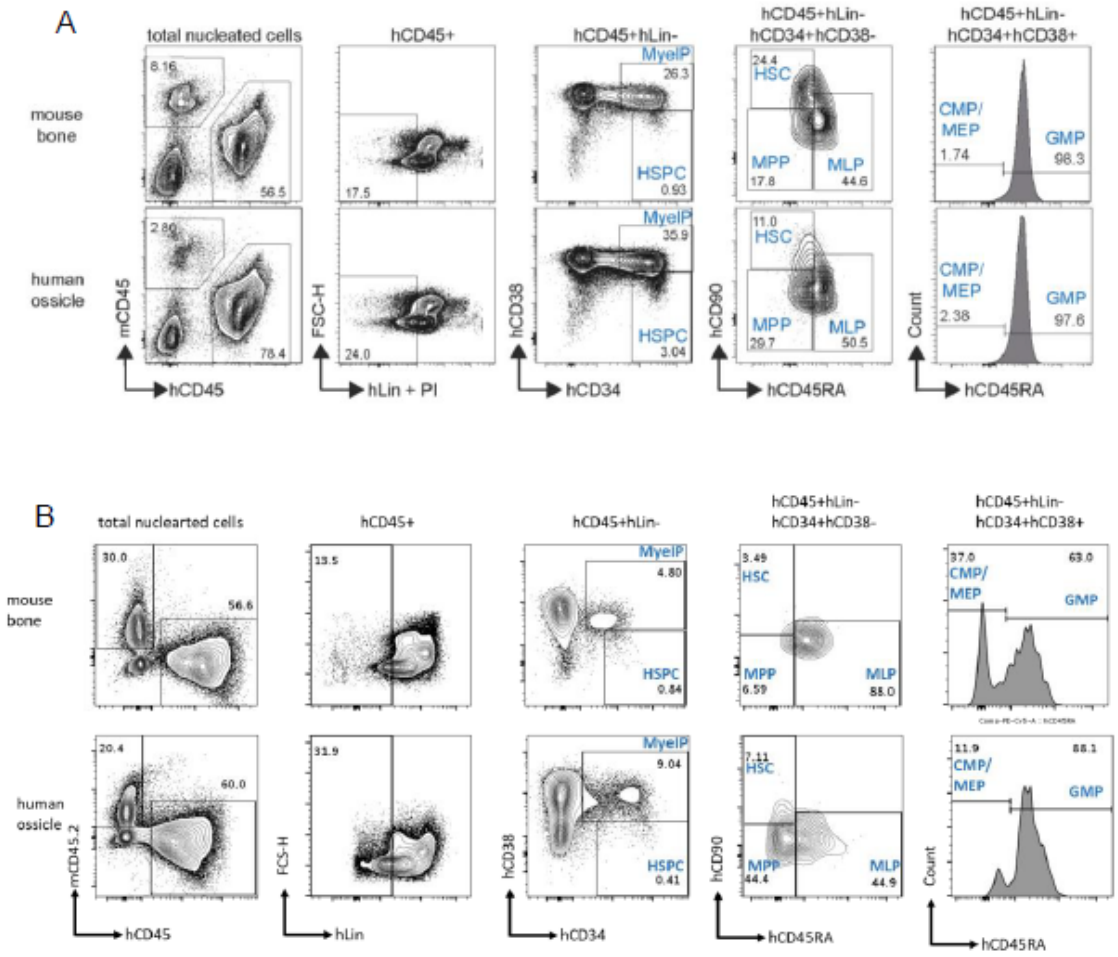

Supplemental Figure 2. Immunophenotype of mature and immature hematopoietic cells in mouse bone and human ossicle engrafted in STRG and MSTRG. Representative immunophenotype of immature hematopoiesis in the mouse bones and the *in vivo*-remodeled human ossicles at 8 weeks after CB transplantation in the STRG mice (A) and the MSTRG mice (B). HSPC, CD45+Lin-CD34+CD38-; MyeIP, CD45+Lin-CD34+CD38+; HSC, CD45+Lin-CD34+CD38-CD90+CD45RA-; MPP, CD45+Lin-CD34+CD38-CD90-CD45RA-; MLP, CD45+Lin-CD34+CD38-CD90-CD45RA+; CMP and MEP, CD45+Lin-CD34+CD38+CD34+CD45RA-; GMP, CD45+Lin-CD34+CD38+CD34+CD45RA+.

Supplemental figure 3

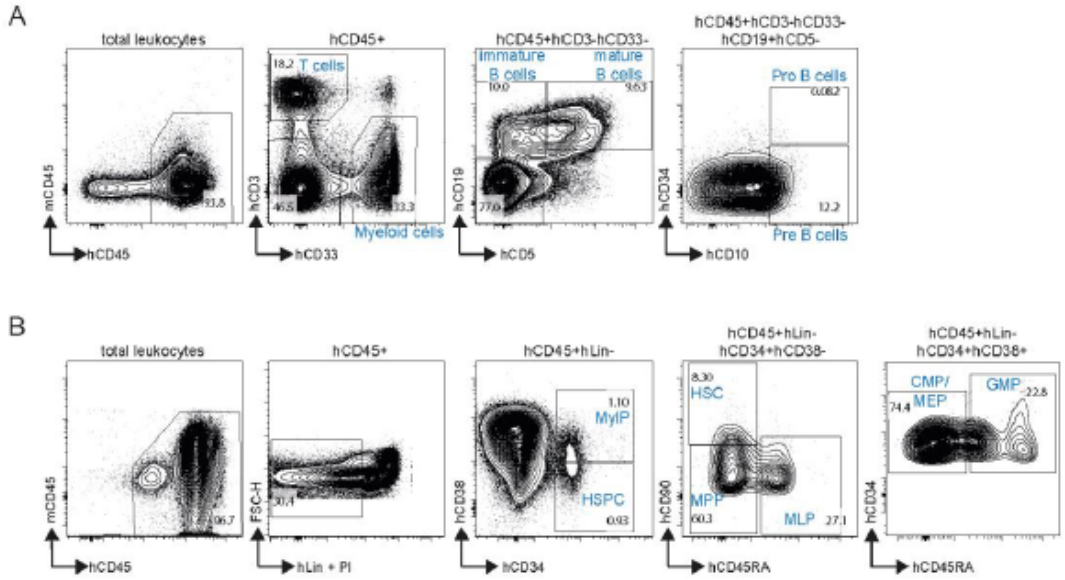

Supplemental Figure 3. Immunophenotype of mature and immature hematopoietic cells in cord blood mononuclear cells. (A) Representative immunophenotype of human mature cells in cord blood mononuclear cells (CB-MNC). Human CD45+ cells are gated for mature T cells (CD45+CD3+CD33-) and myeloid cells (CD45+CD3-CD33+). CD45+CD3-CD33- cells are sub-divided into mature (CD45+CD3-CD33-CD19+CD5+), and immature B cells (CD45+CD3-CD33-CD19+CD5-) that are further differentiated to pre- (CD45+CD3-CD33-CD19+CD5-CD34-CD10+) and pro-B cells (CD45+CD3-CD33-CD19+CD5-CD34+CD10+). (B) Representative immunophenotype of human hematopoietic cells in CB-MNC. Human CD45+, human Lin- cells are gated for hematopoietic stem and progenitor cells (HSPC, CD34+CD38-) and myeloid Progenitors (MyeIP, CD34+CD38+). HSPCs are sub-divided based on CD90 and CD45RA expression into hematopoietic stem cells (HSC, CD90+CD45RA-), multipotent progenitors (MPP, CD90-CD45RA-) and multi-lymphoid progenitors (MLP, CD90+CD45RA+). MyeIP are sub-divided into common myeloid progenitors and megakaryocyte erythroid progenitors (CMP and MEP, CD34+CD45RA-), and granulocyte macrophage progenitors (GMP, CD34+CD45RA+).

Supplemental materials and methods

Mice

hTPO^{KI} hSIRPα^{Tg} Rag2$^{-/-}$ IL2Rcγ$^{-/-}$ Balb/c mice (STRG) or hM-CSF^{KI} hTPO^{KI} hSIRPα^{Tg} Rag2$^{-/-}$ IL2Rcγ$^{-/-}$ Balb/c mice (MSTRG) were generated by intercrossing the human TPO[9] and M-CSF[16] knock-in mouse with human SIRPα transgenic mouse[17]. All mice were maintained at the University Hospital Zurich or Kumamoto University animal facility according to the guidelines of the Swiss Federal Veterinary Office or of Kumamoto University, and all the experiments were approved by the Veterinäramt of Kanton Zurich, Zurich, Switzerland or Kumamoto University.

MSC isolation, *in vitro* culture, and *in vivo* implantation.

Human mesenchymal stromal cells (MSCs) were isolated from human bone marrow aspirates and processed previously reported[5]. The human bone marrow biopsies were approved by the Cantonal ethics committee of Zurich, Switzerland or the ethics committee of Kumamoto University. Shortly, MSCs were expanded for maximum four passages and seeded onto type I collagen meshes (round disks with 6-mm-diameter and 2-mm-thickness; Ultrafoam, Davol) at a density of 33×10^6cells/cm^3 and cultured in a serum-free chondrogenic medium (DMEM supplemented with penicillin-streptomycin glutamine (Invitrogen), HEPES (Invitrogen), sodium pyruvate (Invitrogen), ITS (Insulin, Transferrin, Selenium) (Invitrogen), Human Serum Albumin 0.12% (CSL Behring), 0.1mM ascorbic acid (Sigma), 10^{-7}M dexamethasone (Sigma) and 10ng/ml TGF-β3 (Novartis)) for 3 weeks, followed by another 2 week culture in a serum-free hypertrophic medium, (DMEM supplemented with 50 nM thyroxine, 10mM β-glycerophosphate (Sigma), 10^{-6}M dexamethasone, and 0.1mM ascorbic acid and 50 pg/mL IL-1β (Sigma)). The resultant human cartilage templates were subcutaneously implanted in pouches on the back of 6-10 week old STRG or MSTRG mice (four samples per mouse).

Human progenitor cell isolation and transplantation

Human CD34+ cells were purified from cord blood by density gradient centrifugation and subsequent immunomagnetic positive selection with anti-human CD34 microbeads (Miltenyi Biotec). Cells were frozen in FBS containing 10% DMSO and kept in liquid nitrogen. The human cord blood biopsies were approved by the Cantonal ethics committee of Zurich, Switzerland, and by Kumamoto University. Four weeks after ossicle implantation, 6-8x10^5 CD34+ cells were pooled from several

donors and injected intravenously into sublethally irradiated (400cGy) STRG or MSTRG mice, followed by analysis at 8 weeks after the transplantation.

Flow cytometry

The implanted ossicles, mouse femurs and tibiae were isolated from mice after euthanization, and separately crushed using a mortal and pestle, followed by enzymatic digestion at 37°C for 45 min in DMEM (Invitrogen), 10% FCS (Invitrogen), 10mM HEPES (Invitrogen), 0.4% collagenase II (Worthington) and 0.02% DNase I (Worthington). The resultant cells were filtered on a 70 µm cell strainer and incubated with human and mouse FcR blocking antibodies (Miltenyi Biotec) and the following antibodies: TRI-COLOR conjugated anti-human lineage antibodies (CD2, CD3, CD4, CD8, CD10, CD11b, CD14, CD19, CD20, CD56, CD235a)(Invitrogen); anti-human CD45-eFluor 450 (clone HI30, eBioscience); anti-human CD90-PE (clone 5E10, Beckton Dickinson (BD Biosciences)); anti-human CD38-FITC (clone HIT2, BD Biosciences); anti-human CD34-PECy7 (clone 8G12, BD Biosciences); anti-human CD45RA-APC eFluor 780 (clone HI100, eBioscience); anti-mouse CD45.2-APC (clone 104, Biolegend). Human cell chimerism in peripheral blood (PB) of human ossicle and mouse bone was determined by anti-human CD3-PECy7 (clone UCHT1, eBioscience), anti-human CD19-APCCy7 (clone HIB19, BD Biosciences), anti-human CD33-APC (clone P67.6, BD Biosciences), anti-human CD45-eFluor 450 (clone HI30, eBioscience) and anti-mouse CD45.2-FITC (clone 104, eBioscience). Dead cells were excluded by Propidium Iodide or Hoechest33342 (Invitrogen). All samples were analyzed on a FACS Aria III (BD Biosciences) or LSR Fortessa (BD Biosciences).

CFU and Serial transplantation

For the colony-forming assay, 1,000 human CD45+Lin-CD34+ cells were sorted from ossicles and femurs, respectively, and plated onto methylcellulose medium (Stem Cell Technologies) containing 100 ng/ml human IL-3, 50 ng/ml human IL-6, 50 ng/ml human IL-11, 50 ng/ml human SCF, 250 ng/ml human TPO, 20 U/ml human EPO, 250 ng/ml human GM-CSF and 50 ng/ml human Flt3L. Cells were maintained at 37°C in 5% CO_2 and scored after 12-14 days, and classified to each hematopoietic cell lineages by their morphologies. For serial transplantation, 4 $x10^5$ human CD45+CD34+ cells FACS-sorted from ossicles and femurs, were serially transplanted into sub-lethally irradiated (400cGy) STRG mice without ossicles, followed by monthly PB and terminal BM analysis for human cell engraftment and differentiation.

Cell cycle analysis assay

Single cell suspensions from human ossicles and mouse bones of STRG were extracellularly stained with TRI-COLOR conjugated anti-human lineage antibodies, anti-human CD45-BV711 (clone HI30, Biolegend), anti-mouse CD45-BV786 (clone 30-F11, Biolegend), anti-human CD90-FITC (clone 5E10, BD), anti-human CD38-APC (clone HIT2, BD), anti-human CD34-PECy7 (clone 8G12, BD), anti-human CD45RA-APC eFluor 780 (clone HI100, eBioscience). After washing with PBS containing 2% human serum (Sigma-Aldrich), cells were fixed with Fixation/Permeabilization buffer (eBioscience) for 30min at 4°C. Cells were intracellularly stained with anti-human Ki67-PE (dilution 1:5, BD) for 45 min at room temperature in Permeabilization buffer (eBioscience). After washing, cells were stained with DAPI (1mg/ml, Invitrogen) for 30 min at 4 °C and immediately analysed on a LSR Fortessa (BD Biosciences). For analysis of MSTRG mouse, single cell suspensions from human ossicle or mouse bone of MSTRG mice were stained with anti-human CD90-PE (clone 5E10, Biolegend), anti-mouse CD45.2-Biotin (clone 104, Biolegend), anti-human CD34-PECy7 (clone 8G12, BD), anti-human CD38-APC (clone HIT2, BD), anti-human CD45-APCCy7 (clone HI30, Biolegend) and Streptavidin-PECy5.5 (Biolegend). After 30 min incubation, cells were washed, and fixed with Fix/Perm Buffer (BD Biosciences) for 20 min on ice. Intracellular staining was done by using anti-human Ki67-FITC (clone ki-67, Biolegend) for 30 min on ice in Perm/Wash Buffer (BD Biosciences). Cells were then stained with Hoechst (10ug/ml, Life technologies) for 10 min at room temperature and analyzed on LSR Fortessa or BD FACSCanto™ II (BD Biosciences).

Histological Staining

Decalcified samples were embedded in paraffin and sections of 5 µm thickness prepared using a microtome (Microm, HM430, Thermo Scientific). Safranin-O, Alizarin red, hematoxylin/eosin, Masson tri-chrome and Alu staining were performed as published previously[5].

Microtomography

Samples were collected and fixed overnight in 1.5% formaldehyde at 4°C. Microtomography of the explants was performed using a tungsten x-ray source at 70 kV and 260 µA with an aluminum filter of 0.5 mm (Nanotome, GE, USA). Transmission images were acquired for 360° with an incremental step size of 0.25°.

Volumes were reconstructed using a modified Feldkamp algorithm (software supplied by manufacturer) at a voxel size of 2.5-3 µm. Thresholding, segmentation and 3D measurements were performed using the VGStudio Max software. After microtomography, samples were decalcified in 15% EDTA solution (Sigma Aldrich) before histology.

Statistical analysis

All data are shown as the mean, unless indicated otherwise. All statistical comparisons were evaluated with Students t-Test; *$p<0.05$; **$p<0.01$; ***$p<0.001$ (two-tailed t-test).

Chapter V:

Phenotypic distribution of the human mesenchymal and blood cells in engineered human hematopoietic organs

Manuscript submitted to Leukemia

Phenotypic distribution of the human mesenchymal and blood cells in engineered human hematopoietic organs (150 charac. Max)

Running title: Characterization of customized human ossicles (max. 50 letters and space)

Paul E Bourgine[1], Kristin Fritsch[2], Sebastien Pigeot[3], Hitoshi Takizawa[4], Leo Kunz[1], Konstantinos D Kokkaliaris[1], Daniel L Coutu[1], Markus G Manz[2*], Ivan Martin[3*], Timm Schroeder[1*].

[1] Department of Biosystems Science and Engineering, ETH Zurich, CH-4058 Basel, Switzerland.
[2] Tissue engineering, Department of Biomedicine, University of Basel and University Hospital Basel, CH-4056 Basel, Switzerland.
[3] Hematology, University Hospital Zurich and University of Zurich, CH-8091 Zurich, Switzerland.
[4] International Research Center for Medical Sciences, Kumamoto University, Kumamoto 860-0811, Japan.
* Corresponding authors

Corresponding authors:

Timm Schroeder: Department of Biosystems Science and Engineering (D-BSSE), ETH Zurich Mattenstrasse 26, 4058 Basel, Switzerland. timm.schroeder@bsse.ethz.ch

And

Ivan Martin: Department of Biomedicine, University of Basel and University Hospital Basel, CH-4056 Hebelstrasse 20, Basel, Switzerland. Ivan.martin@usb.ch

And

Markus G Manz: Department of Hematology, University Hospital Zurich and University of Zurich. CH-8091 Rämistrasse 100, Zürich. manz@usz.ch

The authors declare no conflicts of interest.

Text: 4,000 words (excluding references only)

Max number of figures/tables: 8

Max number of references: 60

ABSTRACT (maximum 200 words)

Hematopoietic Stem Cells (HSCs) reside in the bone marrow (BM) niche, a unique microenvironment tightly orchestrating their functions. The cellular and molecular composition of the human BM niche and its interactions with HSCs are predominantly investigated using murine animals, which do not fully reflect the biology of the human system. As promising recent alternative model, human BM-derived mesenchymal stromal cells (hMSCs) are used to generate ectopic human ossicles (hOss) in mice, capable to engraft transplanted human HSCs. However, the functional distribution of the human microenvironment remains to be assessed. Here, we combined the use of genetic tools and confocal microscopy to engineer and subsequently characterize wild type and SDF1α overexpressing hOss. We describe that genetic manipulation of hMSCs is compatible with hOss formation, and allows identifying their fate distribution as human niche cells in a quantitative fashion. We also identified physical interactions between the implanted hMSCs and human CD45+/CD34+/CD90+ hematopoietic cells enriched in functional HSCs, thus supporting the exploitation of hMSCs as a cellular vector for the delivery of factors influencing human blood reconstitution. The design and characterization of customized humanized hematopoietic organs is expected to help decoding the interactions between the hematopoietic and the stromal compartments, within clinically relevant physiological or pathological settings.

INTRODUCTION

The life-long production of all human blood-cell lineages is ensured by hematopoietic stem cells (HSCs)[1,2]. In adults, HSC functions are maintained and tightly regulated in the specialized bone marrow (BM) microenvironment, referred to as BM niche[1,2]. This environment is defined by unique physical properties[3–5] and includes differentiated cells, extracellular matrix and signaling factors[6,7] essential for cell differentiation, survival[8] and self-renewal[1,9]. However, the precise cellular and molecular composition of the human hematopoietic niche remains elusive[10]. Our understanding of human hematopoiesis largely relies on the analogy made with the mouse system[11]. In reality, despite commonly inherited genetic traits, HSC basic biology differs across species and the corresponding interactions with their niches are not fully conserved[10,12]. In consequence, information derived from

murine studies does not systematically correlate with the human system, raising concerns about their direct relevance toward therapeutic developments[12].

Advanced xenotransplantation models offer robust engraftment and development of human hematopoiesis in mouse bones[13]. This has significantly contributed to the progressive understanding of human HSC functions in healthy and pathological set-ups[14,15]. However, such humanized mouse models are incompatible with the organizational and functional study of the HSC niche, since the BM microenvironment remains entirely murine.

As an alternative, the possibility to engineer ectopic humanized ossicles (hOss) using human BM-derived mesenchymal stromal cells (hMSCs) is receiving increasing attention[14,16,17], with demonstration of robust human blood engraftment in both healthy and malignant scenarios[14,18,19]. While this is attributed to the presence of hMSCs, their contribution in the functional organization of the niche remains to be investigated.

Here, we propose the genetic engineering of hMSCs together with the use of a recently developed deep multicolor imaging confocal analysis[20] in order to achieve a first quantitative assessment of the distribution and role of hMSCs in hOss. We previously reported a developmental approach to bone organ formation, by *in vitro* chondrogenic priming of hMSCs. Following hypertrophic cartilage (hyC) formation, the generated tissues remodel into hOss upon subcutaneous implantation in humanized mice[16] by recapitulating the endochondral ossification process[21]. We target the further exploitation of this approach to engineer and characterize customized hematopoietic bone organs - here exemplified by the generation of niches overexpressing stromal derived factor 1 alpha (SDF1α) –, in order to assess the composition and distribution of the human cellular compartments.

The validation of the methodology bears relevance toward deciphering the human hematopoietic system using advanced and modular/tunable models of higher translational relevance.

METHODS

Isolation and culture of hMSCs

hMSCs were isolated from human bone-marrow aspirates from the iliac crest, after ethical approval (EKBB, Ref. 78/07) and informed donor consent from patients. Bone marrow aspirates (20 mL volume) were harvested from healthy donors (N≥3) using a biopsy needle inserted through the cortical bone, and immediately transferred into plastic tubes

Data are presented as means ± standard error of the mean and were analyzed using the GraphPad Prism software. Single comparison was performed using the non-parametric Mann Whitney t-test assuming a non-gaussian distribution of the values. Multiple comparisons were performed using the one way ANOVA assuming a non-gaussian distribution of the values. Statistical significant differences were defined as: * =$p < 0.05$, ** = $p < 0.01$, *** = $p < 0.001$.

RESULTS

Primary hMSCs can be genetically engineered without altering their capacity to form hypertrophic cartilage

Prior to cartilage formation, hMSCs were transduced (**Figure 1A**) using a VENUS (mock control) or VENUS-SDF1α lentivirus respectively (**Supplementary Figure S4A**). The transduction allowed the generation of homogenous VENUS and VENUS-SDF1α hMSCs populations (> 93% and 96% using VENUS and VENUS-SDF1α viruses respectively, **Figure 1B**). The VENUS-SDF1α transduction led to a significant SDF1α overexpression (31-fold increase in RNA levels as compared to VENUS hMSCs, **Figure 1C**).

Cells were subsequently seeded on collagen meshes and primed to form hyC. Over the 5 week course of *in vitro* culture, the total number of cells in the hyC remained stable ($1.3x10^6$ and $1.2\ x10^6$ at week 1 and week 5 respectively, **Supplementary Figure S4B**). During this period, the monitoring of proteins in hyC supernatant revealed comparable release profiles of angiogenic (vascular endothelial growth factor - VEGF), osteoinductive (bone morphogenetic protein 2 – BMP-2), bone remodeling (matrix metalloproteinase 13 - MMP-13), and inflammatory (interleukin 8 – IL-8) factors, suggesting similar development of the templates by untransduced (primary hyC) or transduced hMSCs (VENUS and VENUS-SDF1α hyC) (**Figure 1D**). VENUS-SDF1α hyC secreted significantly higher amounts of SDF1α (4-fold increase at Day 3, **Figure 1D**) though a progressive decrease was observed over time.

At the end of the *in vitro* culture, histological analysis indicated the successful formation of mature hyC in all groups, characterized by the large presence of glycosaminoglycans (Safranin-O, **Figure 1E**) and a mineralized ring at the periphery of the tissue (Alizarin red, **Figure 1E**). Differentiation was confirmed by RT-PCR, revealing activation of chondrogenic (Collagen 2, Sox 9, **Figure 1F**) and hypertrophic genes (RUNX2, ALP, BSP, OSX, **Figure 1F**) in

all hyC. Importantly, VENUS-SDF1α hyC were shown to maintain a marked SDF1α overexpression (**Figure 1F**) as compared to primary and VENUS hyC.

Hypertrophic cartilage with a targeted SDF1α enrichment can be generated

After demonstrating the similar quality of hyC derived from primary or VENUS hMSCs, VENUS hyC were further used as the control group allowing for the tracing of hMSCs via the VENUS signal.

Multicolor confocal analysis of thick hyC sections was performed to investigate the presence and distribution of cells and SDF1α in the templates. VENUS cells were homogenously distributed within the tissue, largely embedded into a collagen type 2-rich matrix with detectable SDF1α proteins (**Figure 2A**). High resolution imaging revealed presence of the cytokine intracellularly in both VENUS and VENUS-SDF1α cells in their corresponding hyC (**Figure 2B**). The SDF1α protein was also found associated with the ECM, as shown by colocalization with collagen type 2, in a more abundant fashion in VENUS-SDF1α samples (**Figure 2B**). To confirm microscopic observations, hyC constructs were lysed and assessed for their content in a panel of growth factors, including SDF1α. VENUS and VENUS-SDF1α hyC displayed comparable proteins content (**Figure 2C** and **Supplementary Figure S4C**) except a 2-fold SDF1α enrichment in the VENUS-SDF1α templates (**Figure 2C**). We thus report the successful tuning of cartilage tissue's composition, through a targeted enrichment in SDF1α content.

The findings above suggest that the previously observed marked decrease of secreted SDF1α over culture time is due to its embedding in the ECM. This applies to VEGF and IL-8, and proteins with undetectable levels in the supernatant were also shown to be incorporated within the ECM of hyC (thrombopoietin - TPO, interleukin 6 - IL-6, matrix metalloproteinase - MMP-9, **Supplementary Figure S4C**). Thus, the engineered hyC consisted of mature cartilage tissues containing a large panel of pro-angiogenic (VEGF, Monocyte chemotactic protein 1 - MCP-1), osteoinductive (BMP-2, bone morphogenetic protein 4 - BMP-4), bone remodeling factors (MMP-9, MMP-13), but also inflammatory cytokines (IL-6, IL-8, Granulocyte colony-stimulating factor - G-CSF, Macrophage colony-stimulating factor - M-CSF) and factors associated with hematopoietic stem cell maintenance (TPO, stem cell factor - SCF, Fms-related tyrosine kinase 3 ligand - Flt3-L).

Molecularly engineered hyC can remodel into humanized bone organs and comprise human MSCs partially reconstituting the human niche

In vitro engineered VENUS and VENUS-SDF1α hyC were subcutaneously implanted in mice (**Figure 3A**). After 6 weeks, when constructs are expected to be remodeled into bone tissue, animals were intravenously transplanted with CD34+ cord-blood derived hematopoietic cells to reconstitute human hematopoiesis (**Figure 3A**). After a total *in vivo* period of 12 weeks, VENUS and VENUS-SDF1α constructs remodeled into ectopic ossicles exhibiting macroscopic evidence of vascularization (**Figure 3B**). Microtomography scans (**Figure 3C**) revealed the formation of mature bone tissue with no quality differences between the two hOss types, consisting in a spheroid organ of 18 ±2.1 mm^3 (**Supplementary Figure S6C**).

Deep confocal analysis on both types of hOss was performed to obtain a comprehensive understanding of the reconstituted BM environment. Progressive sectioning of hOss allowed gathering substantial 3D information (**Figure 3D** and **Supplementary Figure S5A**), and indicated an intense vascularization surrounding the hOss with its cavity largely filled by BM cells (**Figure 3D** and **Supplementary Figure S5A**). The hOss were also shown to be connected to the host nervous system as shown by evidences of innervation (peripherin, **Supplementary Figure S5B**).

The presence of hMSCs in both VENUS and VENUS-SDF1α organs was evidenced by the VENUS signal. Staining with SDF1α revealed the strong presence of the protein in the marrow (**Figure 3E**), highly expressed by blood cells[23]. The SDF1α protein could still be detected in hMSCs-derived cells from VENUS-SDF1α hOss (**Figure 3E**). Remarkably, in the engineered hOss hMSCs were associated with an important fate diversity following the remodeling of hyC. This includes hMSCs abundantly found in the bone marrow stroma, exhibiting a fibroblastic-like shape and positivity for CD90 (Stromal cells, **Figure 3F**), but also hMSCs differentiated into the osteogenic lineage in the form of osteocytes embedded in the bone matrix (Osteocytes, **Figure 3F**) and lining osteoblasts (Osteoblasts, **Figure 3F**). HMSCs were also found in close association with the vasculature (Vascular associated, **Figure 3F**), both to arterioles and sinusoids (**Supplementary Figure S5C**). To a lower extent, we also identified hMSCs differentiated into the adipogenic lineage, as shown by the presence of VENUS positive adipocytes (**Supplementary Figure S5D**).

The fate quantification of the hMSC populations in both VENUS and VENUS-SDF1α organs was performed by applying isosurface segmentation strategies. We first segmented the

VENUS signal (**Supplementary Figure S6A**) in corresponding hOss sections (**Supplementary Figure S6B**), and normalization with the mean volume of hOss (**Supplementary Figure S6C**) allowed us obtaining the average number of hMSCs objects per hOss. From the $1.2x10^6$ hMSCs present in the hyC at the time of implantation, only $0.1x10^6$ were still populating the hOss, corresponding to a 90% decrease (**Supplementary Figure S6D**). To corroborate this finding, flow-cytometry quantification of VENUS cells after hOss digestion was also performed, estimating the number of hMSCs per hOss at 0.06M (**Supplementary Figure S6D**), but this method likely does not allow for the efficient retrieval of bone embedded cells.

Further segmentation strategies (**Supplementary Figure S7A** and **S7B**) allowed quantifying the previously identified populations. In both hOss types, VENUS cells were abundantly found within the stromal compartment (Stromal, 45% and 47% in VENUS and VENUS-SDF1α hOss respectively, **Figure 3G**). A large fraction (47% and 50%, respectively; **Figure 3G**) was directly associated with vasculature (0-1µm distance to vessels), as confirmed by random dots distribution (**Supplementary Figure S7C**). In addition, osteocytes were found to represent respectively 36% and 41% of VENUS cells (**Figure 3G**) while osteoblasts were less abundant (19% in VENUS hOss versus 12% in VENUS-SDF1α hOss, **Figure 3G**). No significant differences could be observed between VENUS and VENUS-SDF1α hOss indicating that the hMSCs genetic modification did not impact on their subsequent fate decisions upon hOss formation.

Human niche cells and human hematopoietic stem/progenitor cells are in close vicinity in humanized ossicles

Flow cytometry of retrieved hOss and corresponding mouse bones (**Supplementary Figure S8A** and **S8B**) revealed the engraftment of human blood cells, as shown by an average hCD45 chimerism level of 40% (**Figure 4A**). VENUS hOss and mouse bones displayed comparable frequencies of naïve and more committed blood populations (**Figure 4A**). In the hOss overexpressing SDF1α, significantly higher frequencies of MPPs and CMPs/MEPs (2.7 and 2.4 fold increase respectively) and superior HSPCs and HSCs content (1.8 and 1.9 fold increase respectively) were observed although without reaching significance. No differences between mouse bones and either hOss conditions were found in the GMPs or MyLPs compartments (**Supplementary Figure S8C**). The functionality of hCD45/CD34+ cells

retrieved from mouse bones or hOss was evaluated by *in vitro* colony formation unit (cfu) assays. Cells were capable to efficiently give rise to all myeloid colonies but the hCD45/CD34+ fraction derived from hOss displayed a significantly higher potential to form hematopoietic colonies (**Supplementary Figure S8D**), including GEmM, than the corresponding population retrieved from mouse bones. No differences were observed between cells retrieved from VENUS or VENUS-SDF1α hOss, suggesting that the SDF1α overexpression did not impact on stem and progenitor functionality. These data validate the generation of SDF1α-customized hOss, composed of an increased frequency of HSPCs without alterations of their functionality.

We further performed confocal microscopy to assess the distribution of human blood cells in the hOss. Those were shown to form heterogenous "islets" of human hematopoiesis in the bone marrow compartment (**Figure 4B**). Multicolor staining was used to identify hMSCs-derived niche cells (positive for VENUS) and particular HSPC populations within engineered hOss. This allowed the localization of a rare subset of HSPCs (hCD45+/CD34+/CD90+) enriched in functional HSCs, which was consistently in close proximity (less than 1µm distance) with VENUS-cells, in both VENUS and VENUS-SDF1α niches (n=9, **Figure 5C**). This singular physical interaction between the human stromal and naïve hematopoietic compartments validates the possibility to combine the use of deep multicolor confocal microscopy, genetic tools and the hOss model to study human niche cells/hematopoietic cells interplay.

DISCUSSION

We report the engineering and characterization of customized human hematopoietic bone organs. The method relies on the genetic modification of primary hMSCs, their priming to recapitulate the developmental program of endochondral ossification[21], and quantitative multidimensional imaging of the reconstituted human bone marrow environment.

The study of hematopoiesis in a humanized context is a primary challenge. The generation of transgenic animals supporting human engraftment is associated with some limitations[24], including a time-consuming single gene targeting, the unpredictable biological outcome (e.g., embryonic lethality, low efficiency, absence of recognizable phenotypes), and often non-tissue specific if at all conditional. Instead, our strategy relies on the exploitation and characterization of the hOss model, using hMSCs as cellular vector for the targeted delivery

of factors influencing the composition of the human blood compartment. The introduced modification is thus strictly related to the BM tissue as ensured by hMSCs-derived niche cells.

The biological validation of the method was performed using SDF1α as a known factor influencing stem cell behavior. SDF1α has been reported both as stem cell chemo-attractant[25–27] and pro-quiescent molecule[28,29], thus offering multiple readouts to validate the effects of its overexpression in hOss. We successfully measured a clear enrichment in CMPs/MEPs, MPPs and HSCs populations in the hOss overexpressing SDF1α. Interestingly, the association of SDF1α with proteoglycans – main constituents of cartilaginous ECM[30] - was reported to strongly promote the migration of HSPCs[31]. This might suggest that the observed effects result from preferential homing at the time of engraftment[25], though a different cycling rate of HSPCs cannot be excluded. Importantly, the molecular modification was shown to specifically impact the human blood composition while not affecting the fate and distribution of implanted hMSCs. The capacity to manipulate hMSCs without impairing their endochondral program was a pre-requisite for the direct assessment of possible SDF1α effects.

Despite pre-existing molecular engineering approaches[32,33], current xenografts models poorly characterized the reconstituted human environment. Here, we used advanced microscopy tools to monitor hMSCs within the engineered tissues, from the *in vitro* hyC stage to the fully remodeled hOss. As easily accessible organs tunable in size, quantitative 3D information on the hOss cellular composition could be retrieved, and offered a comprehensive understanding of the human niche in this *in vivo* setting. This revealed that hMSCs displayed an unsuspected degree of plasticity in the model, giving rise to several niche phenotypes, including lining osteoblasts, osteocytes, stromal cells and adipocytes. Distance analyses revealed a strong association of hMSCs with vasculature, but also direct physical interactions with HSPCs. Importantly, only a reduced fraction of hMSCs were found in the engineered hOss. This can be explained by the extensive *in vitro* and *in vivo* period combined with the limited self-renewing capacity of hMSCs that were primed toward differentiation[34,35]. It also leaves space for optimization of the approach to achieve superior degree of humanization. The use of immortalized hMSCs[36,37] could represent a valuable option, with the combined advantage to potentially increase the standardization of cartilage

and bone organ production, and reduce the substantial variations associated with humanized models[22].

However, despite a limited number hMSCs had significant effects on the engraftment of human blood cells. These findings reinforced the idea that hMSCs are key cellular players of the hematopoietic niche[1,2], and suggest a contact-triggered regulation of HSPCs by the mesenchymal compartment, which was so far only previously reported in mouse studies[22].

Collectively, the essential role of hMSCs and their proximity to HSPCs in the hOss model supports their use for the delivery of putative niche factors. The paradigm of engineered customized human HSC niches, here exemplified with SDF1α, can be further explored with additional factors putatively affecting stem cell homing/localization/function in healthy or pathological scenarios (e.g. by engraftment of leukemic primary material), but also impacting the human niche compartment. In fact, in addition to the blood compartment the hOss could be valuable for the identification of specific human niche cells populations, derived from the implanted hMSCs. This could reveal to be of particular importance in pathologic scenarios, in which the role of the stroma and associated factors in disease evolution remain elusive[11,38]. Our model could thus help deciphering the complex phenotypes and functions associated with hMSCs[35,39] in myeloid and/or lymphoid malignancies.

ACKNOWLEDGEMENTS

This study was supported in part by the SystemsX (StemSysMed grant #2014/266 to MGM, TS and IM), and Division III programs (grant # 31003A_156430 to IM) of the Swiss National Science Foundation.

AUTHORSHIP CONTRIBUTIONS

PEB, IM, TS and MGM designed the research. PEB, KF and SP performed experiments. PEB, KF, SP, HT, LK, KK and DC analyzed data. PEB, TS, IM and MGM wrote the manuscript. TS, IM and MGM financed the project.

DISCLOSURE OF CONFLICTS OF INTEREST

The authors declare no conflicts of interest.

REFERENCES

1 Méndez-Ferrer S, Michurina T V, Ferraro F, Mazloom AR, Macarthur BD, Lira SA *et al.* Mesenchymal and haematopoietic stem cells form a unique bone marrow niche. *Nature* 2010; **466**: 829–34.

2 Morrison SJ, Scadden DT. The bone marrow niche for haematopoietic stem cells. *Nature* 2014; **505**: 327–34.

3 Guilak F, Cohen DM, Estes BT, Gimble JM, Liedtke W, Chen CS. Control of Stem Cell Fate by Physical Interactions with the Extracellular Matrix. Cell Stem Cell. 2009; **5**: 17–26.

4 Keung AJ, Healy KE, Kumar S, Schaffer D V. Biophysics and dynamics of natural and engineered stem cell microenvironments. Wiley Interdiscip. Rev. Syst. Biol. Med. 2010; **2**: 49–64.

5 Engler AJ, Sen S, Sweeney HL, Discher DE. Matrix Elasticity Directs Stem Cell Lineage Specification. *Cell* 2006; **126**: 677–689.

6 Zhang CC, Lodish HF. Cytokines regulating hematopoietic stem cell function. *Curr Opin Hematol* 2008; **15**: 307–311.

7 Rieger MA, Hoppe PS, Smejkal BM, Eitelhuber AC, Schroeder T. Hematopoietic cytokines can instruct lineage choice. *Science* 2009; **325**: 217–218.

8 Knapp DJHF, Hammond CA, Aghaeepour N, Miller PH, Pellacani D, Beer PA *et al.* Distinct signaling programs control human hematopoietic stem cell survival and proliferation. *Blood* 2016; **129**: 307–319.

9 Kunisaki Y, Frenette PS. The secrets of the bone marrow niche: Enigmatic niche brings challenge for HSC expansion. *Nat Med* 2012; **18**: 864–865.

10 van Pel M, Fibbe WE, Schepers K. The human and murine hematopoietic stem cell

niches: Are they comparable? Ann. N. Y. Acad. Sci. 2015. doi:10.1111/nyas.12994.

11 Schepers K, Campbell TB, Passegu?? E. Normal and leukemic stem cell niches: Insights and therapeutic opportunities. Cell Stem Cell. 2015; **16**: 254–267.

12 Doulatov S, Notta F, Laurenti E, Dick JE. Hematopoiesis: A human perspective. Cell Stem Cell. 2012; **10**: 120–136.

13 Rongvaux A, Willinger T, Martinek J, Strowig T, Gearty S V, Teichmann LL *et al.* Development and function of human innate immune cells in a humanized mouse model. *Nat Biotechnol* 2014; **32**: 364–372.

14 Reinisch A, Thomas D, Corces MR, Zhang X, Gratzinger D, Hong W-J *et al.* A humanized bone marrow ossicle xenotransplantation model enables improved engraftment of healthy and leukemic human hematopoietic cells. *Nat Med* 2016; **22**: 812–821.

15 Antonelli A, Noort WA, Jaques J, de Boer B, de Jong-Korlaar R, Brouwers-Vos AZ *et al.* *Establishing human leukemia xenograft mouse models by implanting human bone marrow-like scaffold-based niches*. 2016 doi:10.1182/blood-2016-05-719021.

16 Scotti C, Piccinini E, Takizawa H, Todorov A, Bourgine P, Papadimitropoulos A *et al.* Engineering of a functional bone organ through endochondral ossification. *Proc Natl Acad Sci U S A* 2013; **110**: 3997–4002.

17 Bourgine PE, Scotti C, Pigeot S, Tchang LA, Todorov A, Martin I. Osteoinductivity of engineered cartilaginous templates devitalized by inducible apoptosis. *Proc Natl Acad Sci U S A* 2014; **111**: 17426–31.

18 Abarrategi A, Foster K, Hamilton A, Mian SA, Passaro D, Gribben J *et al.* Versatile humanized niche model enables study of normal and malignant human hematopoiesis. *J Clin Invest* 2017; **127**: 543–548.

19 Martine LC, Holzapfel BM, McGovern JA, Wagner F, Quent VM, Hesami P *et al.*

Engineering a humanized bone organ model in mice to study bone metastases. *Nat Protoc* 2017; **12**: 639–663.

20 Coutu DL, Kokkaliaris KD, Kunz L ST. Three-dimensional map of non-hematopoetic bone and bone marrow cells and molecules. *Nat Biotechnol* 2017.in press.

21 Kronenberg HM, Kronenberg HM. Developmental regulation of the growth plate. *Nature* 2003; **423**: 332–6.

22 Rongvaux A, Willinger T, Takizawa H, Rathinam C, Auerbach W, Murphy AJ *et al.* Human thrombopoietin knockin mice efficiently support human hematopoiesis in vivo. *Proc Natl Acad Sci U S A* 2011; **108**: 2378–83.

23 Dar A, Kollet O, Lapidot T. Mutual, reciprocal SDF-1/CXCR4 interactions between hematopoietic and bone marrow stromal cells regulate human stem cell migration and development in NOD/SCID chimeric mice. Exp. Hematol. 2006; **34**: 967–975.

24 Devoy A, Bunton-Stasyshyn RK a, Tybulewicz VLJ, Smith AJH, Fisher EMC. Genomically humanized mice: technologies and promises. *Nat Rev Genet* 2012; **13**: 14–20.

25 Lapidot T, Kollet O. The essential roles of the chemokine SDF-1 and its receptor CXCR4 in human stem cell homing and repopulation of transplanted immune-deficient NOD/SCID and NOD/SCID/B2mnull mice. *Leukemia* 2002; **16**: 1992–2003.

26 Aiuti A, Webb IJ, Bleul C, Springer T, Gutierrez-Ramos JC. The chemokine SDF-1 is a chemoattractant for human CD34+ hematopoietic progenitor cells and provides a new mechanism to explain the mobilization of CD34+ progenitors to peripheral blood. *J Exp Med* 1997; **185**: 111–20.

27 Mohle R, Bautz F, Rafii S, Moore MA, Brugger W, Kanz L. The chemokine receptor CXCR-4 is expressed on CD34+ hematopoietic progenitors and leukemic cells and mediates transendothelial migration induced by stromal cell-derived factor-1. *Blood*

1998; **91**: 4523–4530.

28 Itkin T, Lapidot T. SDF-1 keeps HSC quiescent at home. Blood. 2011; **117**: 373–374.

29 Tzeng YS, Li H, Kang YL, Chen WG, Cheng W, Lai DM. Loss of Cxcl12/Sdf-1 in adult mice decreases the quiescent state of hematopoietic stem/progenitor cells and alters the pattern of hematopoietic regeneration after myelosuppression. *Blood* 2011; **117**: 429–439.

30 Roughley PJ, Lee ER. Cartilage proteoglycans: Structure and potential functions. Microsc. Res. Tech. 1994; **28**: 385–397.

31 Netelenbos T, Zuijderduijn S, Van Den Born J, Kessler FL, Zweegman S, Huijgens PC *et al.* Proteoglycans guide SDF-1-induced migration of hematopoietic progenitor cells. *J Leukoc Biol* 2002; **72**: 353–62.

32 Carretta M, de Boer B, Jaques J, Antonelli A, Horton SJ, Yuan H *et al.* Genetically engineered mesenchymal stromal cells produce IL-3 and TPO to further improve human scaffold-based xenograft models. *Exp Hematol* 2017; **51**: 36–46.

33 Chen Y, Jacamo R, Shi YX, Wang RY, Battula VL, Konoplev S *et al.* Human extramedullary bone marrow in mice: A novel in vivo model of genetically controlled hematopoietic microenvironment. *Blood* 2012; **119**: 4971–4980.

34 Ito K, Suda T. Metabolic requirements for the maintenance of self-renewing stem cells. *Nat Rev Mol Cell Biol* 2014; **15**: 243–256.

35 Nombela-Arrieta C, Ritz J, Silberstein LE. The elusive nature and function of mesenchymal stem cells. *Nat Rev Mol Cell Biol* 2011; **12**: 126–131.

36 Shi S, Gronthos S, Chen S, Reddi A, Counter CM, Robey PG *et al.* Bone formation by human postnatal bone marrow stromal stem cells is enhanced by telomerase expression. *Nat Biotechnol* 2002; **20**: 587–591.

37 Bourgine P, Le Magnen C, Pigeot S, Geurts J, Scherberich A, Martin I. Combination of immortalization and inducible death strategies to generate a human mesenchymal stromal cell line with controlled survival. *Stem Cell Res* 2014; **12**: 584.

38 Schepers K, Pietras EM, Reynaud D, Flach J, Binnewies M, Garg T *et al.* Myeloproliferative neoplasia remodels the endosteal bone marrow niche into a self-reinforcing leukemic niche. *Cell Stem Cell* 2013; **13**: 285–299.

39 Mo M, Wang S, Zhou Y, Li H, Wu Y. Mesenchymal stem cell subpopulations: phenotype, property and therapeutic potential. Cell. Mol. Life Sci. 2016; **73**: 3311–3321.

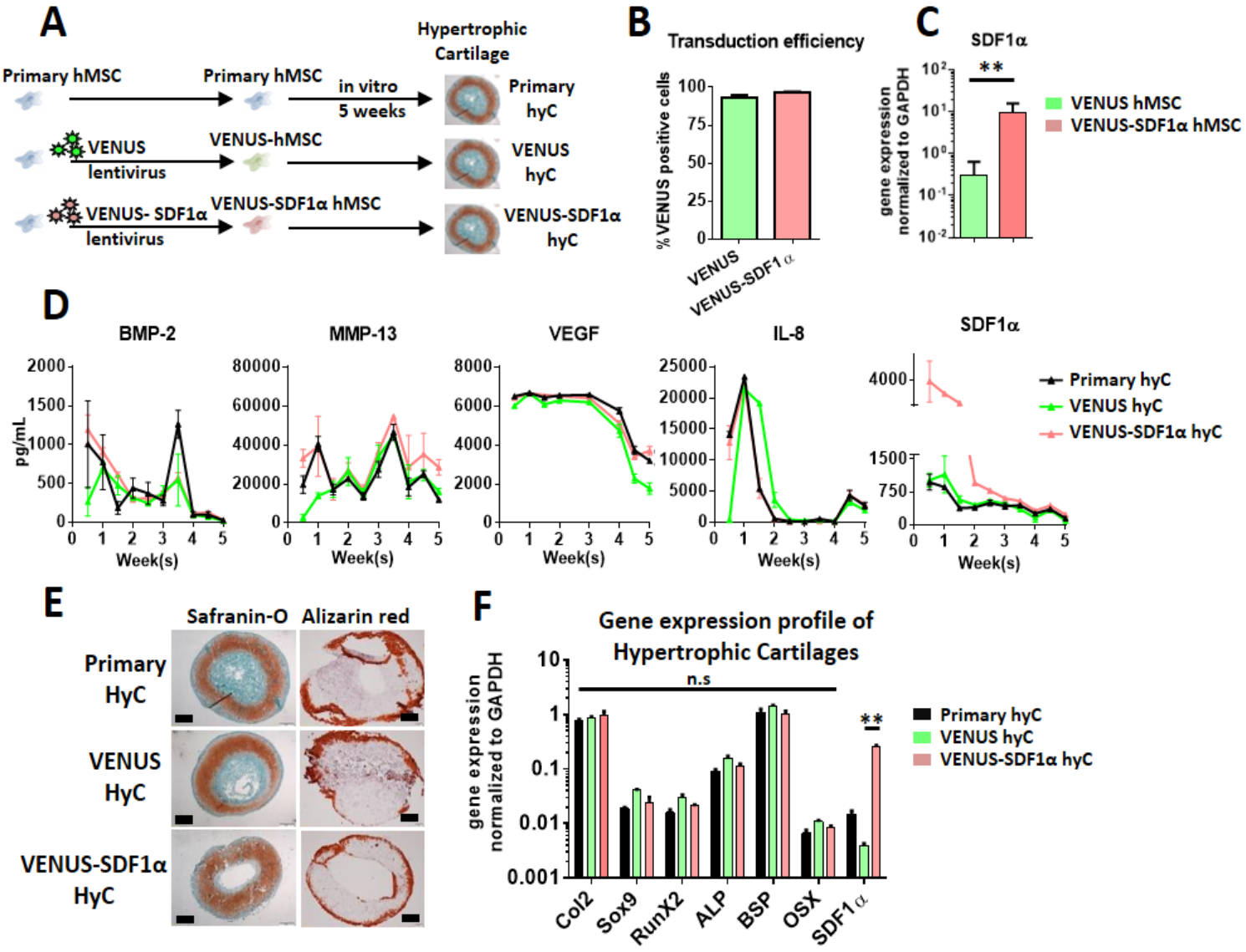

Figure 1. Primary hMSC can be genetically engineered without altering their capacity to form hypertrophic cartilage. (A) Experimental design for generation of hypertrophic cartilage (hyC). SDF1α: stromal derived factor 1 alpha. (B) Primary hMSC were successfully transduced with the VENUS and VENUS- SDF1α lentiviruses, as assessed by flow cytometry. n≥4 biological replicates. (C) The VENUS-SDF1α transduction led to a significantly higher expression of SDF1α levels in corresponding cells prior to hyC formation. **p<0.01, ***p<0.001. n≥5 biological replicates. BMP-2: bone morphogenetic protein 2. MMP-13: matrix metalloproteinase 13. VEGF: vascular endothelial growth factor. IL-8: interleukin 8. (D) All hyC display similar protein secretion patterns during in vitro culture time but VENUS-SDF1α hyC release higher amount of SDF1α. n≥3 biological replicates. (E) VENUS and VENUS-SDF1α successfully displayed features of mature hypertrophic cartilage tissue following the 5 weeks of in vitro culture, as assessed by histological analysis. Safranin-O staining reveals the presence of glycoamynoglycans (red) while Alizarin red the presence of mineralized tissue (red). Scale bar = 500µm. (F) After 5 weeks of in vitro culture, VENUS-sdf1α hyC successfully displayed a typical hypertrophic molecular profile while exhibiting a significant SDF1α increased. n≥4 biological replicates. Col2: collagen type 2. RunX2: Runt-related transcription factor 2. ALP: alkalyne phosphatase. BSP: bone sialoprotein. OSX: osterix.

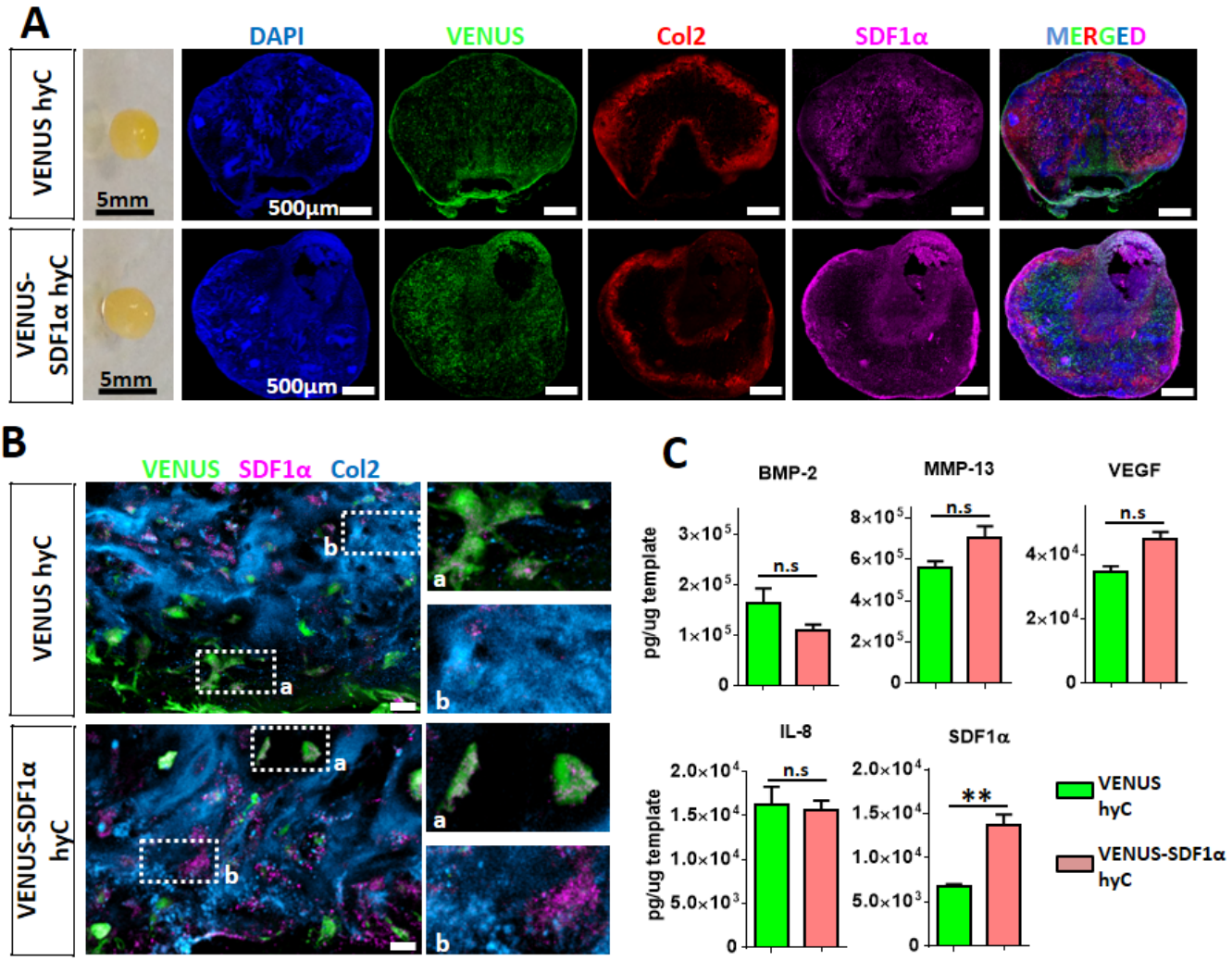

Figure 2. Hypertrophic cartilage with a targeted SDF1α enrichment can be generated. (A) VENUS and VENUS-SDF1α hyC consist in cartilage pellets (macroscopic view, left) in which hMSC (VENUS positive) and the SDF1α protein are found abundantly in the collagen-rich matrix, as assessed by immunofluorescence analysis of thick hyC sections. Col2: collagen type 2. Scale bar = 500µm. (B) SDF1α is found more abundant in the ECM of VENUS-SDF1α hyC, as revealed by high resolution immunofluorescence imaging. Scale bar = 20µm. Col2: collagent type 2. (C) A significant and specific SDF1α enrichment is obtained in the VENUS-SDF1α hyC, as assessed by protein quantification. n= 3 biological repeats. **p<0.01.

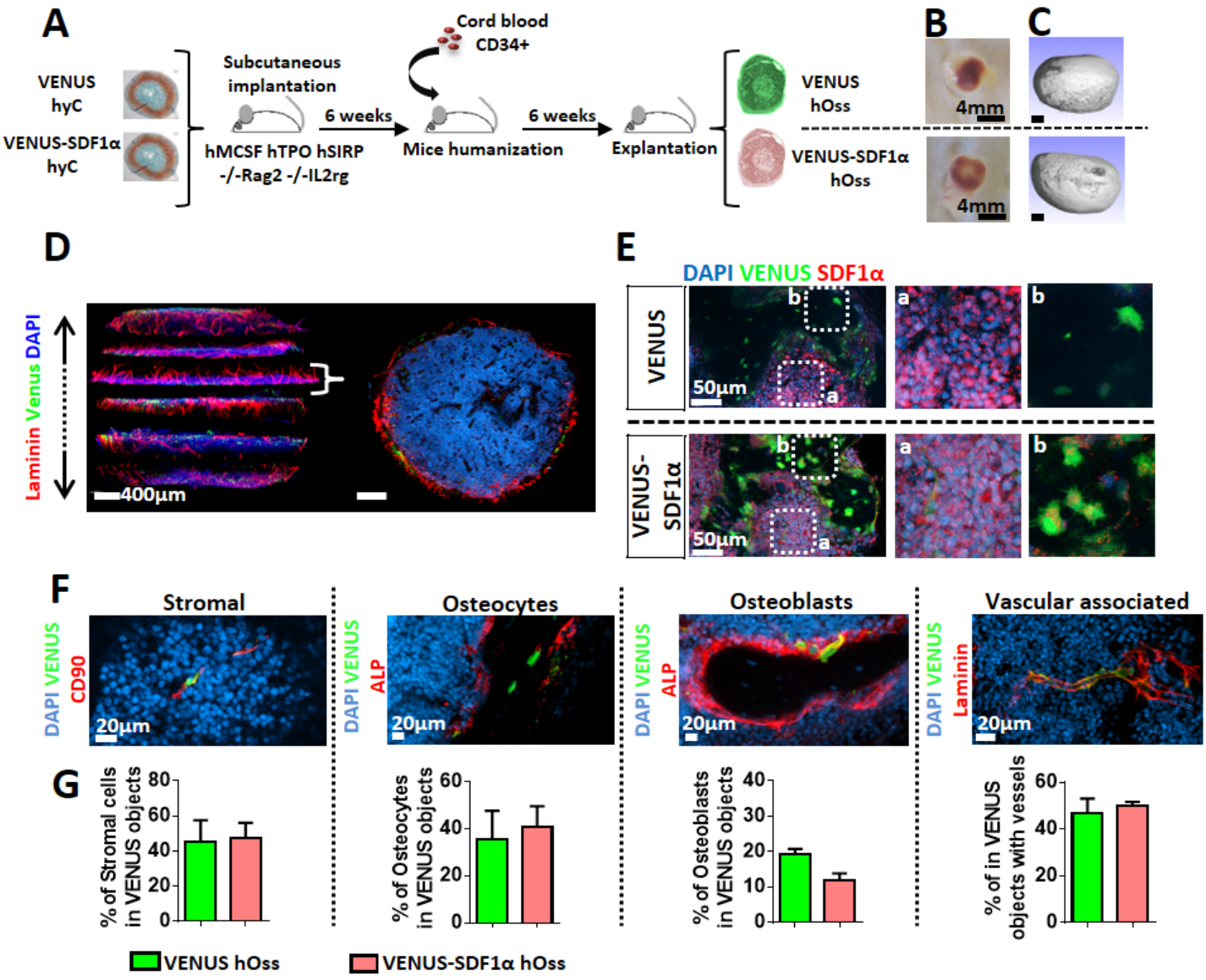

Figure 3. Molecularly engineered hyC can remodel into humanized bone organs and comprise human MSCs partially reconstituting the human niche. (A) Experimental design for the generation of humanized ossicles (hOss). Engineered hyC are implanted into immunocompromised animals. Mice are humanized 6 weeks later by intravenous transplantation of human CD34+ isolated from cord blood. Constructs are retrieved 6 weeks later for analysis. (B) VENUS and VENUS-SDF1α hyC successfully remodelled into ossicles, as shown macroscopically by blood colonization and (C) by microtomography scans revealing the formation of mature bone tissue. Ossicles were retrieved after 12 weeks *in vivo*. Scale bar = 0.5mm. (D) Multidimensional confocal immunofluorescence imaging allows for the reconstitution of hOss for 3D quantitative information retrieval (left). Top view of a transversal hOss section (right) illustrating the internal bone marrow cavity (DAPI) and intense peripheric vascularization (lamimin). Scale bar = 400µm. (E) The SDF1α protein was expressed by blood cells, and also found more abundantly in VENUS cells from the VENUS-SDF1α ossicles. Right and b = magnification panels. (F) Implanted hMSCs (VENUS positive) demonstrate a fate plasticity by acquiring multiple niche-cell phenotypes. Scale bar = 20µm. (G) Fate quantification of Venus hMSC based on the segmentation of immunofluorescence data. Stromal cells: venus+/CD90+/stroma localization. Osteocytes: venus+/ALP-/localization in bone nodules. Osteoblasts: venus+/ALP+/localization at the bone and bone marrow interface. Vasculature associated: venus+/distance to lamimin+ vessels < 1µm. ALP: alkalyne phosphatase. n≥3 biological replicates.

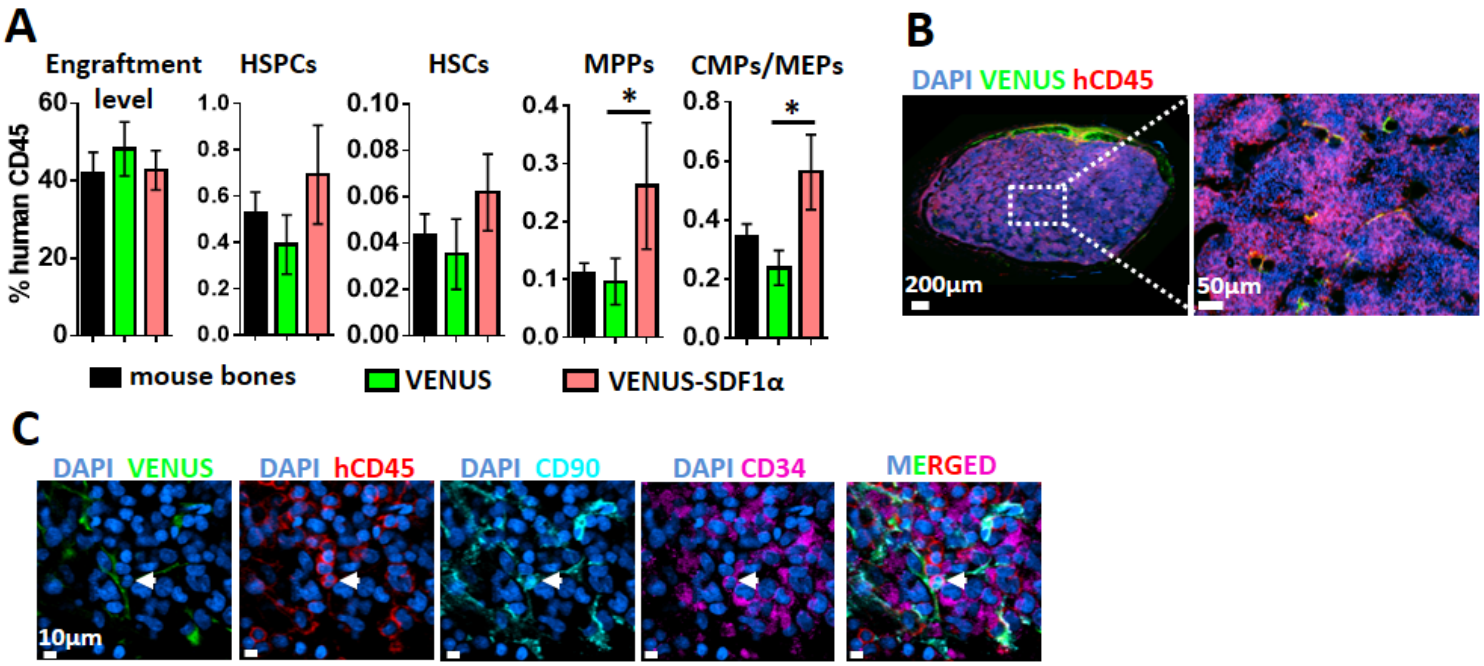

Figure 4. Human niche cells and human hematopoietic stem/progenitors cells are in close vicinity in humanized ossicles. (A) SDF1α overexpressing ossicles displayed an higher frequencies of human blood populations, as assessed by flow cytometry. n≥18 biological replicates. (B) Humanized ossicles display a chimeric blood composition organized in 'islets' of human hematopoieisis. (C) Deep confocal analysis of hOss allows for the identification and localization of a rare HSPCs subset (hCD45/CD34/CD90), found directly in contact with hMSC-derived niche cells (n=9).

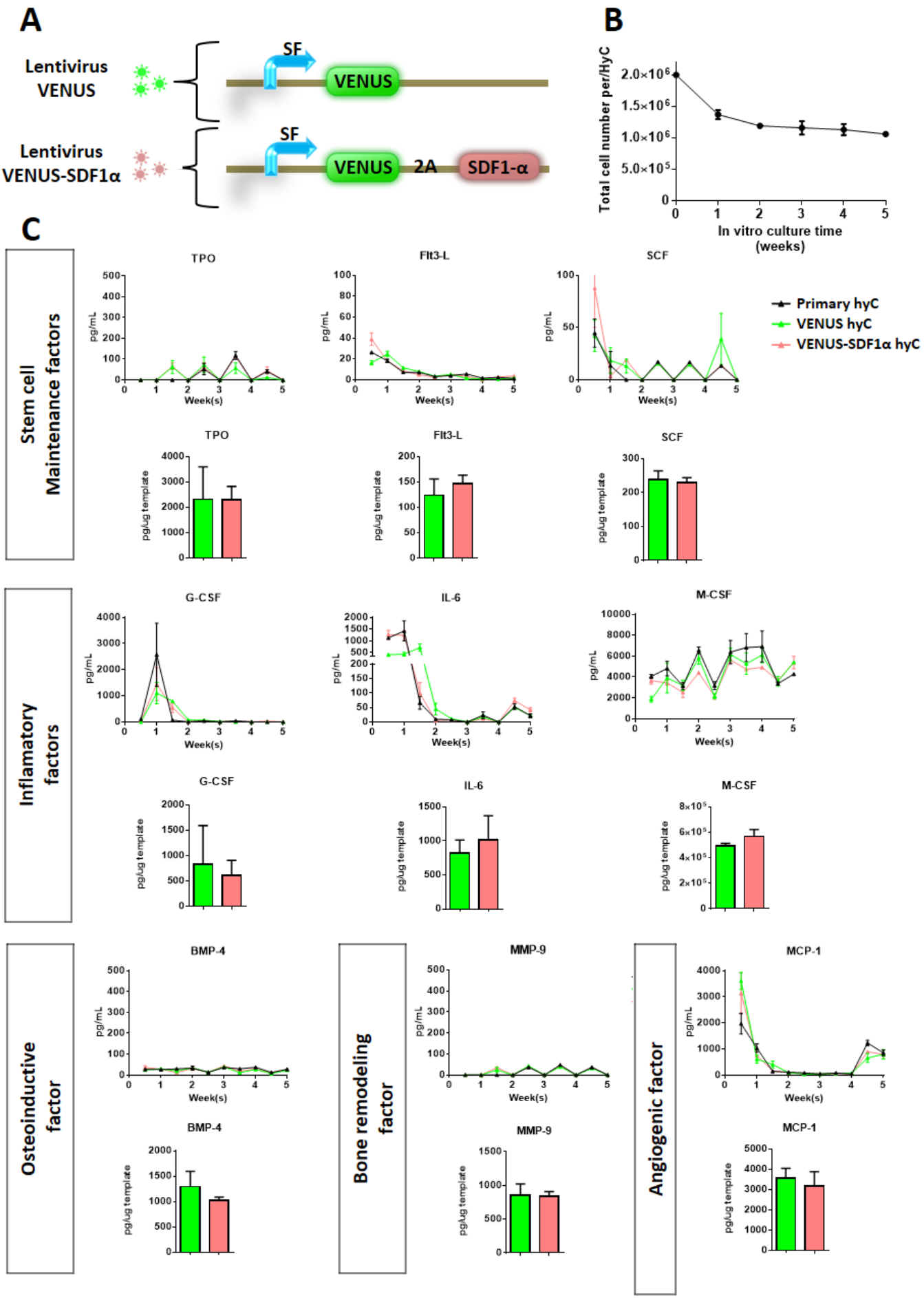

Figure S4. (A) Lentivectors map. (B) Quantification by DNA content of hMSC number in hyC over in vitro culture time. n=3 biological replicates. (C) Protein analysis in the supernatant (timeline over 5 weeks of in vitro culture) and in lysed hyC at the end of the in vitro culture. TPO: thrombopoietin. Flt3-L: Fms-related tyrosine kinase 3. SCF: stem cell factor. G-CSF: Granulocyte colony-stimulating factor. IL-6: interleukin 6. M-CSF: Macrophage colony-stimulating factor. MMP-9: matrix metalloproteinase. MCP-1: Monocyte chemotactic protein 1. BMP-4: bone morphogenetic protein 4. n=3 biological replicates.

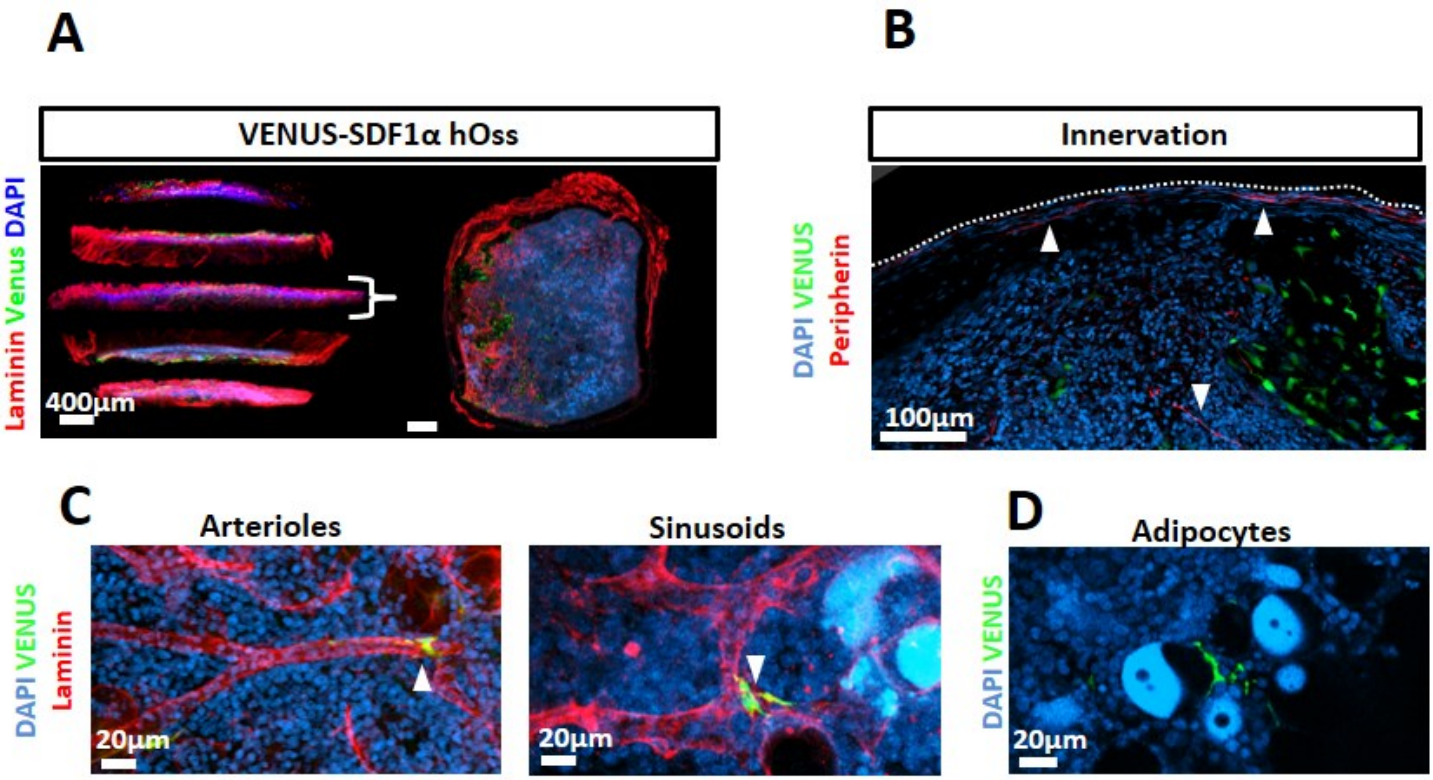

Figure S5. (A) Multidimensional confocal immunofluorescence imaging of VENUS-SDF1αhOss for 3D quantitative information retrieval (left). Top view of a transversal hOss section (right) illustrating the internal bone marrow cavity (DAPI) and intense peripheric vascularization (lamimin). Scale bar = 400µm. (B) Humanized ossicles display evidences of innervation (arrows), proving connection to the host nervous system. Sclale bar = 100µm. (C) Implanted hMSC (VENUS positive) are detected in association with the established vasculature, which includes both arterioles (left) and sinusoids (right). Scale bar = 20µm. (D) Implanted hMSCs (VENUS positive) differentiate into adipocytes, as assessed by the presence of cytosolic lipid droplets autofluorescent in the blue channel (DAPI). Scale bar = 20µm.

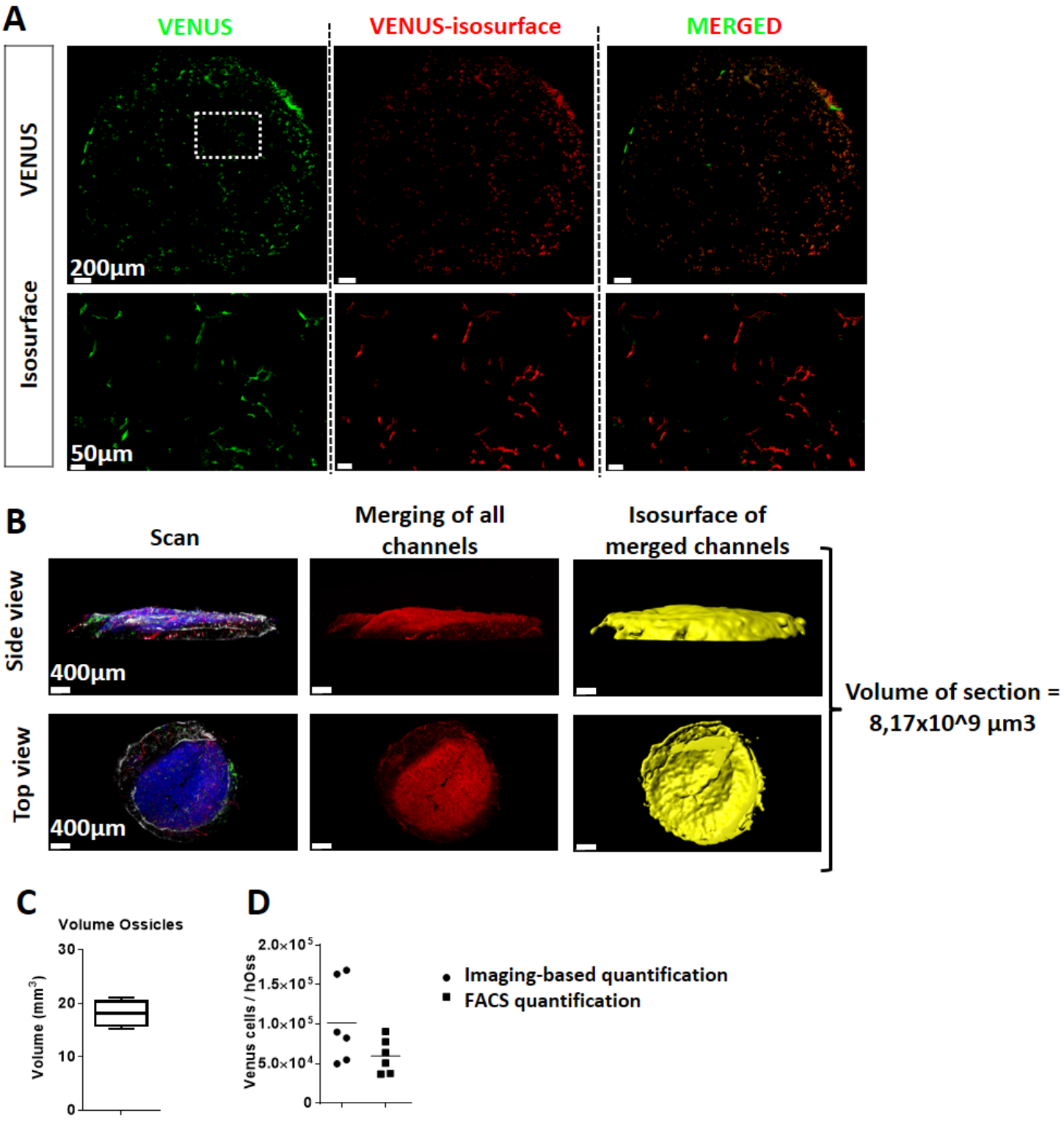

Figure S6. (A) Generation of isosurfaces for hMSC-VENUS fate determination/quantification using the Imaris software. (B) Generation of isosurafeces of whole sections based on the combination of all channels using the Imaris software. This is used to derive the volume of section scanned and normalized the number of objects per volume of section. (C) Mean volume of hOss calculated by microtomography. n=6 biological replicates. (D) Quantification of VENUS expressing hMSC by imaging, or by FACS following digestion of hOss. One point represents one ossicle.

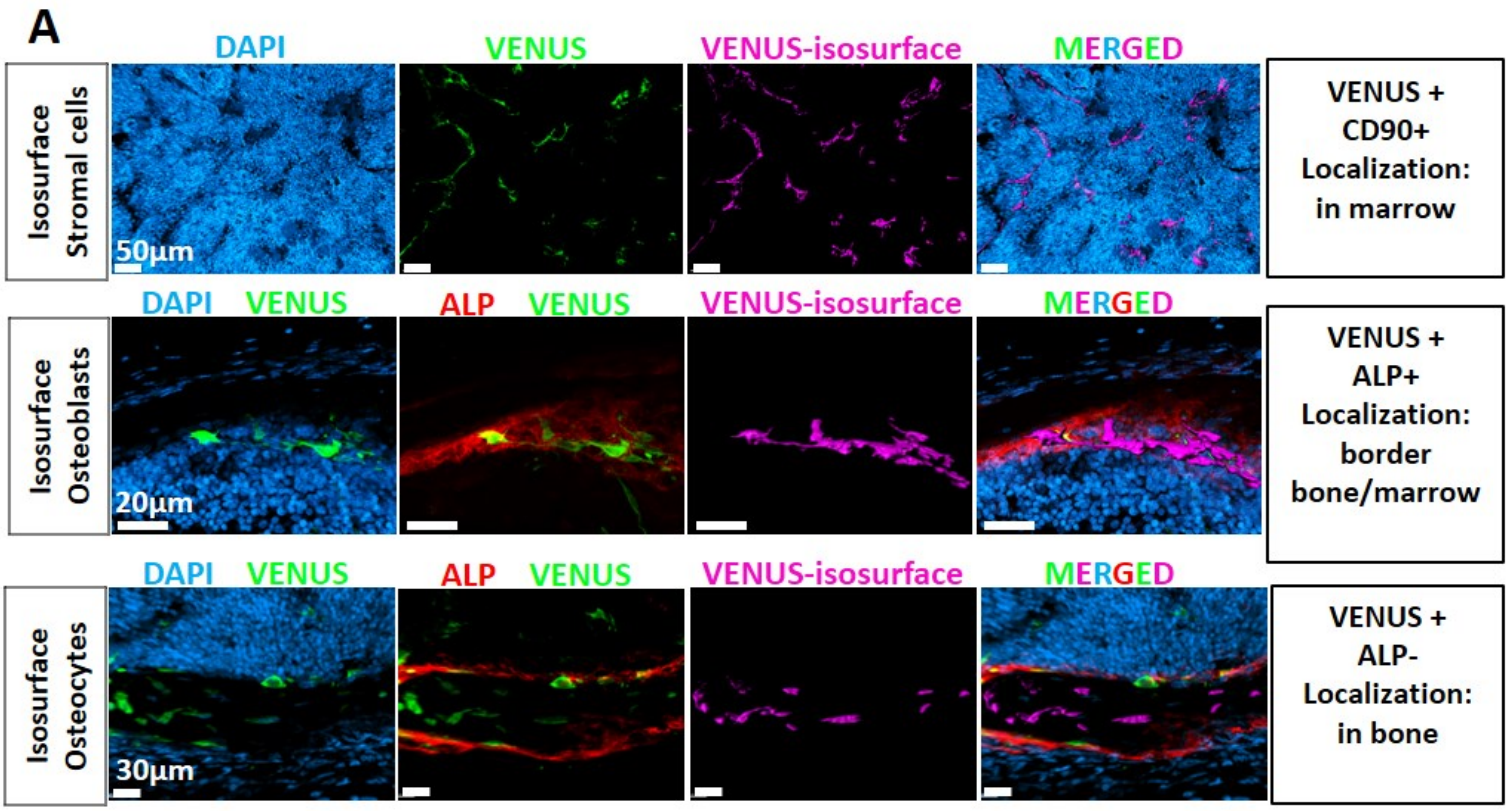

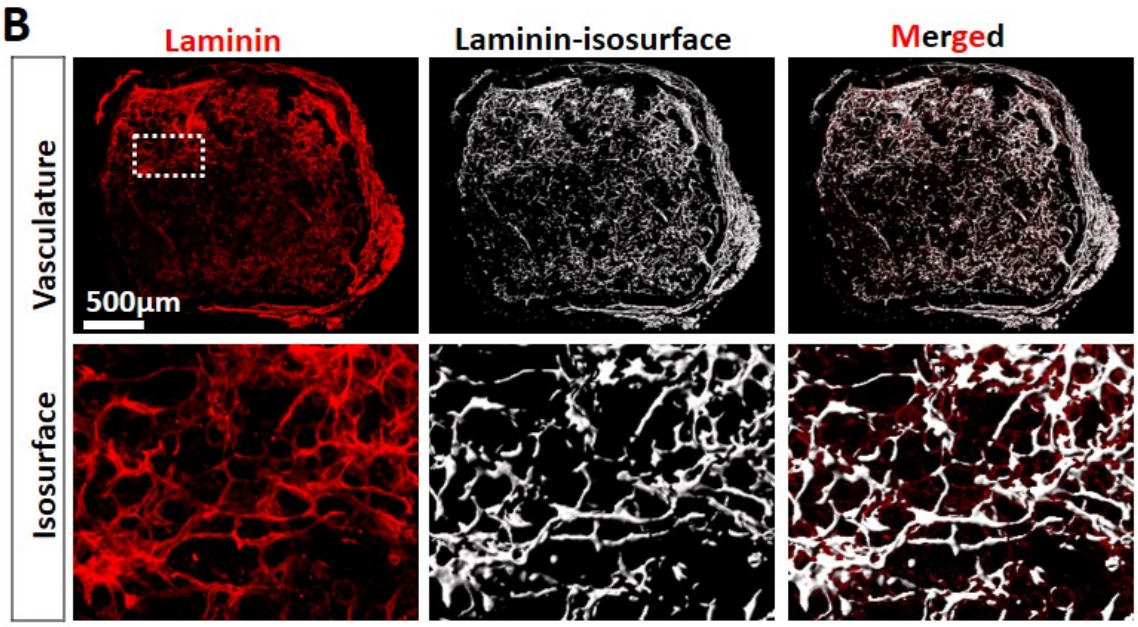

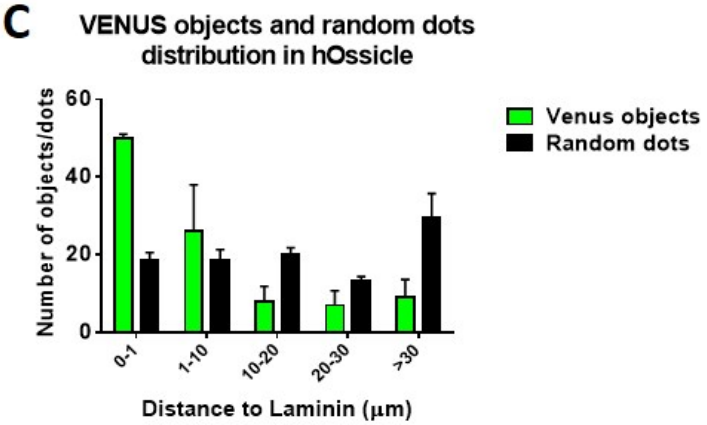

Figure S7. (A) Rationale and representative example leading to the generation of isosurfaces for hMSC-VENUS fate determination/quantification. ALP: alkalyne phosphatase. (B) Generation of vasculature isosurfaces based on laminin expression. (C) Distance transform between VENUS objects and Laminin, and comparison with random dots distribution.

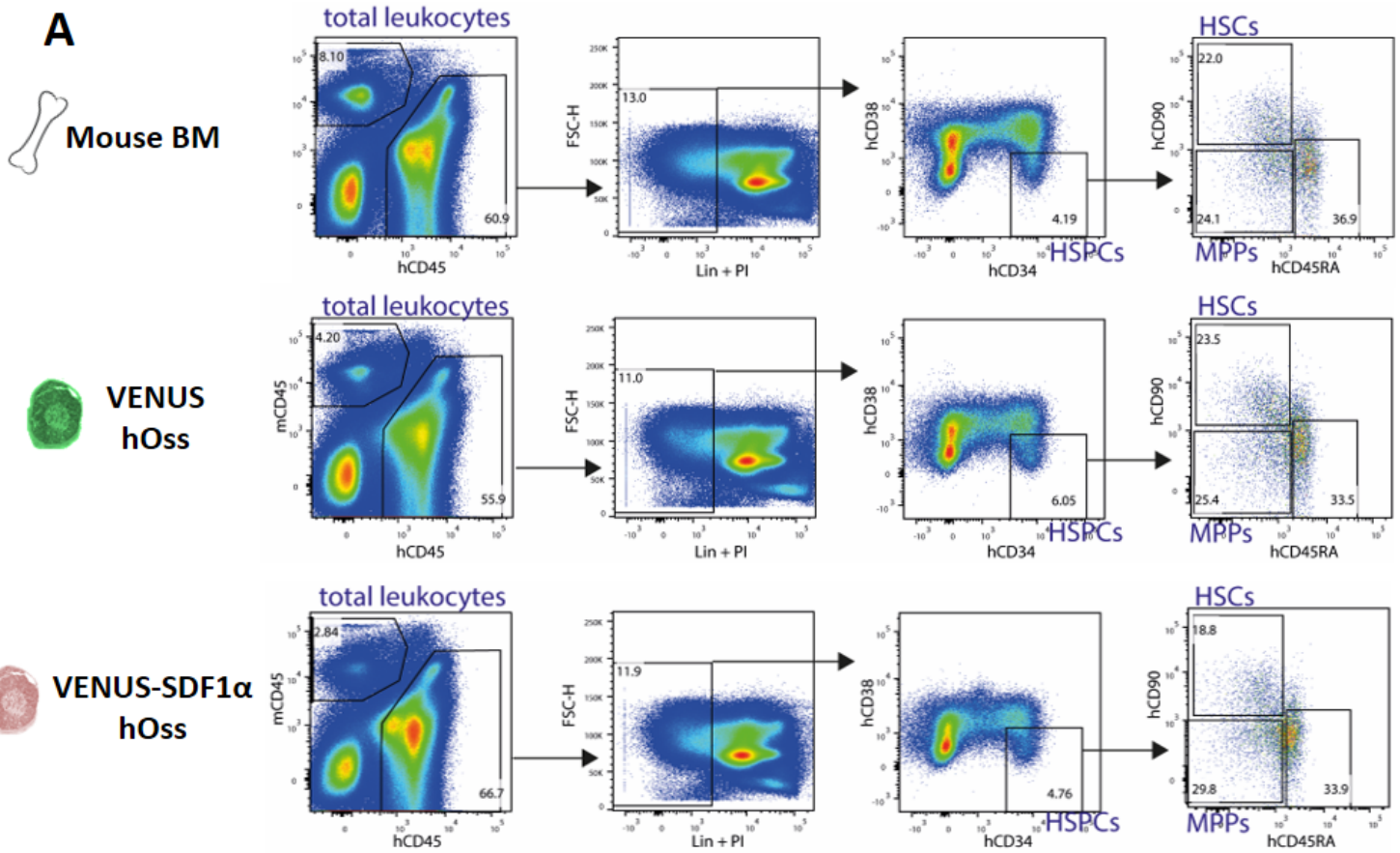

B

Population	Surface phenotype
HSPCs	Lin- CD34+ 38-
HSCs	Lin- hCD45+ CD34+ CD38- CD45RA- CD90+
MPPs	Lin- hCD45+ CD34+ CD38- CD45RA- CD90-
MylPs	Lin- hCD45+ CD34+ CD38- CD45RA+ CD90-
CMPs/MEPs	Lin- hCD45+ CD34+ CD38+ CD45RA-
GMPs	Lin- hCD45+ CD34+ CD38+ CD45RA+

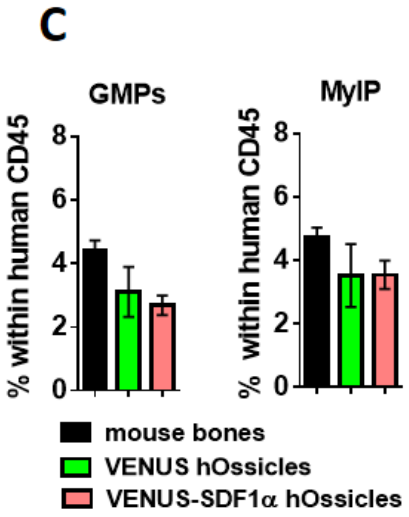

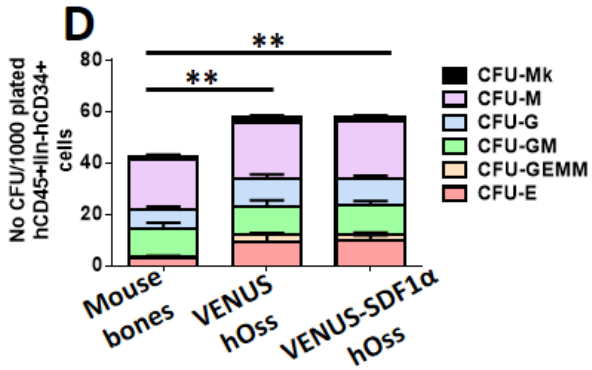

Supp Figure 8. (A) Gating strategy for analysis of HSPCs populations engrafted in mouse bones or humanized ossicles. (B) Phenotypic markers defining HSPCs, HSCs, MPPs, MylPs, CMPs/MEPs and GMPs populations. (C) Flow cytometry-derived frequencies of GMP amd MyLP populations in engineered hOss and mouse bones at the end of the 12 weeks *in vivo* period. n ≥12. (D) (E) Human CD45+/CD34+ cells maintained in VENUS and VENUS-SDF1α ossicles displayed a superior capacity to form myeloid colonies *in vitro*. CFU: colony forming unit. GEmM: Colony-forming unit-Granulocyte, Erythroid, macrophage, Megakaryocyte. GM: Colony-forming unit-granulocyte and macrophage. E: colony forming unit-erythroid. G: colony forming unit granulocyte. M: colony forming unit macrophage. n ≥12 biological replicates. *p<0.05, **p<0.01.

Chapter VI:

Conclusion and perspectives

Thesis summary

Endochondral ossification is a developmental process occurring both during bone formation with the creation of the BM and bone repair reinstating the normal bone function and properties. In this thesis we proposed to harness the properties of endochondral ossification to tackle bone repair and the interactions of human stroma with human HSC. This was pursued by the in vitro generation of HyC, a critical intermediate in endochondral ossification.

Indeed, despite important progresses in biomaterials and cell therapies, there is a clear need for off-the-shelf products for bone regeneration as most existing products remain limited. In fact, the clinical gold standard remains autologous bone graft. In the chapter 2, we demonstrate the potential of tissue engineering and devitalized HyC for bone formation. By engineering BM-MSC with an inducible apoptotic cassette, the resulting devitalization leads to better preservation of the ECM as opposed to standard devitalization techniques. The developed ECM can induce bone formation by osteoinduction recapitulating biological processes. The validation of biologically active devitalized grafts for bone formation is a major step towards the development of an off-the-shelf product bypassing the use of autologous materials and extensive doses of growth factors.

Chapter 3 tackles the upscaling and standardization of a potential off-the-shelf production as well as direct comparison of the apoptosis devitalized ECM against a clinical allograft gold standard in an immunocompetent orthotopic animal model. Engineered BM-MSCs seeded on a collagen sponge scaffold in an upscaled perfusion bioreactors generate uniform and homogenous HyC improving the standardization of the graft generation envisioning the use of GMP compatible bioreactors for streamline processing of devitalized HyC. The upscaled devitalized HyC led to increased bone formation both by osteoconduction and osteoinduction confirming the potential of devitalized ECM as allograft for bone regeneration.

Chapters 4 deals with the validation of a model for human HSC engraftment in a humanized stroma. This comes from the simple analysis that despite extensive HSC niche studies, very few have to do with the actual human HSC niche and direct correlation to human is often admitted. It is therefore primordial to develop models capable of analyzing the direct interactions between human stromal cells and human HSC in the bone marrow niche. By using in vitro generated human HyC and subsequent in vivo implantation and CD34+ cells transplantation we could demonstrate that a humanized stroma is favorable to long term engraftment of self-renewing hematopoietic progenitors and promote their quiescence.

Following up on the chapter 4, chapter 5 aimed at further describing this humanized ossicle model by further engineering the implanted human stromal cells and HyC by overexpression of a critical HSC quiescence and homing factor: CXCL12. We could convincingly show that human MSC genetic engineering did not alter their capacity to undergo endochondral ossification. Moreover, they could be harnessed to functionally modify the human HSCs and progenitors' composition within the generated ossicles. Further engineering with a VENUS reporter allowed the quantification of human stromal cells fate in the remodeled ossicles after 12 weeks in vivo. Using this model, interactions between human stromal cells and human hematopoietic progenitors could be visualized and quantified.

In conclusion, this thesis showed that by following a developmental tissue engineering program both translational and fundamental research could be carried out, respectively for bone repair and the study of human HSC niches. In the first case, in vitro upscaled perfusion bioreactor devitalized tissues are used as bone substitute material for bone grafting. In the second case, in vitro living tissues are implanted in humanized mice to generate ectopic bone organ with human stroma and hematopoietic compartments in order to study their interactions. It shows the versatility and potential of this tissue engineered model for two distinct biological areas.

Future perspectives

For the bone…

The work presented in this thesis bring about major progresses towards envisioning new osteoinductive bone substitute material based on tissue engineered grafts. Nevertheless, crucial steps need to be tackled to bring this strategy further to be used as a clinical product. First of all, the cell source need to be standardized to obtain reproducible results with unlimited and easy to access cells. To this purpose, the use of a cell line carrying the apoptotic cassette and capable to undergo chondrogenic differentiation is of primary importance. Then, the development of a good manufacturing practice (GMP) bioreactor is required to comply with the necessary requirements to reach the clinic. Finally, an efficient and reliable storing strategy needs to be developed. All of these aspects are currently being developed by me and others in the lab. An immortalized cell line carrying the apoptotic cassette has been engineered [81] but could not reproducibly undergo chondrogenic differentiation. We further engineered this cell line with the major osteoinductive protein, the bone morphogenetic protein 2 (BMP2). This newly generated cell line proved to efficiently and reproducibly undergo chondrogenic differentiation and remodel into bone upon in vivo subcutaneous ectopic implantation in immunodeficient mice (Fig.7). Furthermore, the remodeling process occurs much

faster than previously observed using primary human BM-MSCs engineered with the apoptototic cassette [81].

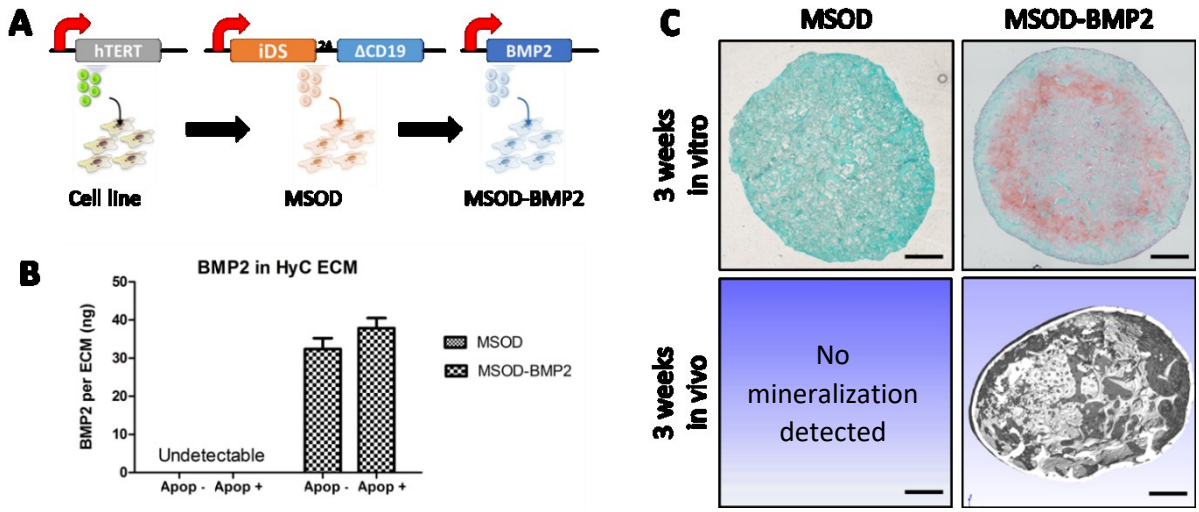

Figure 7: Generation and characterization of the MSOD-BMP2 cell line. (A) Schematic representation of the genetic engineering steps towards the creation of the MSOD-BMP2 cell line. (B) BMP2 protein content in the different HyC after 3 weeks of chondrogenic differentiation in vitro, pre (Apop-) or post (Apop +) apoptosis decellularization. (C) Histological stainings and microtomography (µCT) of the decellularized generated HyC tissues, before (3 weeks in vitro) and after in vivo implantation (3 weeks in vivo). Glycosaminoglycan (GAG, Safranin-O staining), a major component of cartilaginous ECM, is only present in the MSOD-BMP2 HyC (red staining) in vitro. µCT analysis after 3 weeks in vivo ectopic implantation represents a cross-section throughout the ossicle with the presence of mature cortical bone and immature trabecular bone. The cartilage tissue generated by MSOD-BMP2 completely remodeled into bone. Tissue generated by the MSOD line did not lead to any mineralization. (Scale bars, 500 µm)

Following this significant step forward, we set out to tackle the storing process by developing a lyophilization (also known as freeze-drying) protocol to preserve and store the in vitro generated HyC before in vivo implantation. Preliminary results confirmed the potential of the devitalized graft for bone remodeling following the lyophilization procedure (Fig. 8). Current and future experiments will aim on one hand at better understanding the recruitment of the host cells leading to a superior remodeling as the one observed with primary BM-MSC. On the other hand, storage and upscaling in a GMP compliant bioreactor experiments are undergoing to move closer to a clinical setup. The final validation before moving to the clinic would be in a large orthotopic animal model such as a primate.

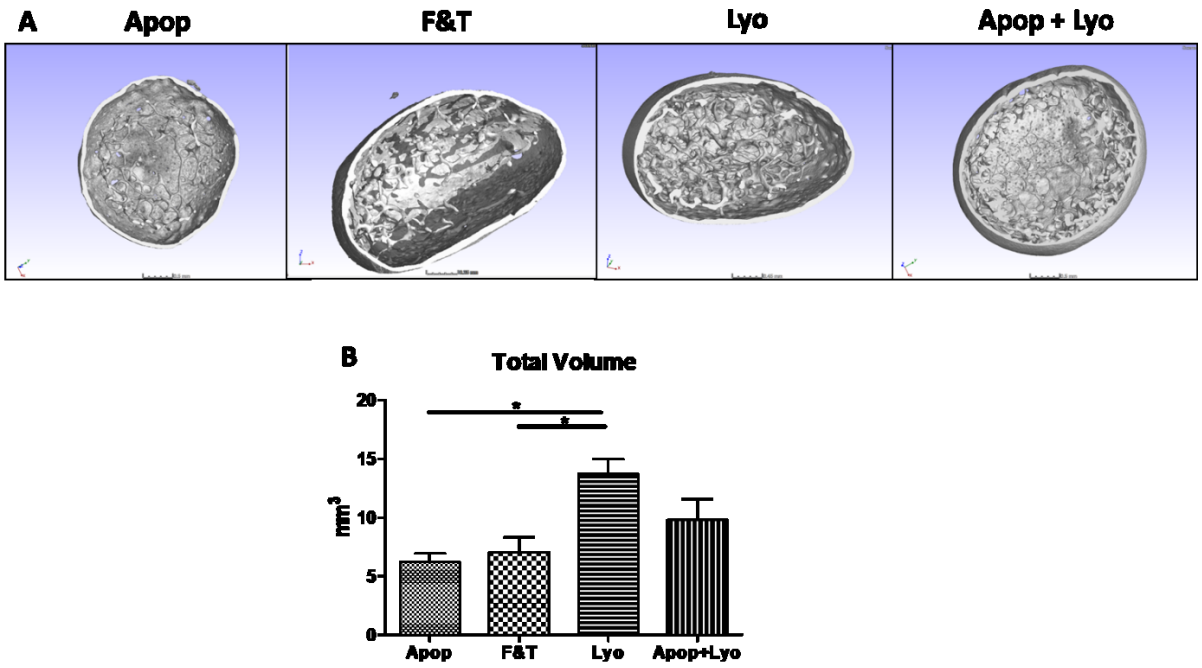

Figure 8: Remodeled HyC following 6 weeks subcutaneous in vivo implantation in immunodeficient mice. MSOD-BMP2 cells were seeded on a collagen scaffold and differentiated toward chondrogenesis as in Fig. 7. Four devitalization conditions were tested: apoptized (Apop), freeze and thaw (F&T), lyophilized (Lyo), apoptized and lyophilized (Apop+Lyo). (A) µCT reconstruction following the 6 weeks in vivo implantation. No structural differences can be observed. (B) Remodeled ossicles volume analysed by µCT. Interestingly, lyophilized tissues led to a significantly bigger size (n=3).

… and the bone marrow

Following years of study in the mouse or using genetically engineered mice, the appeal for human ectopic ossicles and HSC engraftment in a humanized stroma is rising [55,56]. The possibility to visualize cellular interactions in an in vivo environment with or without modification of the human stroma or hematopoietic cells opens up a whole field of possibilities to study the human HSC niche. Other main factors involved in the HSC engraftment and homeostasis such as Scf could be targeted for genetic engineering. These strategies could be coupled with conditional knock-in or knock-out to allow an in vivo temporal control. Similar approaches could be coupled with leukemic cells transplantation providing an adequate model for allele specific leukemia.

Finally, primary BM-MSC form diseased patients such as myelodysplastic syndromes (MDS) could be used to recreate an analogous stromal environment as in the patients allowing a more precise study of this specific stromal environment. Despite being an attractive approach, low number of diseased BM-MSC can be obtained and generating HyC is poorly reproducible and (Fig. 9).

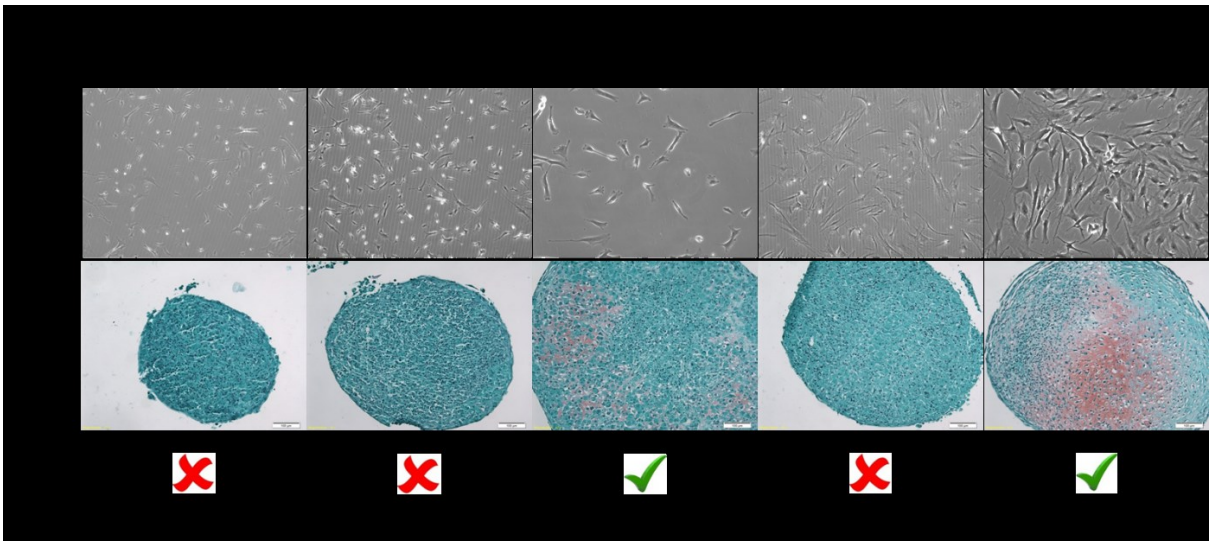

Figure 9: 3D chondrogenic differentiation of BM-MSCs from 5 different patients affected with MDS disease. Cells expansion was difficult and low numbers of tissues could be generated. Only 2 patients (3 & 5) showed slight chondrogenesis (assessed by GAG deposition in red on the safranin-O staining) following 3 weeks in vitro culture. The red cross shows the absence of chondrogenesis, the green tick shows the presence of chondrogenesis. The ratio at the bottom correspond to the number of chondrogenic tissues out of all the tissues generated.

Nevertheless, combining these cells with more chondrogenic cells or even the MSOD-BMP2 cell line could lead to a mixed environment allowing both in vivo bone remodeling and the generation of a specific MDS environment. Also, other techniques allow the generation of in vivo subcutaneous ossicles such as synthetic gels coupled with specific growth factors such as BMP2. It could be envisioned to couple MDS BM-MSC inside those BMP2 synthetic gels to generate ossicles with a MDS stromal environment.

To conclude, the work carried out in this thesis paves the way for clinical applications in the orthopedic regenerative medicine using devitalized in vitro engineered tissue grafts. In another way, the use of similar in vitro generated graft but keeping the living cells allows the generation of a powerful tool to study the human HSC niche and opens the door to many potential studies.

Bibliography

[1] Bjorn R. Olsen, Anthony M. Reginato, and Wenfang Wang, Bone Development (2000).

[2] H. Hojo, A.P. McMahon, S. Ohba, An Emerging Regulatory Landscape for Skeletal Development, Trends in genetics TIG 32 (12) (2016) 774–787.

[3] B. Clarke, Normal bone anatomy and physiology, Clinical journal of the American Society of Nephrology CJASN 3 Suppl 3 (2008) S131-9.

[4] R.S. Taichman, Blood and bone: Two tissues whose fates are intertwined to create the hematopoietic stem-cell niche, Blood 105 (7) (2005) 2631–2639.

[5] H. Fonseca, D. Moreira-Gonçalves, H.-J.A. Coriolano, J.A. Duarte, Bone quality: The determinants of bone strength and fragility, Sports medicine (Auckland, N.Z.) 44 (1) (2014) 37–53.

[6] F. Lamoureux, M. Baud'huin, L. Duplomb, D. Heymann, F. Redini, Proteoglycans: Key partners in bone cell biology, BioEssays news and reviews in molecular, cellular and developmental biology 29 (8) (2007) 758–771.

[7] R. Florencio-Silva, G.R.d.S. Sasso, E. Sasso-Cerri, M.J. Simões, P.S. Cerri, Biology of Bone Tissue: Structure, Function, and Factors That Influence Bone Cells, BioMed research international 2015 (2015) 421746.

[8] F. Long, Building strong bones: Molecular regulation of the osteoblast lineage, Nature reviews. Molecular cell biology 13 (1) (2011) 27–38.

[9] L. Yang, K.Y. Tsang, H.C. Tang, D. Chan, K.S.E. Cheah, Hypertrophic chondrocytes can become osteoblasts and osteocytes in endochondral bone formation, Proceedings of the National Academy of Sciences of the United States of America 111 (33) (2014) 12097–12102.

[10] A.D. Berendsen, B.R. Olsen, Bone development, Bone 80 (2015) 14–18.

[11] T.A. Franz-Odendaal, Induction and patterning of intramembranous bone, Frontiers in bioscience (Landmark edition) 16 (2011) 2734–2746.

[12] H.M. Kronenberg, Developmental regulation of the growth plate, Nature 423 (6937) (2003) 332–336.

[13] E.M. Thompson, A. Matsiko, E. Farrell, D.J. Kelly, F.J. O'Brien, Recapitulating endochondral ossification: A promising route to in vivo bone regeneration, Journal of tissue engineering and regenerative medicine 9 (8) (2015) 889–902.

[14] N. Ortega, D. Behonick, D. Stickens, Z. Werb, How proteases regulate bone morphogenesis, Annals of the New York Academy of Sciences 995 (2003) 109–116.

[15] E. Kozhemyakina, A.B. Lassar, E. Zelzer, A pathway to bone: Signaling molecules and transcription factors involved in chondrocyte development and maturation, Development (Cambridge, England) 142 (5) (2015) 817–831.

[16] K.Y. Tsang, D. Chan, K.S.E. Cheah, Fate of growth plate hypertrophic chondrocytes: Death or lineage extension?, Development, growth & differentiation 57 (2) (2015) 179–192.

[17] M.J. Hilton (Ed.), Skeletal development and repair: Methods and protocols, Humana Press, New York, 2014.

[18] S.M. Oliveira, I.F. Amaral, M.A. Barbosa, C.C. Teixeira, Engineering endochondral bone: In vitro studies, Tissue engineering. Part A 15 (3) (2009) 625–634.

[19] S.M. Oliveira, D.Q. Mijares, G. Turner, I.F. Amaral, M.A. Barbosa, C.C. Teixeira, Engineering endochondral bone: In vivo studies, Tissue engineering. Part A 15 (3) (2009) 635–643.

[20] K. Pelttari, A. Winter, E. Steck, K. Goetzke, T. Hennig, B.G. Ochs, T. Aigner, W. Richter, Premature induction of hypertrophy during in vitro chondrogenesis of human mesenchymal stem cells correlates with calcification and vascular invasion after ectopic transplantation in SCID mice, Arthritis and rheumatism 54 (10) (2006) 3254–3266.

[21] C. Scotti, B. Tonnarelli, A. Papadimitropoulos, A. Scherberich, S. Schaeren, A. Schauerte, J. Lopez-Rios, R. Zeller, A. Barbero, I. Martin, Recapitulation of endochondral bone formation using human adult mesenchymal stem cells as a paradigm for developmental engineering, Proceedings of the National Academy of Sciences of the United States of America 107 (16) (2010) 7251–7256.
[22] C. Scotti, E. Piccinini, H. Takizawa, A. Todorov, P. Bourgine, A. Papadimitropoulos, A. Barbero, M.G. Manz, I. Martin, Engineering of a functional bone organ through endochondral ossification, Proceedings of the National Academy of Sciences of the United States of America 110 (10) (2013) 3997–4002.
[23] F. Aria, T. Suda, Regulation of Hematopoietic Stem Cells in the Osteoblastic Niche, in: Y. Choi (Ed.), Osteoimmunology: Interactions of the immune and skeletal systems / edited by Yongwon Choi, Springer, New York, London, 2007, pp. 61–67.
[24] P. Bianco, P.G. Robey, Skeletal stem cells, Development (Cambridge, England) 142 (6) (2015) 1023–1027.
[25] S. Doulatov, F. Notta, E. Laurenti, J.E. Dick, Hematopoiesis: A human perspective, Cell stem cell 10 (2) (2012) 120–136.
[26] C. Antoniani, O. Romano, A. Miccio, Concise Review: Epigenetic Regulation of Hematopoiesis: Biological Insights and Therapeutic Applications, Stem cells translational medicine (2017).
[27] M. Moschetta, Y. Kawano, K. Podar, Targeting the Bone Marrow Microenvironment, Cancer treatment and research 169 (2016) 63–102.
[28] S.J. Morrison, D.T. Scadden, The bone marrow niche for haematopoietic stem cells, Nature 505 (7483) (2014) 327–334.
[29] S. Coskun, K.K. Hirschi, Establishment and regulation of the HSC niche: Roles of osteoblastic and vascular compartments, Birth defects research. Part C, Embryo today reviews 90 (4) (2010) 229–242.
[30] C. Nombela-Arrieta, G. Pivarnik, B. Winkel, K.J. Canty, B. Harley, J.E. Mahoney, S.-Y. Park, J. Lu, A. Protopopov, L.E. Silberstein, Quantitative imaging of haematopoietic stem and progenitor cell localization and hypoxic status in the bone marrow microenvironment, Nature cell biology 15 (5) (2013) 533–543.
[31] L.M. Calvi, D.C. Link, The hematopoietic stem cell niche in homeostasis and disease, Blood 126 (22) (2015) 2443–2451.
[32] R. Schofield, The relationship between the spleen colony-forming cell and the haemopoietic stem cell, Blood cells 4 (1-2) (1978) 7–25.
[33] J. Zhang, C. Niu, L. Ye, H. Huang, X. He, W.-G. Tong, J. Ross, J. Haug, T. Johnson, J.Q. Feng, S. Harris, L.M. Wiedemann, Y. Mishina, L. Li, Identification of the haematopoietic stem cell niche and control of the niche size, Nature 425 (6960) (2003) 836–841.
[34] L.M. Calvi, G.B. Adams, K.W. Weibrecht, J.M. Weber, D.P. Olson, M.C. Knight, R.P. Martin, E. Schipani, P. Divieti, F.R. Bringhurst, L.A. Milner, H.M. Kronenberg, D.T. Scadden, Osteoblastic cells regulate the haematopoietic stem cell niche, Nature 425 (6960) (2003) 841–846.
[35] A. Wilson, E. Laurenti, G. Oser, R.C. van der Wath, W. Blanco-Bose, M. Jaworski, S. Offner, C.F. Dunant, L. Eshkind, E. Bockamp, P. Lió, H.R. Macdonald, A. Trumpp, Hematopoietic stem cells reversibly switch from dormancy to self-renewal during homeostasis and repair, Cell 135 (6) (2008) 1118–1129.
[36] L. Ding, S.J. Morrison, Haematopoietic stem cells and early lymphoid progenitors occupy distinct bone marrow niches, Nature 495 (7440) (2013) 231–235.
[37] B. Sacchetti, A. Funari, S. Michienzi, S. Di Cesare, S. Piersanti, I. Saggio, E. Tagliafico, S. Ferrari, P.G. Robey, M. Riminucci, P. Bianco, Self-renewing osteoprogenitors in bone marrow sinusoids can organize a hematopoietic microenvironment, Cell 131 (2) (2007) 324–336.

[38] G.M. Crane, E. Jeffery, S.J. Morrison, Adult haematopoietic stem cell niches, Nature reviews. Immunology 17 (9) (2017) 573–590.
[39] D. Toscani, M. Bolzoni, F. Accardi, F. Aversa, N. Giuliani, The osteoblastic niche in the context of multiple myeloma, Annals of the New York Academy of Sciences 1335 (2015) 45–62.
[40] L. Ding, T.L. Saunders, G. Enikolopov, S.J. Morrison, Endothelial and perivascular cells maintain haematopoietic stem cells, Nature 481 (7382) (2012) 457–462.
[41] V.W.C. Yu, D.T. Scadden, Hematopoietic Stem Cell and Its Bone Marrow Niche, Current topics in developmental biology 118 (2016) 21–44.
[42] F. Ugarte, E.C. Forsberg, Haematopoietic stem cell niches: New insights inspire new questions, The EMBO journal 32 (19) (2013) 2535–2547.
[43] T. Nagasawa, H. Kikutani, T. Kishimoto, Molecular cloning and structure of a pre-B-cell growth-stimulating factor, Proceedings of the National Academy of Sciences of the United States of America 91 (6) (1994) 2305–2309.
[44] Y. Feng, C.C. Broder, P.E. Kennedy, E.A. Berger, HIV-1 entry cofactor: Functional cDNA cloning of a seven-transmembrane, G protein-coupled receptor, Science (New York, N.Y.) 272 (5263) (1996) 872–877.
[45] T. Nagasawa, S. Hirota, K. Tachibana, N. Takakura, S. Nishikawa, Y. Kitamura, N. Yoshida, H. Kikutani, T. Kishimoto, Defects of B-cell lymphopoiesis and bone-marrow myelopoiesis in mice lacking the CXC chemokine PBSF/SDF-1, Nature 382 (6592) (1996) 635–638.
[46] Y. Nie, Y.-C. Han, Y.-R. Zou, CXCR4 is required for the quiescence of primitive hematopoietic cells, The Journal of experimental medicine 205 (4) (2008) 777–783.
[47] B.A. Anthony, D.C. Link, Regulation of hematopoietic stem cells by bone marrow stromal cells, Trends in immunology 35 (1) (2014) 32–37.
[48] J.E. TILL, E.A. McCULLOCH, A direct measurement of the radiation sensitivity of normal mouse bone marrow cells, Radiation research 14 (1961) 213–222.
[49] B.L. Pike, W.A. Robinson, Human bone marrow colony growth in agar-gel, Journal of cellular physiology 76 (1) (1970) 77–84.
[50] M.A. Moore, N. Williams, D. Metcalf, In vitro colony formation by normal and leukemic human hematopoietic cells: Characterization of the colony-forming cells, Journal of the National Cancer Institute 50 (3) (1973) 603–623.
[51] D.E. Mosier, R.J. Gulizia, S.M. Baird, D.B. Wilson, Transfer of a functional human immune system to mice with severe combined immunodeficiency, Nature 335 (6187) (1988) 256–259.
[52] J.M. McCune, R. Namikawa, H. Kaneshima, L.D. Shultz, M. Lieberman, I.L. Weissman, The SCID-hu mouse: Murine model for the analysis of human hematolymphoid differentiation and function, Science (New York, N.Y.) 241 (4873) (1988) 1632–1639.
[53] R. Namikawa, H. Kaneshima, M. Lieberman, I.L. Weissman, J.M. McCune, Infection of the SCID-hu mouse by HIV-1, Science (New York, N.Y.) 242 (4886) (1988) 1684–1686.
[54] S. Kamel-Reid, J.E. Dick, Engraftment of immune-deficient mice with human hematopoietic stem cells, Science (New York, N.Y.) 242 (4886) (1988) 1706–1709.
[55] A. Reinisch, N. Etchart, D. Thomas, N.A. Hofmann, M. Fruehwirth, S. Sinha, C.K. Chan, K. Senarath-Yapa, E.-Y. Seo, T. Wearda, U.F. Hartwig, C. Beham-Schmid, S. Trajanoski, Q. Lin, W. Wagner, C. Dullin, F. Alves, M. Andreeff, I.L. Weissman, M.T. Longaker, K. Schallmoser, R. Majeti, D. Strunk, Epigenetic and in vivo comparison of diverse MSC sources reveals an endochondral signature for human hematopoietic niche formation, Blood 125 (2) (2015) 249–260.
[56] A. Reinisch, D. Thomas, M.R. Corces, X. Zhang, D. Gratzinger, W.-J. Hong, K. Schallmoser, D. Strunk, R. Majeti, A humanized bone marrow ossicle xenotransplantation model enables improved engraftment of healthy and leukemic human hematopoietic cells, Nature medicine 22 (7) (2016) 812–821.

[57] A. Schindeler, M.M. McDonald, P. Bokko, D.G. Little, Bone remodeling during fracture repair: The cellular picture, Seminars in Cell & Developmental Biology 19 (5) (2008) 459–466.
[58] S.J. Roberts, N. van Gastel, G. Carmeliet, F.P. Luyten, Uncovering the periosteum for skeletal regeneration: The stem cell that lies beneath, Bone 70 (2015) 10–18.
[59] S. Stegen, N. van Gastel, G. Carmeliet, Bringing new life to damaged bone: The importance of angiogenesis in bone repair and regeneration, Bone 70 (2015) 19–27.
[60] T.A. Einhorn, L.C. Gerstenfeld, Fracture healing: Mechanisms and interventions, Nature reviews. Rheumatology 11 (1) (2015) 45–54.
[61] Y. Fillingham, J. Jacobs, Bone grafts and their substitutes, The bone & joint journal 98-B (1 Suppl A) (2016) 6–9.
[62] Dr. Madhukar Rajaram Wagh, Dr. Dilip Ravalia, Bone Regeneration and Repair: Current and Future Aspects.
[63] A.-M. Yousefi, P.F. James, R. Akbarzadeh, A. Subramanian, C. Flavin, H. Oudadesse, Prospect of Stem Cells in Bone Tissue Engineering: A Review, Stem cells international 2016 (2016) 6180487.
[64] J.N. Fisher, G.M. Peretti, C. Scotti, Stem Cells for Bone Regeneration: From Cell-Based Therapies to Decellularised Engineered Extracellular Matrices, Stem cells international 2016 (2016) 9352598.
[65] E. Gomez-Barrena, P. Rosset, D. Lozano, J. Stanovici, C. Ermthaller, F. Gerbhard, Bone fracture healing: Cell therapy in delayed unions and nonunions, Bone 70 (2015) 93–101.
[66] P. Rosset, F. Deschaseaux, P. Layrolle, Cell therapy for bone repair, Orthopaedics & traumatology, surgery & research OTSR 100 (1 Suppl) (2014) S107-12.
[67] A.J. Friedenstein, I.I. Piatetzky-Shapiro, K.V. Petrakova, Osteogenesis in transplants of bone marrow cells, Journal of embryology and experimental morphology 16 (3) (1966) 381–390.
[68] A.J. Friedenstein, K.V. Petrakova, A.I. Kurolesova, G.P. Frolova, Heterotopic of bone marrow. Analysis of precursor cells for osteogenic and hematopoietic tissues, Transplantation 6 (2) (1968) 230–247.
[69] P. Bianco, Stem cells and bone: A historical perspective, Bone 70 (2015) 2–9.
[70] M.N. Knight, K.D. Hankenson, Mesenchymal Stem Cells in Bone Regeneration, Advances in wound care 2 (6) (2013) 306–316.
[71] X. Wang, Y. Wang, W. Gou, Q. Lu, J. Peng, S. Lu, Role of mesenchymal stem cells in bone regeneration and fracture repair: A review, International orthopaedics 37 (12) (2013) 2491–2498.
[72] F. de Francesco, G. Ricci, F. D'Andrea, G.F. Nicoletti, G.A. Ferraro, Human Adipose Stem Cells: From Bench to Bedside, Tissue engineering. Part B, Reviews 21 (6) (2015) 572–584.
[73] B. Lindroos, R. Suuronen, S. Miettinen, The potential of adipose stem cells in regenerative medicine, Stem cell reviews 7 (2) (2011) 269–291.
[74] P. Janicki, G. Schmidmaier, What should be the characteristics of the ideal bone graft substitute? Combining scaffolds with growth factors and/or stem cells, Injury 42 Suppl 2 (2011) S77-81.
[75] L. Roseti, V. Parisi, M. Petretta, C. Cavallo, G. Desando, I. Bartolotti, B. Grigolo, Scaffolds for Bone Tissue Engineering: State of the art and new perspectives, Materials science & engineering. C, Materials for biological applications 78 (2017) 1246–1262.
[76] D. Wendt, S.A. Riboldi, M. Cioffi, I. Martin, Potential and bottlenecks of bioreactors in 3D cell culture and tissue manufacturing, Advanced materials (Deerfield Beach, Fla.) 21 (32-33) (2009) 3352–3367.
[77] I. Martin, D. Wendt, M. Heberer, The role of bioreactors in tissue engineering, Trends in biotechnology 22 (2) (2004) 80–86.

[78] H. Lu, T. Hoshiba, N. Kawazoe, G. Chen, Comparison of decellularization techniques for preparation of extracellular matrix scaffolds derived from three-dimensional cell culture, Journal of biomedical materials research. Part A 100 (9) (2012) 2507–2516.
[79] P.M. Crapo, T.W. Gilbert, S.F. Badylak, An overview of tissue and whole organ decellularization processes, Biomaterials 32 (12) (2011) 3233–3243.
[80] T.W. Gilbert, T.L. Sellaro, S.F. Badylak, Decellularization of tissues and organs, Biomaterials 27 (19) (2006) 3675–3683.
[81] P. Bourgine, C. Le Magnen, S. Pigeot, J. Geurts, A. Scherberich, I. Martin, Combination of immortalization and inducible death strategies to generate a human mesenchymal stromal cell line with controlled survival, Stem cell research 12 (2) (2014) 584–598.

Curriculum Vitae

Personal information

First and last name	**Sébastien Pigeot**
Address	Strassburgerallee 75, 4055 Basel (Switzerland)
Telephone(s)	Mobile +41 76 264 9414
E-mail(s)	sebastien.pigeot@gmail.com
Nationality	French

Education and training

Dates	**From 04/2013 (Defense on 01/03/1018)**
Occupation Held	PhD Student in Cell Biology
Main activities and responsabilities	Tissue Engineering for bone regeneration, 3D bioreactor culture, Molecular biology
Name of the laboratory/Institution	Department Biomedicine, University of Basel University Hospital Basel
Dates	**03/2015**
Title of qualification awarded	LTK Module 1:Introductory course in laboratory animal science
Principal subjects / occupational skills covered	Animal experimentation on Mice and Rats
Name and type of organisation	University of Zürich & FELASA
Dates	**09/2008 → 09/2011**
Title of qualification awarded	Diplôme d'Ingénieur en Biotechnologie, Master of Biotechnology and Therapeutic Applications
Principal subjects / occupational skills covered	All important aspects of biotechnology are covered: from molecular biology to microbiology, plant physiology, biocomputing and bioprocessing; additional lectures in patent law, economics and professional language courses Chosen specialization in the third year: Synthetic Biology
Name and type of organisation	École Supérieure de Biotechnologie Strasbourg, ESBS (Trinational Engineering School) Strasbourg (France)
Dates	**09/2010 → 09/2011**
Title of qualification awarded	Master in Drugs Sciences, Biotechnology and Therapeutical Innovations.
Principal subjects / occupational skills covered	Drugs registration, patents
Name and type of organisation	Faculty of Pharmacy, Strasbourg University (France)
Dates	**09/2007 - 06/2008**
Title of qualification awarded	Bachelor in Biological Sciences, 5th and 6th semester
Principal subjects / occupational skills covered	General knowledge in different aspects of biology such as molecular biology, Genetic, Cellular biology, Microbiology and food microbiology.
Name and type of organisation	Heriot-Watt University Edinburgh (Scotland)

Dates	**09/2005 – 07/2007**
Title of qualification awarded	Higher National Diploma (HND), 1st to 4th semester
Principal subjects / occupational skills covered	Fundamental and practical teaching. General knowledge in biology, biochemistry, molecular biology, genetic, cellular biology, microbiology, pharmacology, organic chemistry Chosen specialization in second year: Biological and Biochemical Analyses.
Name and type of organisation	Institut Universitaire de Technologie (IUT), Université de La Rochelle La Rochelle (France)
Dates	**2005**
Title of qualification awarded	High school diploma with mention cum laude. (Baccalauréat)
Principal subjects / occupational skills covered	Scientific section Main subjects covered: mathematics, physics, chemistry, natural sciences.
Name and type of organisation	Lycée Bernard Palissy Saintes (France)

Work and practical experience

Dates	**From 04/2013 (defense on 01/03/2018)**
Occupation Held	PhD Student in Cell Biology
Main activities and responsabilities	Tissue Engineering for bone regeneration, 3D bioreactor culture, Molecular biology
Name of the laboratory/Institution	Department Biomedicine, University of Basel University Hospital Basel
Dates	**28/11/2011 – 29/07/2012**
Occupation Held	Research apprentice
Main activities and responsabilities	Construction and test in vitro of several vectors in order to suppress HIV through a combination of different shRNAs. Test of Zinc Finger Nucleases construct in vitro in human cells. It involved cloning, cell culture, transfection, virus packaging, transduction, luciferase assay, northern blot, work with radioactive materials, in vitro transcription.
Name of the laboratory/Institution	John Rossi's Laboratory Beckmann Research Institute – City of Hope, Duarte, CA, USA
Dates	**28/06/2011 – 26/08/2011**
Occupation held	Research Apprentice
Main activities and responsabilities	Construction and test in vitro of several vectors in order to suppress HIV through a combination of different shRNAs. It involved cloning, cell culture, transfection, virus packaging, transduction, luciferase assay, northern blot, work with radioactive materials.
Name of the laboratory/Institution	John Rossi's Laboratory Beckmann Research Institute – City of Hope Duarte, CA, USA
Dates	**11/2009 - 11/2010**
Occupation held	iGEM competition (International Genetically Engineered Machine) / Synthetic Biology
Main activities and responsibilities	Creation of a controllable specific protein degradation system. The project was built up in its entirety by a group of undergraduate students from the idea to its conception through sponsoring, personal research and manipulation.
Dates	**15/06/2009 – 15/08/2009**

Occupation held	Laboratory internship
Main activities and responsibilities	Purification and crystallization of the proteasome β subunit from A. fulgidus.
Name of the laboratory/Institution	Department Chemie, Lehrstuhl für Biochemie, Technische Universität München (TUM) Munich (Germany)
Dates	**04/2007 – 06/2007**
Occupation held	Laboratory internship
Main activities and responsibilities	Screening of patients affected by myeloproliferative disease by allelic discrimination using single nucleotide polymorphisms (SNPs).
Name of the laboratory/Institution	INSERM U790: Stem cells and hematopoiesis Institut Gustave Roussy Villejuif (France)

Talks, Posters (Seminars)

Dates and structure	**02/2017 ➔ Poster/Seminar**
Title	Engineered bone organs to study and environmentally regulate the engraftment of human hematopoietic stem cells within human origin niches.
Event/Journal	International Society of Stem Cell Research (ISSCR) Regional event, Basel, Switzerland
Dates and structure	**02/2016 ➔ Poster/Seminar**
Title	Engineered bone organs for the engraftment and maintenance of human hematopoietic stem cells in mice
Event/Journal	Gordon Research Conference on bone and teeth, Galveston, TX, USA.
Dates and structure	**05/2014 ➔ Poster/Seminar**
Title	Osteoinductivity of engineered hypertrophic cartilage devitalized by apoptosis induction
Event/Journal	Swiss Stem Cell Network, Geneva, Switzerland
Dates and structure	**05/2012 ➔ Poster/Seminar**
Title	Combinatorial approach using MGMT P140K transgene and multiplexed RNAs in gene therapy against HIV-1
Event/Journal	American Society of Gene & Cell Therapy (ASGCT) Annual Meeting, Philadelphia, PA, USA.

List of Publications

2018**:** Kristin Fritsch*, Sébastien Pigeot*, Paul E. Bourgine, Xiaomin Feng, Timm Schroeder, Ivan Martin, Markus G. Manz, Hitoshi Takizawa. Engineered humanized bone organs maintain human hematopoiesis in vivo. Exp. Hem. In Press.

2017: P. E. Bourgine, E. Gaudiello, B. Pippenger, C. Jaquiery, T. Klein, S. Pigeot, A. Todorov Jr., S. Feliciano, A. Banfi, I. Martin. Engineered Extracellular Matrices as Biomaterials of Tunable Composition and Function. Adv. Funct. Mater.

2014: Bourgine PE, Scotti C, Pigeot S, Tchang LA, Todorov A, Martin I. Osteoinductivity of engineered cartilaginous templates devitalized by inducible apoptosis. PNAS.

2014: Bourgine P, Le Magnen C, Pigeot S, Geurts J, Scherberich A, Martin I. Combination of immortalization and inducible death strategies to generate a human mesenchymal stromal cell line with controlled survival. Stem Cell Research.

Manuscripts

Paola Occhetta, Sébastien Pigeot et al. Developmentally inspired programming of adult human mesenchymal stromal cells towards stable chondrogenesis. PNAS, in revision.

Paul Bourgine, Kristin Fritsch, Sébastien Pigeot et al. Phenotypic distribution of the human mesenchymal and blood cells in engineered human hematopoietic organs. Leukemia, in revision.

Julien Guerrero, Sébastien Pigeot et al. Fractionated human adipose tissue as a native biomaterial for the generation of a bone organ by endochondral ossification. Acta Biomaterialia, in revision.

Sébastien Pigeot et al. Devitalized bioreactor based hypertrophic cartilage as regenerative material for bone defects. Manuscript in preparation.

Personal skills and competences

Mother tongue(s) **French**

Other language(s) English, German

Self-assessment

English	Proficient user (understanding, writing and speaking), also in scientific fields
German	Good understanding and speaking, basics in writing

Social skills and competences

Strong teamwork and communication skills, Open minded, Good adaptability

Example(s)

Teamwork and communication skills	Participation on iGEM 2010; Group projects form important parts of the ESBS curriculum
Open minded / adaptability	Studies and internship abroad

Computer skills and competences: Routine use of bioinformatics tools (NCBI, Blast, Primer3, PDB, etc.)
Well-based knowledge of the MS-Office applications (Word, Excel, Powerpoint)

Driving licence: Class B (since 2005)